THE EFFECTS OF SHIGA TOXIN 1 ON CYTOKINE AND CHEMOKINE PRODUCTION AND APOPTOSIS IN A HUMAN MONOCYTIC CELL LINE

A Dissertation

by

LISA MARGARET HARRISON

Submitted to the Office of Graduate Studies of
Texas A&M University
in partial fulfillment of the requirements for the degree of

DOCTOR OF PHILOSOPHY

August 2004

Major Subject: Medical Sciences

THE EFFECTS OF SHIGA TOXIN 1 ON CYTOKINE AND CHEMOKINE PRODUCTION AND APOPTOSIS IN A HUMAN MONOCYTIC CELL LINE

A Dissertation

by

LISA MARGARET HARRISON

Submitted to Texas A&M University
in partial fulfillment of the requirements
for the degree of

DOCTOR OF PHILOSOPHY

Approved as to style and content by:

Vernon L. Tesh (Chair of Committee)	David N. McMurray (Member)
James E. Samuel (Member)	Rajesh Miranda (Member)
John M. Quarles (Head of Department)	

August 2004
Major Subject: Medical Sciences

ABSTRACT

The Effects of Shiga Toxin 1 on Cytokine and Chemokine Production and Apoptosis in a Human Monocytic Cell Line. (August 2004)

Lisa Margaret Harrison, B.S., University of California at Davis

Chair of Advisory Committee: Dr. Vernon L. Tesh

Severe bloody diarrhea and subsequent serious post-diarrheal illnesses, including the hemolytic uremic syndrome and central nervous system complications, may develop following infections with Shiga toxin (Stx)-producing bacteria. The cytotoxic actions of Stxs destroy the microvasculature of organs, preventing function. A role for the cytokines tumor necrosis factor-alpha (TNF-α) and interleukin-1 beta (IL-1β) in exacerbating disease may lie in their ability to up-regulate the Stx receptor, Gb_3, on endothelial cell surfaces. A main source of proinflammatory cytokines is the macrophage, thus leading us to utilize the monocytic/macrophage-like cell line, THP-1, as a model for cytokine production in Stx pathogenesis.

In addition to treating THP-1 cells with purified Stx1, cells were also treated with lipopolysaccharides (LPS), since bacterial LPS are known to be potent inducers of cytokines, and may be present during infection. Undifferentiated THP-1 cells are sensitive to Stx1 and do not produce TNF-α or

IL-1β, while differentiated THP-1 cells, a better model for resident tissue macrophages, are less sensitive to Stx1 and produce TNF-α and IL-1β. Prolonged expression of TNF-α mRNA over a 12 h time course experiment led us to inquire whether the extended elevation of transcripts involved Stx1-induced mRNA stability. Our data suggest that the presence of Stx1 increases the stabilities of TNF-α and IL-1β transcripts. In contrast to TNF-α, the level of secreted IL-1β protein does not correlate with the level IL-1β mRNA, suggesting an alteration of post-translational processing and/or secretion of IL-1β. Differentiated THP-1 cells produce chemokines in response to Stx1 and/or LPS treatments. Chemokines may enhance the destruction of tissue cells during an infection by mediating an inflammatory cell influx. Comparison of cytokine and chemokine mRNA and protein kinetics suggests that the regulation of expression may differ between individual cytokines and chemokines.

Extension of experimental time courses demonstrated THP-1 cell sensitivity to killing by Stx1, especially in the presence of LPS. Further experiments revealed that undifferentiated and differentiated THP-1 cells were induced to undergo apoptosis following treatment with Stx1, LPS, and Stx1+LPS, and that caspase activation was involved. Collectively, these results allowed us to propose a model of the role of macrophages in Stx1 pathogenesis.

ACKNOWLEDGEMENTS

I would like to sincerely thank my advisor Dr. Vernon L. Tesh for all of his patience, guidance, and support during the past six years of my graduate studies. Dr. Tesh has gone out of his way to help me with every aspect of graduate school, especially during the preparation of the papers presented in this dissertation. I am so grateful for having him as a mentor. I would also like to thank the members of my committe, Dr. David N. McMurray, Dr. James E. Samuel, and Dr. Rajesh Miranda, for their advice on my project and for their assistance with reviewing manuscripts. Additionally, I would like to thank Dr. Rajesh Miranda, Dr. Wei-Jung Chen, and Dr. Shannon Sedberry Allen for their help with the statistical analysis of my data.

For the work presented in Chapter II, the expert technical assistance of Dr. Gregory Foster, Cassandra Armstrong, Dr. Amminikutty Jeevan, Dr. Todd Lasco, and Ilona van Haaften is gratefully acknowledged. For their excellent assistance with the work presented in Chapter III, I would like to thank Christel van den Hoogen, Ilona van Haaften, and Christopher N. Thompson. I would also like to thank Ilona van Haaften, Christel van den Hoogen, Dr. Rama Cherla, and Sang-Yun Lee for their contributions to Chapter IV. Additionally, I would like to thank Dr. Cheleste Thorpe for the gift of purified Stx1 B-subunits and IL-8 cDNA probes, and Jane Miller for expert assistance with the FACS analyses.

TABLE OF CONTENTS

CHAPTER Page

LIST OF FIGURES

FIGURE Page

LIST OF TABLES

CHAPTER I

INTRODUCTION

Shigella dysenteriae type 1 and enterohemorrhagic *E. coli* (EHEC) are the major enteric pathogens that produce a family of protein toxins known as Shiga toxins. *Shigella dysenteriae* type 1 produces Shiga toxin (Stx), while EHEC can produce one or more Stxs designated Stx1, Stx2, Stx2c, Stx2d, Stx2e, and Stx2f. Stx and Stx1 are essentially identical except for one amino acid difference (50,124). Stx2 and its variants differ more significantly from Stx/Stx1, leading to different levels of toxicity in animal models of disease, as well as different receptor preferences (10,78,106,131). Stxs are AB_5 toxins that are composed of a single 32 kDa A-subunit that contains the enzymatic activity of the toxin, and five 7.7 kDa B-subunits which form a pentameric ring that is involved in binding to the toxin receptor on target cells (25). The cell surface receptor for Stxs is the glycolipid Gal ($\alpha1\rightarrow4$)-Gal ($\beta1\rightarrow4$)-Glc ($\beta1\rightarrow1$) ceramide (globotriaosylceramide or Gb_3; 5,49,65), although Stx2e tends to have a higher affinity for Gb_4, which contains an additional terminal sugar (N-acetylgalactosamine or GalNac) (10,78,106). Susceptibility to Stxs may not only depend on the expression of Gb_3 on cell surfaces, but may also depend on the expression of the correct isoform of

---

This dissertation follows the format and style of the journal Infection and Immunity.

Gb_3 in glycolipid-rich microdomains (1,17,93). Furthermore, Gb_3 fatty acid isoforms may affect the intracellular trafficking of Stxs, and thus the outcome of disease (1).

Once Stx is bound to its receptor, it is then endocytosed via a clathrin-coated pit into an endosome (109). The toxin then undergoes retrograde transport through the *trans*-Golgi network, the Golgi stack, and the endoplasmic reticulum, where it may gain access to the cytosol (109). Cleavage of the A-subunit into the A_1 (~28 kDa) and A_2 (~4 kDa) fragments is thought to occur through the action of furin or a furin-like protease during the retrograde transport of the toxin through the cell (26). If the cleavage does not occur at this point, calpain, a cytosolic protease, also has the ability to cleave the A subunit (26). The A_1 fragment possesses the enzymatic N-glycosidase activity of the Stx, which causes depurination of a single adenine residue located on a prominent loop structure near the 3' end of 28S rRNA of the 60S ribosomal subunit (16,111). Depurination, at this site on ribosomes, blocks elongation factor-1-dependent aminoacyl-tRNA binding, preventing peptide elongation and thus, inhibiting protein synthesis (45,89,111).

While the main reservoir for *S. dysenteriae* is man, the main reservoir for EHEC is livestock such as cows and sheep (63). The spread of EHEC from animal to man usually occurs via the ingestion of contaminated food. Drinking

contaminated water and spread by the fecal-oral route from person-to-person contact are alternative means of infection (77). Following infection with *S. dysenteriae* type 1, bacillary dysentery, a severe form of bloody diarrhea may develop. EHEC infections result in hemorrhagic colitis which is also a severe form of bloody diarrhea, but less severe in duration and mortality than bacillary dysentery (77,132). The difference in severity is due, in part, to the fact that *S. dysenteriae* is an invasive organism, while EHEC are noninvasive. In contrast to *S. dysenteriae*, EHEC form attaching and effacing lesions on the surface of the colonic mucosa (3). While initiating attaching and effacing lesions, the bacteria are able to attach intimately to the surface of the intestinal epithelium of the large intestine and translocate bacterial proteins into the host cell. The translocated proteins trigger signaling cascades within the host cell, which affect the cytoskeletal framework that maintains the integrity of the microvilli on the apical surface. The result is microvilli retraction, and subsequent actin condensation beneath the bacteria to form pedestal-like structures. Also, permeability between adjacent cells increases along with activation of chloride secretion into the lumen. Malabsorption due to microvilli retraction, in concert with the release of water into the lumen, caused by increased intercellular permeability and chloride secretion, all contribute to diarrhea. Increased intestinal permeability may also make it possible for Stxs to gain access to the microvasculature of the lamina propria via a paracellular mechanism. However,

Hurley *et al* recently reported that a mechanism for active transcellular transport of Stxs across epithelial barriers might exist (43). Once in the submucosa, Stxs may damage endothelial cells, resulting in release of blood into the lumen, and Stx access to the bloodstream (117).

In addition to causing intestinal damage, Stxs target the kidneys and central nervous system of humans for additional impairment. The actions of Stxs on the glomerular microvasculature can lead to the development of the Hemolytic Uremic Syndrome (HUS) (54). HUS is the most common cause of acute renal failure in children (117). In the US, most HUS cases are due to a single *E. coli* serotype, O157: H7, although there are multiple other STEC serotypes that can cause HUS (90). Approximately 5-8% of children with Stx-associated diarrhea develop HUS (90). HUS has been clinically defined as a triad of features: microangiopathic hemolytic anemia, thrombocytopenia, and acute renal failure (27). Microangiopathic hemolytic anemia involves endothelial cell damage of the small blood vessels in the glomerulus, resulting in blood clot formation and hence, destruction or deformation of red blood cells circulating through damaged blood vessels. Thrombocytopenia is a decrease in circulating blood platelet levels due to platelet aggregation at damaged blood vessel sites, where they participate in blood clot formation. Acute renal failure results when the blood purification function of the kidneys is obstructed due to the formation of intraglomerular blood clots. Without normal renal function,

urine is not produced and nitrogenous wastes are not filtered into the urine, resulting in severe, prolonged morbidity and mortality. Stx action on the microvasculature of the brain is thought to be the cause of CNS injury. An inflammatory response results in severe cerebral edema and can lead to seizures, stroke, coma, and death (116).

Other possible contributors to the pathogenic effects of Stxs leading to HUS may include proinflammatory cytokines and chemokines. Numerous studies have shown that many endothelial cell types are not very sensitive to the cytotoxic actions of Stxs unless they are pre-exposed to the proinflammatory cytokines tumor necrosis factor-α (TNF-α) and interleukin-1β (IL-1β). TNF-α and IL-1β have been shown to up-regulate Gb_3 on the surface of a variety of endothelial cell types, rendering them more susceptible to the cytotoxic actions of Stxs (15,71,72,98,139,142). Furthermore, in some HUS patients, serum and urinary levels of TNF-α are elevated (130). In addition, Harel *et al.*showed selective induction of chloramphenicol aminotransferase (CAT) activity in the kidneys of mice harboring a TNF-α promoter::CAT transgene following Stx infusion (37). These data suggest that TNF-α and IL-1β may contribute to the pathogenesis of HUS by rendering blood vessels in the colon, kidneys, and CNS more susceptible to the destructive action of Shiga toxins. The main source of proinflammatory cytokines is the macrophage. In 1996, van Setten *et al.*

demonstrated that TNF-α and IL-1β were produced by nonadherent human monocytes following treatment with Stx1 (140). Our lab has chosen to concentrate on the interaction of Stxs with mature, macrophage-like cells, rather than immature monocytes. The nonadherent monocytic cell line THP-1, which is representative of the immature, circulating monocytes, can be differentiated into a mature-macrophage like state by treating cells with the phorbol ester phorbol 12-myristate 13-acetate (138). Differentiated THP-1 cells are less sensitive to Stxs, express macrophage-like surface receptors, and are able to produce cytokines following treatment with Stxs (99), rendering it more representative of resident tissue macrophages. Previous work in our lab has demonstrated that both murine and human macrophages are capable of producing TNF-α and IL-1, *in vitro*, following treatment with Stxs (99,133). The *in vivo* and *in vitro* data suggest that: i) TNF-α and IL-1β are involved in the pathogenesis of HUS; ii) following toxin stimulation, macrophages are a possible source of TNF-α and IL-1β; and iii) TNF-α production may be localized to sites of toxin-mediated damage. In chapter I, we describe experiments that further investigated the kinetics of TNF-α mRNA, as well as IL-1β mRNA and protein kinetics in Stx1-, LPS-, and Stx1+LPS-treated THP-1 cells. We also examined the role of transcript stability in the prolonged elevation of TNF-α and

IL-1β mRNAs to determine whether transcript stability may contribute to Stx pathogenesis through extending the expression of TNF-α and IL-1β.

In addition to the contribution of proinflammatory cytokines to Stx pathogenesis, chemokines may also add to the pathology caused by Stxs through the recruitment of inflammatory cells to the sites of infection. The migration of neutrophils to the sites of infection, along with the release of their antimicrobial products, may also damage the host tissues. There is evidence for IL-8 involvement in neutrophil-mediated damage in the intestine (35,144). Migration of neutrophils to the lumen of patients infected with *S. dysenteriae* or EHEC has been reported as well (119). IL-8 has also been found in the urine and serum of some HUS patients, along with the migration of monocytes and neutrophils to their kidneys (141). Furthermore, IL-8 transcript stabilization, IL-8 production, and increased paracellular permeability has been demonstrated in intestinal epithelial cells, *in vitro*, following the administration of Stxs (44,91,136,137). The purpose of the experiments in chapter II was to expand on the findings of chapter I to explore chemokine expression in macrophages. Due to reports proposing a role for IL-8 in Stx pathogenesis, and a possible role for transcript stabilization in IL-8 expression in epithelial cells, we set out to determine if our macrophage model fit into the same category, as a source for IL-8 and other chemokines following exposure to Stxs.

The observation that Shiga toxins, potent protein synthesis inhibitors, induce the expression of proinflammatory proteins is somewhat paradoxical. We sought, therefore, to characterize the mechanisms by which Shiga toxins stimulate cytokine production. In order to determine whether transcription factors are involved in initiating Stx-induced TNF-α gene expression, our lab performed electrophoretic mobility shift assays on nuclear extracts prepared from Shiga toxin stimulated THP-1 cells and human peripheral blood monocytes and probed with radiolabeled nuclear factor-κB (NF-κB) and activator protein-1 (AP-1) consensus oligonucleotides (105). NF-κB and AP-1 were chosen because of other reports implicating their involvement in TNF-α gene activation in macrophages following LPS stimulation (100,114). We were able to detect the nuclear translocation and DNA binding activities of the transcriptional activators NF-κB and AP-1. However, this finding alone does not rigorously prove their involvement in the activation of TNF-α gene expression.

Additional work in our lab examined TNF-α mRNA expression in differentiated THP-1 cells following stimulation with LPS, Stx1, or LPS+Stx1 (105). THP-1 cells have been reported to possess many of the biological properties of primary human monocytes (2). Our experiments showed that TNF-α mRNA levels remained elevated longer in cells stimulated with Stx1 or

LPS+Stx1 than in cells stimulated with LPS alone (105). Thus, Shiga toxins appear to regulate TNF-α expression at both transcriptional and post-transcriptional levels. This led us to speculate that TNF-α and possibly IL-1β mRNAs may be stabilized in macrophages stimulated with Stxs. Furthermore, the levels of TNF-α production seen in cells treated with Stx appeared to be due to the presence of the holotoxin since Stx1 B-subunit or the Stx1 A-subunit mutant are both unable to induce TNF-α protein (23). The intracellular retrograde transport of Stx through the Golgi apparatus into the ER may be necessary for cytokine and chemokine production since a recent report indicated that treatment with the Golgi apparatus inhibitor, Brefeldin A, prevents IL-8 production in Caco-2 cells (148). Stx-induced TNF-α mRNA stability can be examined by measuring mRNA half-life. One way to do this is by utilizing the transcriptional inhibitor, Actinomycin D. Following transcriptional inhibition, mRNA decay can be monitored and a half-life calculated.

There are two main types of determinants of mRNA stability, *cis*- and *trans*-acting determinants (103). *Cis*-acting determinants are located on the mRNA molecule itself, while *trans*-acting determinants are located elsewhere in the cell. *Cis*-acting determinants include 5′ untranslated regions, mRNA coding regions, and 3′ untranslated regions, which may contain AU rich elements and 3′ Poly (A) tails. Deadenylation of poly (A) tails has been described as the first

step of decay for many mRNAs. Poly (A) tails may also form complexes with poly (A)-binding proteins, which have been found to protect mRNAs from rapid degradation, *in vitro*. Therefore, poly (A) tails protect mRNA from rapid or indiscriminate degradation. In addition, poly (A) tails are linked to translation, where a minimal poly (A) length is required for translation initiation. AU rich elements, on the other hand, tend to make mRNAs unstable. They include AUUUA pentamers, which facilitate degradation of the mRNA body, and U-rich regions, which promote deadenylation as well as enhance the AUUUA function. Unstable cytokine mRNAs contain AU rich elements in their 3' untranslated regions (6).

Trans-acting determinants vary from mRNA to mRNA and are regulated in some way, depending on environmental factors, cell growth rate, or stimuli. They can either stabilize or destabilize mRNA when acting alone, or when combined with other *trans*-acting determinants. Poly (A)-binding proteins and binding proteins of AU rich regions are two examples of *trans*-acting determinants. Poly (A)-binding proteins appear to be involved in the accumulation of 80S ribosomal mRNA complexes and the formation of translationally active ribosomes (40). Also, when poly (A)-binding proteins are depleted from a mixture, mRNA is rapidly degraded, but when they are replenished in a mixture lacking poly (A)-binding proteins, mRNAs are restabilized. AU binding proteins also influence mRNA stability. Some AU

binding protein levels have been found to increase or decrease at the same time that mRNAs are stabilized in response to a stimulus. Other AU binding protein levels correlate inversely with mRNA half-life. In other words, when the level of AU binding protein decreases, mRNA half-life increases, or when the level of AU binding protein increases, mRNA half-life decreases (103).

In addition to inhibiting protein synthesis, recent studies have indicated that Stxs are capable of inducing apoptosis, or programmed cell death, in various cell types. Programmed cell death is a way for cells to die without causing an inflammatory response, and involves shrinking of cells, loss of intercellular contacts, chromatin condensation, nuclear fragmentation, cytoplasmic blebbing, and cellular fragmentation. Necrosis, on the other hand involves cell swelling, lysis, and subsequent release of cytoplasmic and nuclear contents into the intercellular milieu, resulting in inflammation (149). Most Stx-related apoptotic studies so far involve epithelial cells, endothelial cells, and B-lymphoma cells. Although the main targets of Stxs appear to be the microvascular endothelial cells of the colon, kidneys, and the CNS, they would be unable to reach these sites without first making their way past the intestinal epithelium and tissue macrophages. In vitro studies involving the intestinal epithelial cell lines Caco-2, HEp-2, and T84 demonstrated that apoptosis was induced following treatment with Stx1 or Stx2, but only in the cells that expressed the toxin receptor Gb_3 on their surfaces (Caco-2 and HEp-2, but not

T84) (51,113). These studies also suggested that the routing of the toxin through the cell was important in determining whether or not apoptosis would occur. The intestinal epithelial cell line, HCT-8, was also induced to undergo apoptosis following treatment with Stx1, in a manner associated with caspase-3 cleavage and DNA fragmentation (120). Furthermore, death of these cells required Stx1 enzymatic activity as well as activation of the MAP kinases p38 and JNK. Besides intestinal epithelial cells, both primary and immortalized human renal cortical and tubular epithelial cells have also been shown to undergo apoptosis following treatment with Stx1 or Stx2 (55,58,127).

There has only been one report with regard to Stx-induced apoptosis in monocytes and macrophages. In 2000, Kojio *et al.* demonstrated that apoptosis is induced in undifferentiated THP-1 cells treated with Stx1 or Stx2, and that this mechanism involves caspase-3 activation, as well as transport of the toxin to the Golgi apparatus (59). In our lab, undifferentiated THP-1 cells were also sensitive to the cytotoxic actions of Stx1, although we did not determine the mode of cell death. However, differentiated THP-1 cells were much more resistant to the cytotoxic effects of Stx1, at least in experiments involved in looking at early signaling events and cytokine production (23,24,99). Furthermore, Stxs did not inhibit protein synthesis in differentiated THP-1 following treatment up to 4 h (23), suggesting that other than production of cytokines, these cells were unaffected by Stxs. A recent study in Burkitt's

lymphoma cells by Tetaud *et al.* demonstrated that apoptosis was not dependent on the inhibition of protein synthesis by Stx1, and that the binding of different ligands to Gb3/CD77, including an anti-Gb_3 mAb, results in the initiation of distinct apoptotic pathways (23,135). Although most of our experiments concentrated on the early events following Stx1 exposure, it is still possible that long-term exposure of differentiated THP-1 cells could have downstream effects of cell function and viability. Experiments conducted in chapters I and II, which set out to determine the prolonged effects of Stx1 on cytokine transcript kinetics and stability in differentiated THP-1 cells, indicated that prolonged exposure to Stx1, especially in concert with LPS, might affect cell viability. Chapter III, therefore, compares the effects of long-term Stx exposure on undifferentiated and differentiated THP-1 cells, and introduces the role of apoptosis of macrophages in Stx pathogenesis.

CHAPTER II

REGULATION OF PROINFLAMMATORY CYTOKINE EXPRESSION BY SHIGA TOXIN 1 AND/OR LIPOPOLYSACCHARIDES IN THE HUMAN MONOCYTIC CELL LINE THP-1*

Overview

Infection with Shiga toxin (Stx)-producing bacteria and the subsequent release of Stxs and endotoxins into the bloodstream may damage blood vessels in the colon, kidneys, and CNS, leading to bloody diarrhea, acute renal failure, and neurological complications. The pro-inflammatory cytokines tumor necrosis factor-α (TNF-α) and interleukin-1β (IL-1β) may contribute to the pathogenesis of Stx-induced vascular lesions by up-regulating toxin receptor expression on endothelial cells. We previously showed that macrophages treated with purified Shiga toxin 1 (Stx1) or lipopolysaccharides (LPS) secrete TNF-α and IL-1β. Northern blot analysis revealed that treatment of the human monocytic cell line THP-1 with LPS induced a rapid and transient increase in TNF-α and IL-1β

---

* Reprinted with permission from Regulation of proinflammatory cytokine expression by Shiga toxin 1 and/or lipopolysaccharides in the human monocytic cell line THP-1 by Lisa M. Harrison, Wilhelmina C. E. van Haaften, and Vernon L. Tesh, 2004, Infection and Immunity, **72:** 2618-2627.

steady-state transcripts. In contrast, Stx1 induced slower but prolonged elevations in cytokine transcripts. The presence of both stimulants resulted in optimal cytokine mRNA induction in terms of kinetics and prolonged expression. Compared to LPS, Stx1 was a poor inducer of IL-1β protein expression, although levels of soluble IL-1β induced by all treatments continually increased over 72 h. IL-1β transcripts were not induced by Stx1 B-subunits. Using the transcriptional inhibitor actinomycin D, we determined that Stx1 or Stx1 + LPS treatment induced cytokine transcripts with increased stability compared to transcripts induced by LPS alone. For all treatments, IL-1β mRNA decay was slower than TNF-α. Collectively, our data suggest that Stxs affect cytokine expression, in part, at the post-transcriptional level by stabilizing mRNAs. Optimal TNF-α expression occurs when both Stxs and LPS are present.

Introduction

Shigella dysenteriae serotype 1 and Shiga toxin-producing *E. coli* (STEC) are causative agents of bacillary dysentery and hemorrhagic colitis, respectively. These bacteria produce potent cytotoxins known as Shiga toxins (Stxs). Shiga toxin produced by *S. dysenteriae* serotype 1 and Shiga toxin 1 (Stx1) produced by STEC are essentially identical toxins. STEC may also express one or more Stxs that are antigenically distinct from Stx1, called Stx2 and Stx2 variants (79,87).

The toxins are thought to damage blood vessels serving the colon (21). In addition to exacerbating intestinal damage associated with infection, Stxs are associated with the development of life threatening post-diarrheal complications (53). The action of Stxs on glomerular and brain microvascular endothelial cells may activate prothrombotic and pro-inflammatory cascades that lead to the development of the hemolytic uremic syndrome (HUS) and central nervous system complications (92,117). Stxs are AB_5 toxins, having a single enzymatic A-subunit in non-covalent association with five identical B-subunits (25,108). Stx B-subunits bind to cells primarily through interaction with the membrane glycolipid receptor globotriaosylceramide (Gb_3) (49,65). Following clathrin-dependent endocytosis, the toxins undergo retrograde transport through the trans-Golgi network and the Golgi apparatus to reach the endoplasmic reticulum and nuclear membranes, where the toxins gain access to the cytosol (108)). During transport, the A-subunit is cleaved and reduced, and once in the cytosol, the enzymatic A_1 fragment mediates the depurination of a single adenine residue located near the 3' end of 28S rRNA of the 60S ribosomal subunit (16,111). The single cleavage event results in the inhibition of peptide elongation, and the loss of protein synthesis (45,89).

While the mechanism of action of Stxs, and the resultant cytotoxicity are well described, the pathogenic mechanism(s) leading to the profound vascular damage seen in HUS is less well understood. Possible contributors to

pathogenesis may include bacterial lipopolysaccharides (LPS) and the pro-inflammatory cytokines tumor necrosis factor-α (TNF-α) and interleukin-1β (IL-1β). Patients with bacillary dysentery or HUS caused by *S. dysenteriae* serotype 1 are frequently endotoxemic (60) and patients with hemorrhagic colitis or HUS caused by STEC frequently present with elevated antibody titers directed against STEC O-antigens (97,52). LPS are known to be potent inducers of cytokine production. TNF-α and IL-1β levels are elevated in the serum and urine of some HUS patients, but are not consistently elevated as in the case with endotoxic shock (130). Although the relative detrimental and beneficial effects of cytokines in the pathogenesis of HUS remain unclear, TNF-α and IL-1β treatment promotes the up-regulation of membrane Gb_3 expression on cultured vascular endothelial cells derived from human umbilical veins, brain, and renal glomeruli, resulting in increased sensitivity to Stxs *in vitro* (15,71,72,98,139,142). These data suggest that TNF-α and IL-1β may contribute to the pathogenesis of HUS by rendering blood vessels in the colon, kidneys, and CNS more susceptible to the destructive action of Stxs. Isogai *et al.* showed that the exogenous administration of TNF-α to mice infected with STEC exacerbated the severity of CNS and glomerular pathology while treatment with a TNF-α inhibitor ameliorated vascular damage (48). The source(s) of cytokines in target organs is not known, but macrophages are known to be major producers of pro-

inflammatory cytokines when stimulated with microbes or microbial products (86,102,145). Human macrophages produce TNF-α and IL-1β when stimulated with purified Stxs *in vitro* (99,140). Infusion of purified Stx1 into mice harboring a TNF-α promoter::chloramphenicol acetyltransferase (CAT) transgene showed selective induction of CAT activity in the kidneys (37). Collectively, these data suggest that tissue macrophages localized to target organs are possible sources of TNF-α and IL-1β.

Our earlier studies suggested that Stxs stimulate cytokine production through activation of the transcription factors, nuclear factor-κB (NF-κB) and activator protein-1 (AP-1) (105). We noted, however, that stimulation of the differentiated human monocytic cell line THP-1 with Stx1 or Stx1 + LPS resulted in the prolonged elevation of TNF-α transcripts compared to cells stimulated with LPS alone. These data suggested that Stxs may regulate cytokine expression at transcriptional and post-transcriptional levels. We hypothesized that cytokine mRNAs may be stabilized in macrophages stimulated with Stxs, explaining in part the prolonged high steady-state levels of TNF-α mRNA extracted from toxin-treated cells. Therefore, we measured the kinetics of TNF-α and IL-1β mRNA induction and determined the rates of mRNA decay through the use of the transcriptional inhibitor actinomycin D. Finally, we examined the

kinetics of Stx1-induced IL-1β protein production and the requirement for the presence of the Stx1 A-subunit in the activation of IL-1β production.

Materials and Methods

Cells. The human myelogenous leukemia cell line THP-1 (138) was purchased from American Type Culture Collection (ATCC; Rockville, MD). Cell cultures were maintained in RPMI 1640 (GibcoBRL; Grand Island, NY) supplemented with 10% fetal bovine serum (FBS; Hyclone Laboratories; Logan, UT), penicillin (100 U/ml) and streptomycin (100 μg/ml) at 37°C in 5% CO_2 in a humidified incubator.

Toxins. Stx1 was expressed from *Escherichia coli* DH5α transformed with the plasmid pCKS112 containing the toxin operon under control of the T7 promoter (131). Stx1 in crude bacterial lysates was purified by sequential ion-exchange, chromatofocusing, and immunoaffinity chromatography as described previously (133). The toxin was assessed for homogeneity by sodium dodecyl sulfate (SDS)-polyacrylamide gel electrophoresis with silver staining and Western blots. The toxin preparation was then passed through ActiClean Etox columns (Sterogene Bioseparations; Carlsbad, CA) to remove trace endotoxin contaminants, and was determined to contain <0.1 ng of endotoxin per ml by the *Limulus* amoebocyte lysate assay (Associates of Cape Cod, Falmouth, ME).

Purified Stx1 B-subunits were the kind gift of Dr. Cheleste Thorpe, Tufts University School of Medicine, Boston, MA. Purified lipopolysaccharides (LPS) derived from *E. coli* O111:B4 were purchased from Sigma Chemical Co. (St. Louis, MO).

Macrophage differentiation and stimulation. The mature macrophage-like state was induced by treating THP-1 cells (10^6 cells per ml) for 48 h with phorbol 12-myristate 13-acetate (PMA; Sigma) at 50 ng/ml in 100-mm culture dishes. Differentiated, plastic-adherent cells were washed twice with cold Dulbecco's phosphate-buffered saline (PBS; Sigma) and incubated with fresh medium lacking PMA, but containing 10% FBS, penicillin (100 U/ml) and streptomycin (100 μg/ml). The medium was then changed every 24 h for 3 additional days. Experiments were performed on the fourth day after removal of PMA. For Northern blot analyses, differentiated cells were treated with LPS (200 ng/ml), Stx1 (400 ng/ml) or both for varying times. We previously demonstrated that these stimulant doses produced maximal cytokine protein secretion in differentiated THP-1 cells *in vitro* (99). The amount of Stxs necessary to cause systemic disease in humans is unknown, but the Stx1 dose used in these experiments represents approximately 4×10^5 Vero cell CD50s, and approximately 1 LD50 for CD-1 mice (131). To determine mRNA decay rates, differentiated THP-1 cells were treated with the same concentrations of stimulants in the presence or absence of the transcriptional inhibitor

actinomycin D (actD; Sigma) using the protocol of Harrold *et al.* (39). Since we have shown that the induction kinetics of TNF-α and IL-1β are slower in response to treatment with Stx1 compared to LPS, actD (5.0 μg/ml) was added to the cells 1 h after LPS stimulation or 2 h after Stx1 or Stx1 + LPS stimulation. Two 1.0 ml aliquots of all cell supernatants were collected and stored at –20^{O}C for use in ELISAs.

Probe synthesis. The human TNF-α and IL-1β cDNA clones were purchased from ATCC, and grown up in LB broth (DIFCO; Detroit, MI) containing ampicillin (50 μg/ml; Sigma) or tetracycline (20 μg/ml; Sigma), respectively. Plasmids containing the TNF-α and IL-1β cDNAs were isolated using the QIAprep Spin Miniprep Kit (QIAGEN; Valencia, CA), and subsequently digested with the restriction endonucleases (New England Biolabs, Beverly, MA) AvaI and HindIII for TNF-α, or PstI for IL-1β. Digestion of the TNF-α cDNA resulted in a 578 bp fragment containing 450 bp of the TNF-α coding region as well as 128 bp of the 3′-untranslated region (3′-UTR). Digestion of the IL-1β cDNA resulted in a 1047 bp fragment containing the entire IL-1β coding region plus 5′- and 3′-UTRs. Fragments were visualized with ethidium bromide following electrophoresis of the digests into 1.2% agarose gels. The 578 bp and 1047 bp DNA fragments were excised and purified using the QIAquick Gel Extraction Kit (QIAGEN). Approximately 25 ng of the TNF-α

and IL-1β cDNA fragments were resuspended in sterile water for use in [α^{32}P]-dCTP random prime labeling reactions employing the Rediprime II kit (Amersham Pharmacia Biotech Inc.; Piscataway, NJ). A 316 bp human glyceraldehyde-3-phosphate dehydrogenase (GAPDH) DNA probe (Ambion Inc.; Austin, TX) was random prime labeled using the Rediprime II kit to detect GAPDH mRNA that served as a mRNA stability control as well as a loading control. Following labeling, unincorporated [α^{32}P]-dCTP was removed using TE-Midi-Select D G-50 Sephadex columns (Shelton Scientific; Shelton, CT). The labeled probes were ready to use after boiling for 5 min.

Northern blot analysis. Total RNA from Stx1- and/or LPS-stimulated, or purified Stx1 B-subunit-stimulated, differentiated THP-1 cells was extracted using the TRIzol Reagent (Gibco Life Technologies) protocol for cell monolayers. Following extraction, total RNA samples (10 μg of each induced by LPS and Stx1 + LPS and 15 μg of each induced by Stx1 and Stx1 B-subunit) were electrophoresed into 1.0% agarose-formaldehyde gels at 50 V for 1.5 h and then transferred to positively charged nylon membranes using the Turboblotter apparatus (Schleicher & Schuell; Keene, NH) for 3 h. Transferred RNA was cross-linked to membranes using a UV cross-linker (Bio-Rad; Hercules, CA). Membranes were washed in 2X SSC + 0.5% SDS for 30-60 min, after which they were pre-hybridized at 42°C for 3 h with salmon testes DNA (Sigma) in a 50%

formamide (Sigma), 10% SDS (Sigma) pre-hybridization solution. Radiolabeled probes were then added to the hybridization buffer overnight at 42°C. After hybridization, blots were rinsed with 2X SSC, washed twice with 2X SSC + 1.0% SDS for 15 min at room temperature, and then washed once with 0.1X SSC + 1.0% SDS for 30 min at 60°C. Blots were dried briefly prior to exposure to a Phosphorimager screen and analyzed using a Phosphorimager (Molecular Dynamics). Membranes were stripped by boiling in 0.1X SSC + 0.1% SDS twice for 15 min and sequentially reprobed with IL-1β and GAPDH probes at 42°C. Quantitation of pixel intensities of the RNA bands was done using ImageQuant software (Molecular Dynamics). Data are expressed as percentage above basal as determined by:

$$\frac{\text{intensity stimulated cells} - \text{intensity unstimulated cells}}{\text{intensity unstimulated cells}} X\ 100$$

IL-1β ELISA. IL-1β production was quantitated using the Human IL-1β Quantikine Sandwich ELISA kit from R&D Systems (Minneapolis, MN). Supernatants from treated cells were centrifuged to remove cellular debris. LPS and Stx1 + LPS samples were diluted 1:10, while Stx1 and Stx1 B-subunit samples were left undiluted. 200 μL of each sample were added to three replicate wells on the ELISA plates for detection of IL-1β. Following the manufacturer's protocol, A_{540} and A_{570} were measured (Dynatech MR5000;

Dynatech Laboratories; Chantilly, VA), and IL-1β production levels were calculated based on a standard curve. The sensitivity of the assay is 1.0 pg/ml.

Statistics. Statistics for experiments were performed with the SAS statistics program (SAS Institute, Cary, NC) or the SPSS statistics program (SPSS, Inc., Chicago, IL). TNF-α and IL-1β mRNA kinetics were analyzed using two-way ANOVAs with the Duncan multiple range test for post-hoc comparisons. IL-1β protein kinetics were analyzed using one-way ANOVAs with the Duncan multiple range test used for post-hoc analysis. Two-way ANOVAs were used to compare differences in cytokine mRNA levels in cells treated with different stimuli in the presence of actD with the Bonferroni correction for multiple comparisons used for post-hoc comparisons. For mRNA half-lives, the data were rank-ordered and subjected to one-way ANOVAs, using the Duncan multiple range tests, to compare mRNA half-lives between the different stimuli. P values ≤ 0.05 were considered significant for the all analyses. All data are presented as means and standards errors of the means from a compilation of at least three independent experiments.

Results

Comparison of TNF-α and IL-1β mRNA kinetics in THP-1 cells stimulated with Stx1, LPS and Stx1 + LPS. Our earlier studies demonstrated

that Stx1 treatment of differentiated THP-1 cells resulted in the induction of relatively stable TNF-α mRNA transcripts (105). Therefore, we extended to 72 h our initial 12 h analysis of TNF-α mRNA induction in differentiated THP-1 cells treated with Stx1 in the presence or absence of LPS. LPS and Stx1 + LPS treatment rapidly induced TNF-α transcripts with peak induction occurring at 30 to 60 min post stimulation (Figure 1a). The peak percentage increase of TNF-α mRNA above basal induced by Stx1+LPS (6245 ± 2050) is roughly double the peak percentage increase induced by LPS alone (3014 ± 1305) and the difference between the two percentages is statistically significant ($p=0.003$). The reduction of steady-state TNF-α mRNA levels to basal values was rapid, although the reduction in mRNA levels following Stx1 + LPS stimulation was delayed compared to treatment with LPS alone. Stx1 was not as potent an inducer of TNF-α transcripts compared to LPS ($p=0.04$) or both stimulants ($p<0.0001$), as Stx1 induced approximately one-tenth the peak percentage increase in TNF-α mRNA levels (808 ± 540) induced by Stx1 + LPS (Figure 1b). However, over a 4 to 12 h time frame, TNF-α transcripts induced by Stx1 appeared relatively stable, with reductions in steady-state mRNA levels appreciable only after 12 h of stimulation.

Given the ability of IL-1β as well as TNF-α to increase Gb_3 expression by vascular endothelial cells *in vitro* (139), we also determined the kinetics of IL-1β

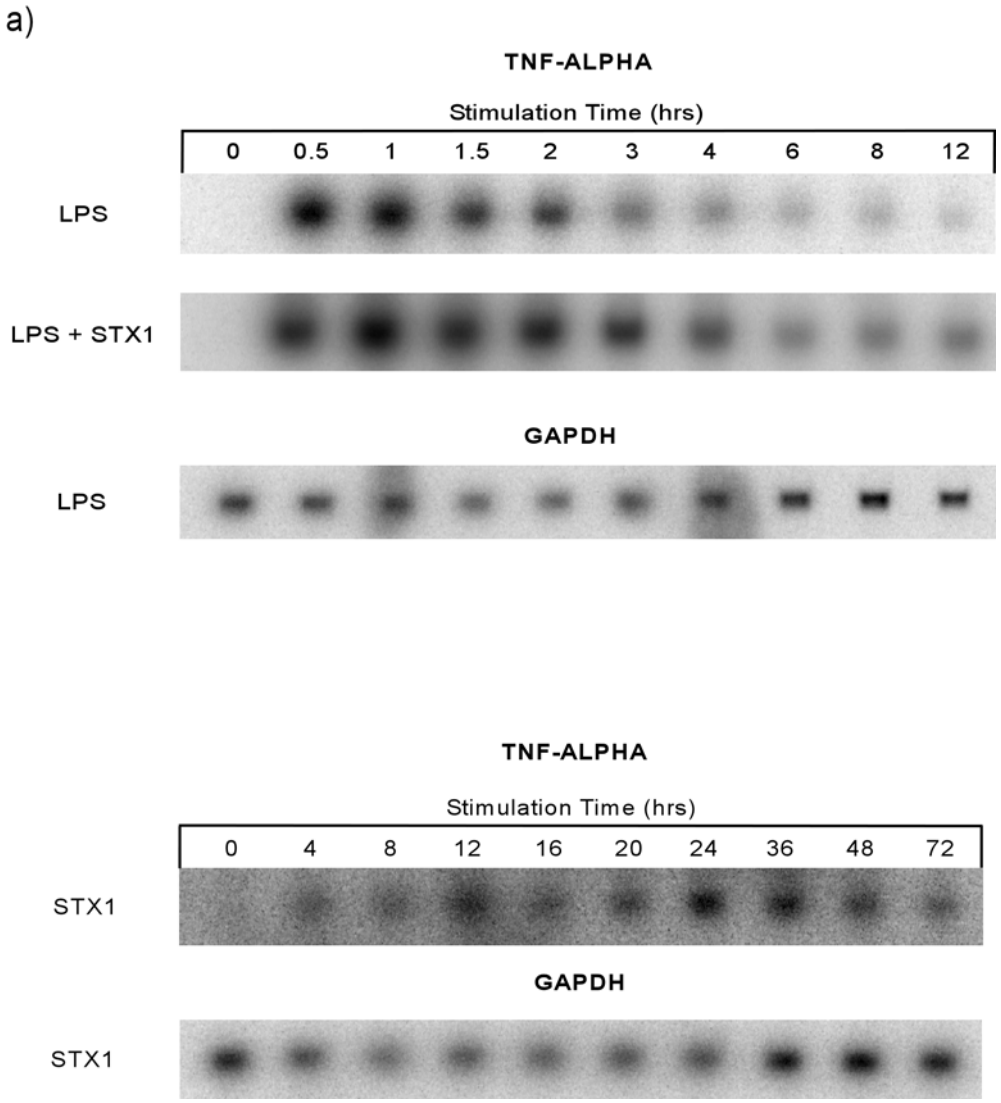

Figure 1. Comparison of TNF-α mRNA kinetics in THP-1 cells stimulated with Stx1, LPS, or Stx1 + LPS. Differentiated THP-1 cells (5 x 10^6 cells/mL) were stimulated with Stx1 (400 ng/mL), LPS (200 ng/mL), or both for 0 to 72 h. Total RNA (10 to 15 µg) was subjected to Northern blot analysis using ^{32}[P]-labeled TNF-α and GAPDH cDNA probes. Hybridization was detected and quantitated using a Phosphorimager and expressed as percentage mRNA above basal (unstimulated) expression. a) Representative Northern blots of Stx1-, LPS-, and Stx1 + LPS-induced TNF-α mRNA. b) Mean intensities of percentage mRNA above basal expression for each time point ± standard error of the means from three independent experiments. An asterisk (*) denotes a significant difference ($p<0.05$) between LPS and Stx1 + LPS treatments. A number sign (#) denotes a significant difference ($p<0.05$) between Stx1 and Stx1 + LPS treatments.

b)

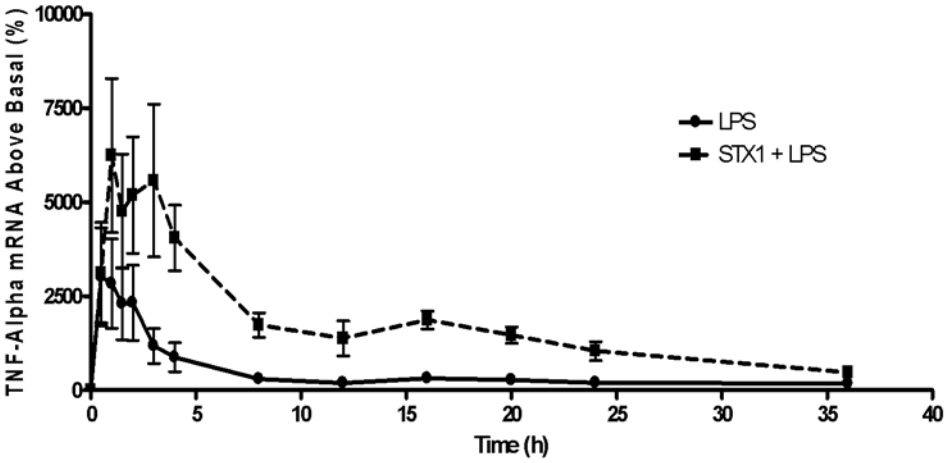

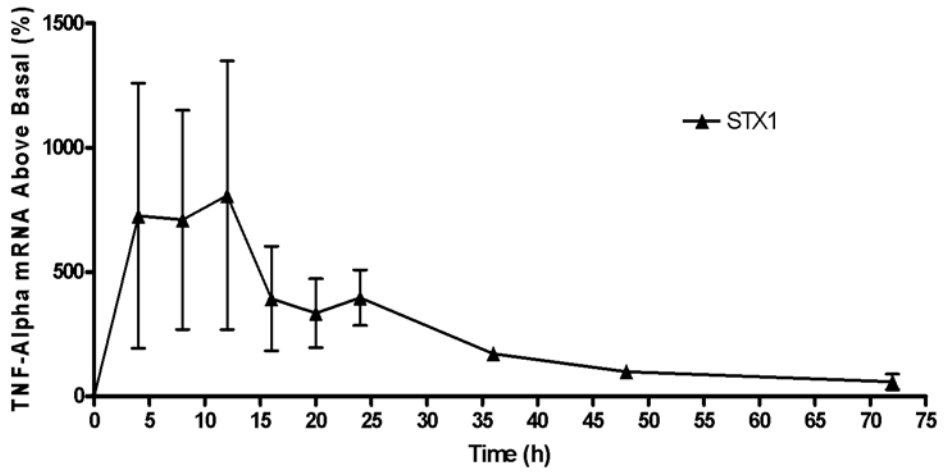

Figure 1 continued

mRNA induction up to 72 h after toxin stimulation. While IL-1β mRNA induction also occurred rapidly in response to LPS or Stx1 + LPS treatment (Figure 2a), the induction kinetics were delayed compared to TNF-α, with peak values achieved at 2 h (LPS treatment) to 4 h (Stx1 + LPS treatment). Treatment of cells with both stimulants did not significantly augment total IL-1β mRNA levels above those induced by LPS alone, in contrast to the increased production of TNF-α transcripts in Stx1 + LPS treated cells. Following treatment with Stx1 alone, IL-1β mRNA was induced with slower kinetics with peak values reached at 24 h (Figure 2b). Regardless of the stimulants used, IL-1β mRNA levels remained elevated longer compared to TNF-α transcripts. In contrast to TNF-α mRNA, IL-1β transcripts appeared to be induced to a higher level by Stx1. The peak percentage increase levels of IL-1β mRNA induced by treatment with LPS (12114 ± 1764) or Stx1 + LPS (11869 ± 2350) were approximately twice that induced by Stx1 alone ($p=0.04$ or $p=0.11$, respectively). The prolonged elevations in steady-state transcript levels suggest that TNF-α and IL-1β expression may be regulated, in part, by Stxs at a post-transcriptional level. An important caveat in the interpretation of these data is that as the treatment times were prolonged, the number of cells detaching from the plates increased, especially with Stx1 + LPS treatment (data not shown). Thus, at the longer time points, the decline in cytokine mRNA levels may be correlated with loss of cell

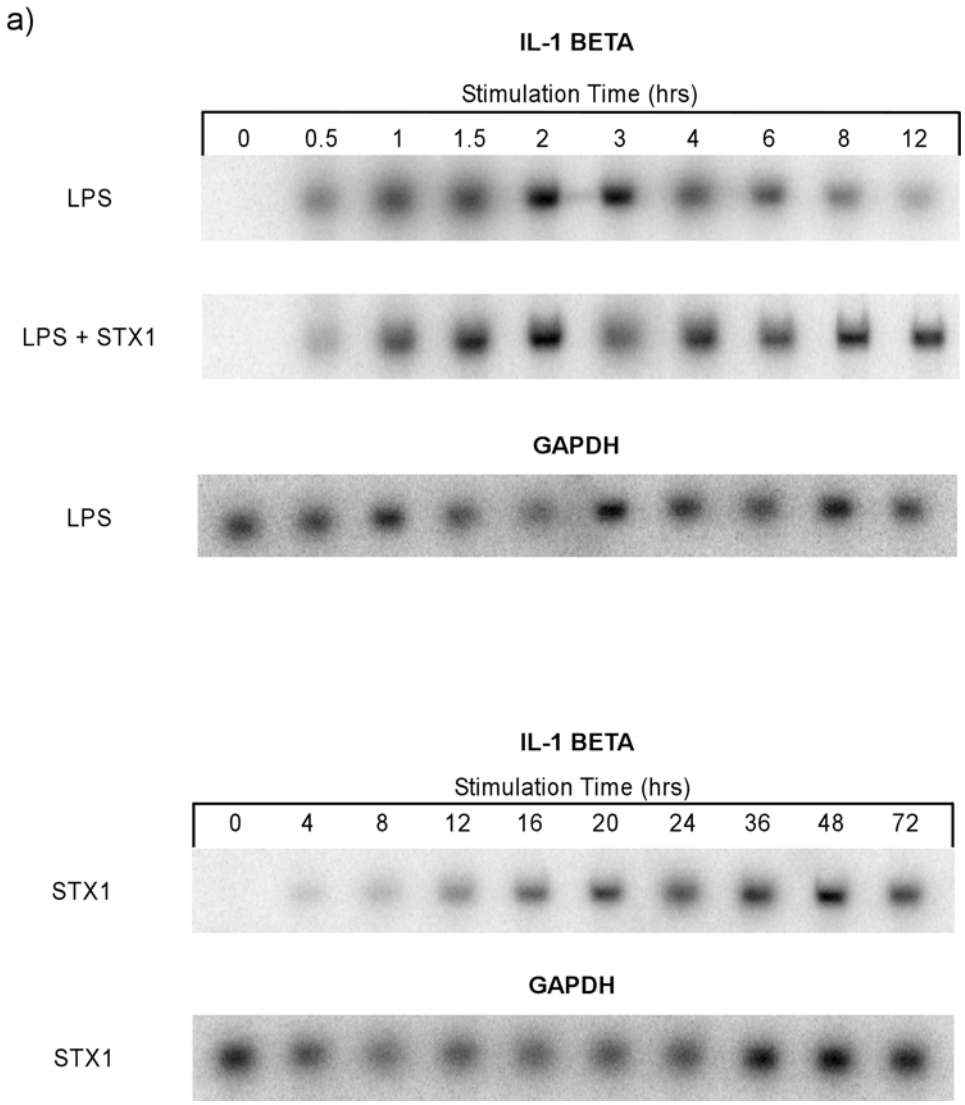

Figure 2. Comparison of IL-1β mRNA kinetics in THP-1 cells stimulated with Stx1, LPS, and Stx1 + LPS. Differentiated THP-1 cells were treated and analyzed as described in the figure legend to Figure 1 except that IL-1β and GAPDH cDNA probes were used. a) Representative Northern blots of Stx1-, LPS-, and Stx1 + LPS-induced IL-1β mRNA. b) Mean intensities of percentage mRNA above basal expression for each time point ± standard error of the means from three independent experiments. A plus sign (+) denotes a significant difference ($P \leq 0.05$) between Stx1 and LPS treatments. A number sign (#) denotes a significant difference ($P \leq 0.05$) between Stx1 and Stx1 + LPS treatments.

b)

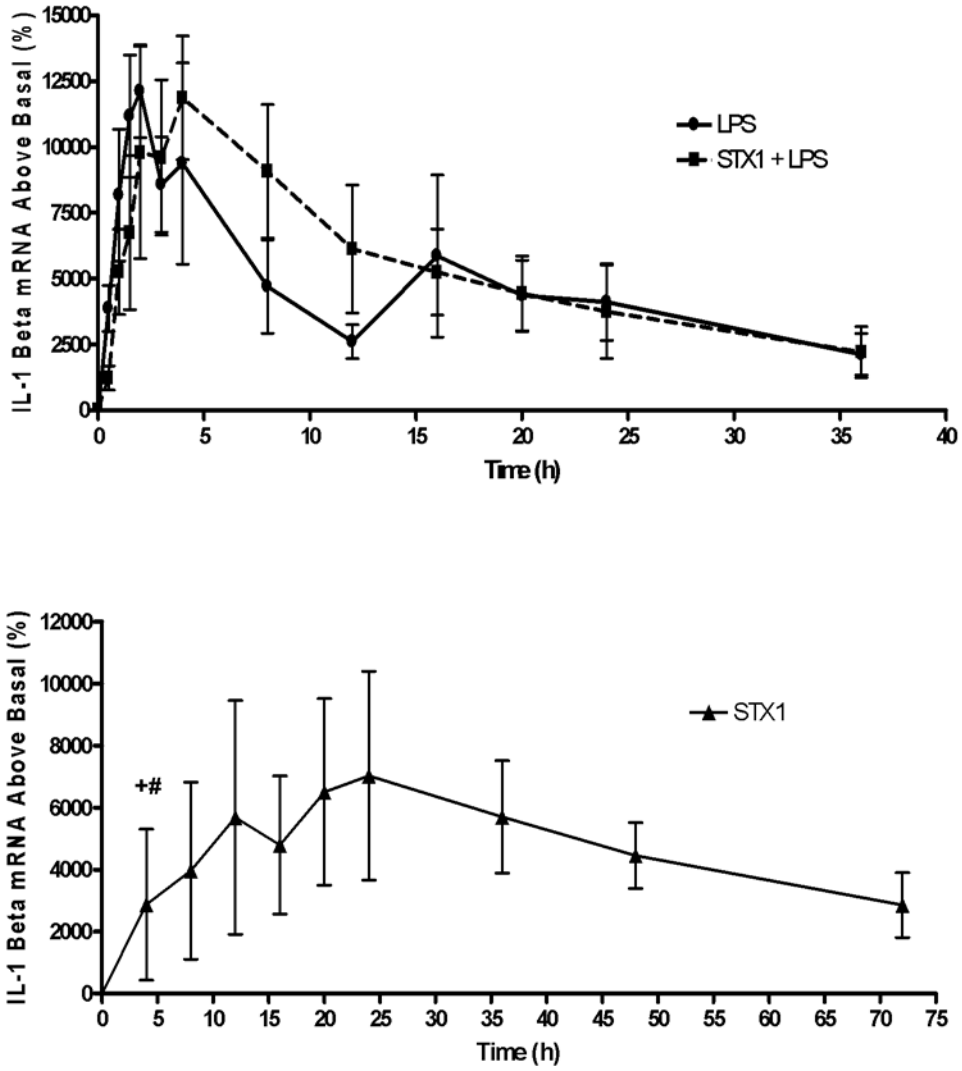

Figure 2 continued

attachment or cell viability associated with Stx1 and/or LPS treatment.

IL-1β protein production in THP-1 cells following Stx1, LPS, and Stx1 + LPS treatment. We previously showed that TNF-α elicited by Stx1 treatment of THP-1 cells was secreted into cell supernatants with maximal values of secreted TNF-α detected approximately 3 h after toxin stimulation (105). However, the kinetics of IL-1β protein production have not been determined in differentiated THP-1 cells treated with Stx1 in the presence or absence of LPS. To demonstrate that IL-1β transcripts were effectively translated in toxin treated cells, we measured IL-1β protein levels in cell supernatants using a sensitive (≈ 1.0 pg/ml) ELISA. The results shown in Figure 3 show that regardless of the stimulant used, IL-1β production increased over 72 h. The kinetics of IL-1β protein production correlated with IL-1β mRNA production for all the treatments, in that IL-1β mRNA production preceded IL-1β protein production. Consistent with levels of mRNA induction, Stx1 appeared to be a less potent inducer of IL-1β protein production and release compared to LPS alone or Stx1 + LPS ($p<0.001$ from 8 h to 72 h), although there appears to be a large discrepancy between IL-1β mRNA and protein production.

IL-1β mRNA and protein production in THP-1 cells requires the Stx1 A-subunit. To determine the possible requirement of Stx1 enzymatic activity in IL-1β production, we stimulated THP-1 cells for 24 h with 400 ng/ml or 800 ng/ml

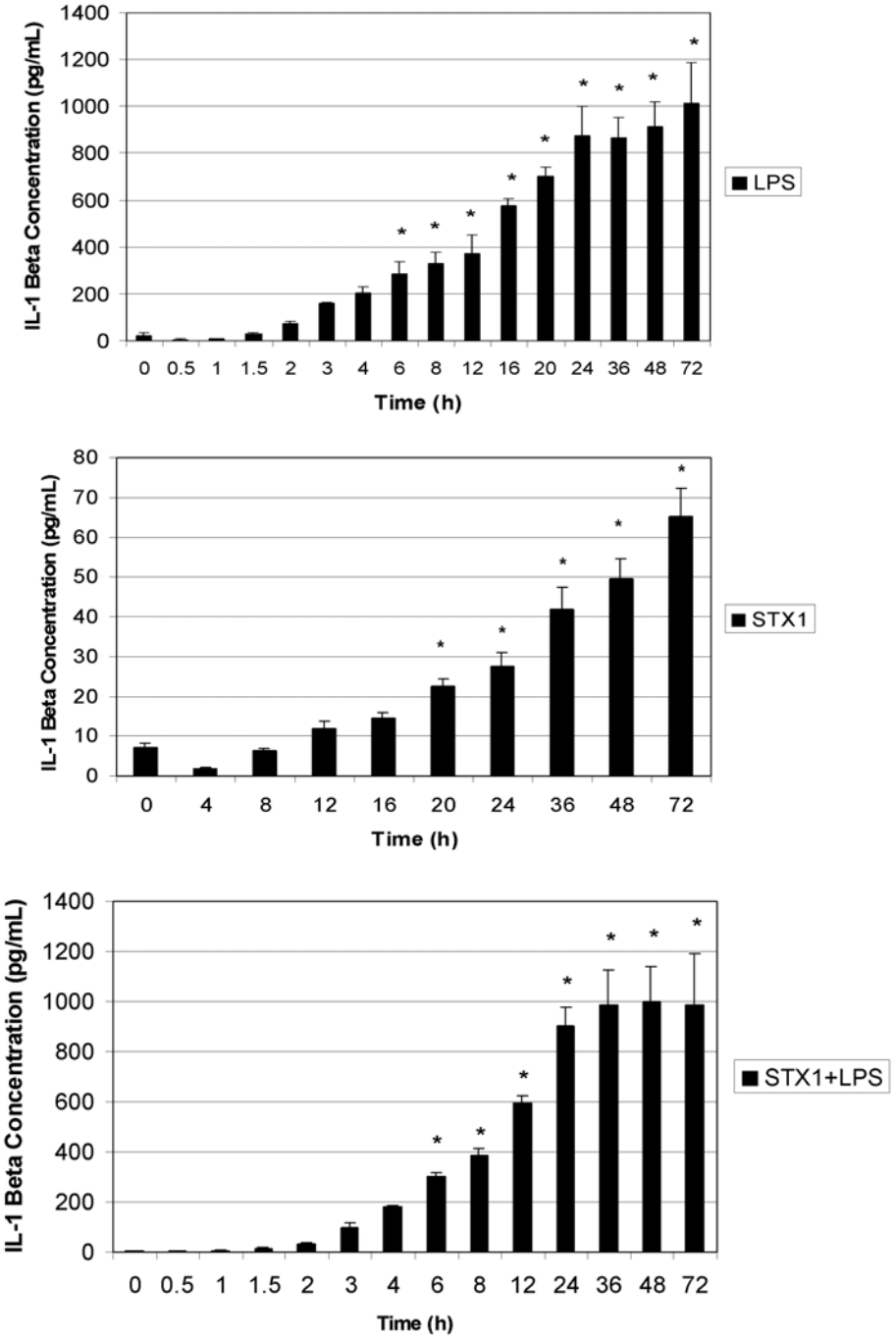

Figure 3. IL-1β protein production by THP-1 cells treated with Stx1, LPS, and Stx1 + LPS. Cell-free supernatants from a) LPS-treated, b) Stx1-treated, and c) Stx1 + LPS-treated cells were collected and analyzed using human IL-1β-specific ELISAs. Data shown are the means ± standard error of the means from triplicate determinations of three independent experiments. An asterisk (*) denotes a significant difference ($P \leq 0.05$) between unstimulated and treated cells.

of purified Stx1 B-subunit or 400 ng/ml of Stx1. Purified Stx1 B-subunit did not result in a significant increase of IL-1β protein over the control, suggesting that the presence of the A subunit may be necessary for IL-1β protein production (Figure 4a). Furthermore, treatment of differentiated THP-1 cells with Stx1 B-subunit did not result in the expression of IL-1β mRNA (Figure 4b).

mRNA stability of TNF-α and IL-1β transcripts induced by Stx1, LPS, and Stx1 + LPS. There are multiple regulatory mechanisms that may account for the prolonged elevation of TNF-α and IL-1β mRNA levels in THP-1 cells stimulated with Stx1 or Stx1 + LPS compared to treatment with LPS alone. We have previously shown that Stx1 treatment of THP-1 cells results in the activation of the ribotoxic stress response and the activation of transcriptional factors NF-κB and AP-1 (24,105). Prolonged activation of these factors may contribute to the phenomenon of elevated cytokine mRNA levels in toxin treated cells. Cytokine expression may also be regulated at post-transcriptional levels, and one of the main mechanisms of post-transcriptional control is regulation of transcript stability (103). Thus, the toxins may disrupt mechanisms that normally facilitate cytokine mRNA decay. We performed Northern blot analysis using the transcriptional inhibitor actD to compare the decay rates of TNF-α and IL-1β mRNAs in THP-1 cells stimulated with Stx1, LPS or Stx1 + LPS. Differentiated THP-1 cells were treated with either Stx1 or Stx1 + LPS for

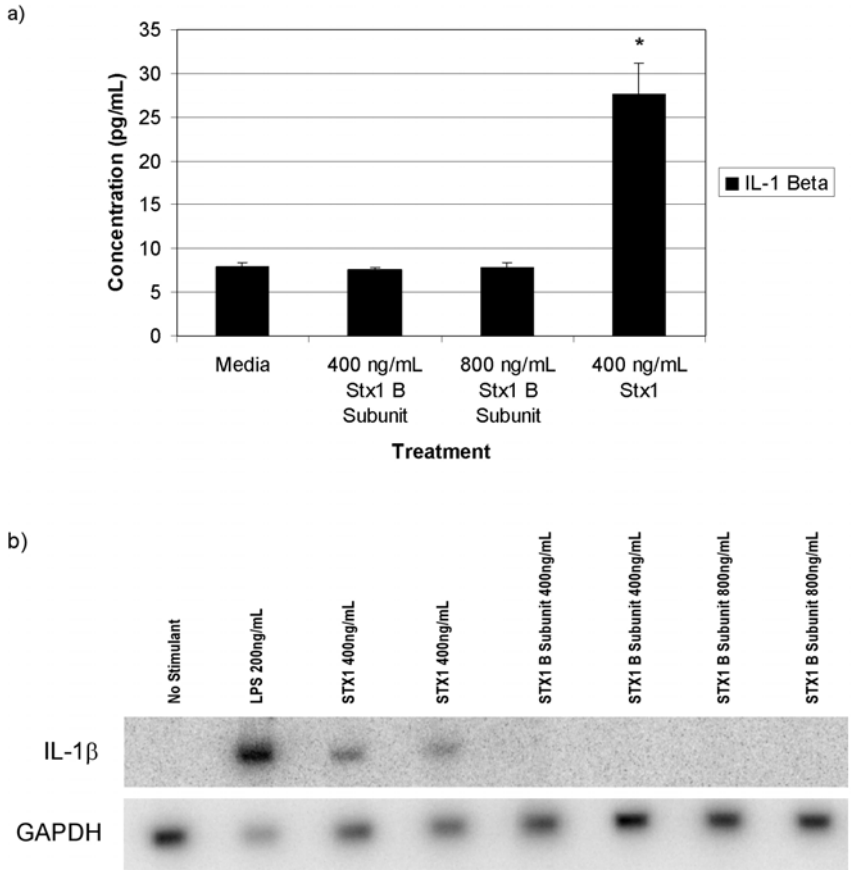

Figure 4. Purified Stx1 B-subunits alone do not induce IL-1β protein or mRNA production in THP-1 cells. Differentiated THP-1 cells (5 X 10^6 cells/mL) were treated with Stx1 B-subunits (400 or 800 ng/mL) for 24 h. a) Cell free supernatants were collected and human IL-1β-specific ELISAs were performed to detect secreted IL-1β. Media collected from untreated cells and cells treated with Stx1 (400 ng/mL) served as negative and positive controls, respectively. Data shown are means ± standard error of the means from triplicate determinations of three independent experiments. An asterisk (*) denotes a significant difference ($P \leq 0.05$) between unstimulated and treated cells. b) Fifteen micrograms of total RNA extracted from cells treated with LPS, Stx1, Stx1 B-subunits, and unstimulated cells were subjected to Northern blot analysis to detect IL-1β mRNA expression.

2h, or LPS for 1 h. ActD (5.0 μg/ml) was added to each plate for 15, 30, 60, 90, 120, and 150 min. The mRNA stability and loading control, GAPDH, showed a stable transcript over the time course of all experiments conducted, and allowed for normalization of TNF-α and IL-1β mRNA levels. Treatment of THP-1 cells with Stx1 or Stx1 + LPS resulted in TNF-α transcript levels that were significantly different from LPS-induced transcript levels ($p \leq 0.001$) after actD addition over time (Figures 5a, 5b). Half- lives for TNF-α transcripts induced by LPS, Stx1, and Stx1 + LPS treatments are shown in Table 1. Statistical analysis revealed that only the half-lives of TNF-α transcripts induced by Stx1 + LPS *vs.* LPS were significantly different ($p \leq 0.05$). For IL-1β transcripts in the presence of actD, Stx1 + LPS and Stx1 treatments resulted in significantly higher transcript levels compared to LPS treatment ($p \leq 0.001$ and $p \leq 0.005$, respectively) (Figures 6a, 6b). Half-lives for IL-1β transcripts induced by LPS, Stx1, and Stx1 + LPS treatments are shown in Table 1. Statistical analysis did not reveal significant differences in the half-lives of IL-1β transcripts induced by LPS *vs.* Stx1. Due to the parameters of the experiment, we cannot accurately estimate the half-life of IL-1β transcripts induced by Stx1 + LPS ($t_{½} > 150$ min).

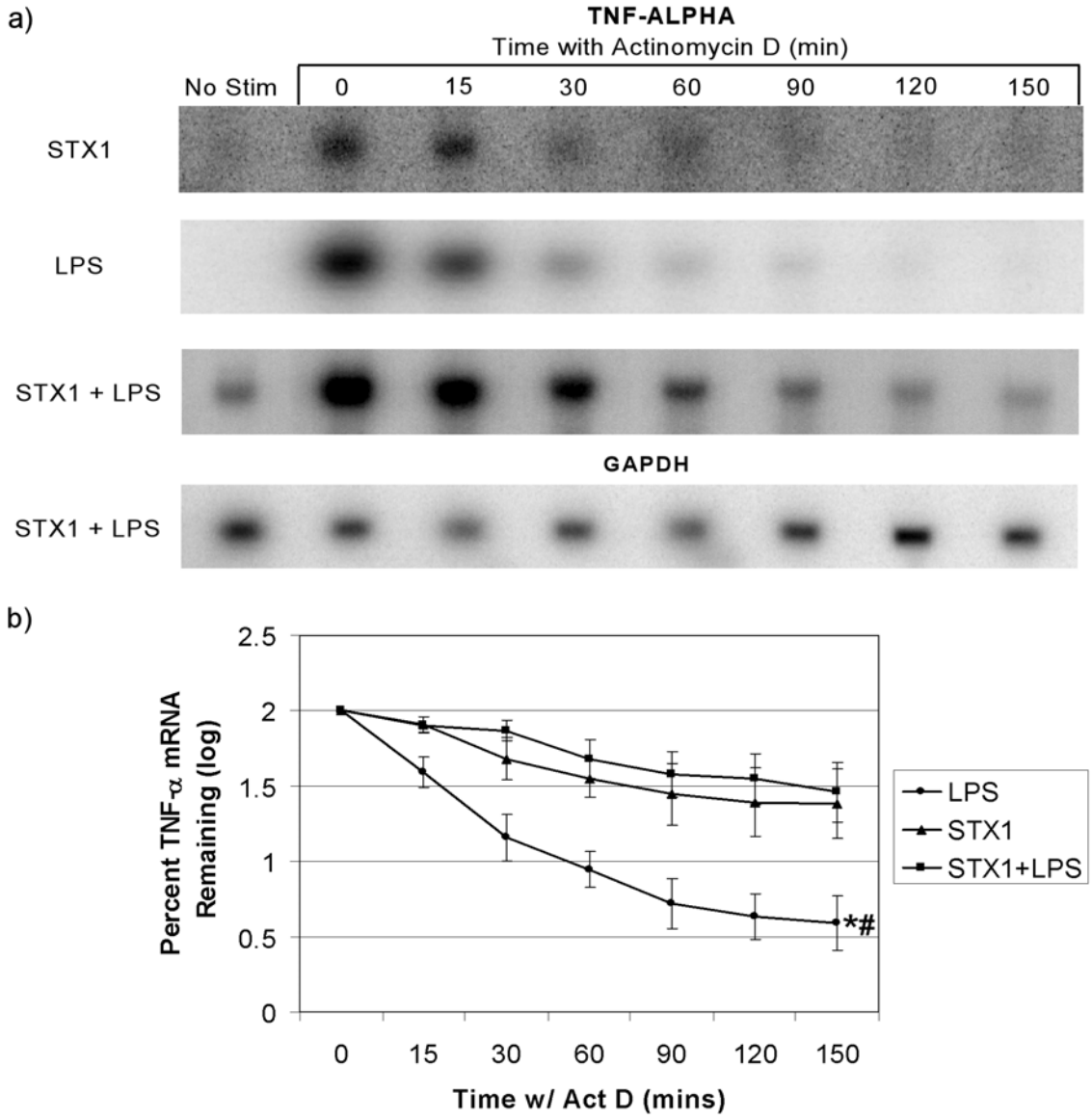

Figure 5. Effects of Stx1 and/or LPS on TNF-α mRNA stability in THP-1 cells. Differentiated THP-1 cells (5 X 10^6 cells/mL) were treated with LPS (200 ng/mL) for 1 h (●), Stx1 (400 ng/mL) for 2 h (▲), or both for 2 h (■). Actinomycin D (Act D) was then added to each plate at a final concentration of 5.0 μg/mL. Total RNA was isolated at each of the indicated time points after Act D addition. Northern blot analysis was performed, and TNF-α mRNA detected and quantitated using a phosphorimager. a) Representative Northern blots probed with ^{32}[P]-labeled TNF-α and GAPDH specific cDNA probes. b) Mean intensities of percentage TNF-α mRNA remaining (log) ± standard error of the means from three independent experiments. An asterisk (*) denotes a significant difference (P≤0.001) between Stx1+LPS and LPS treatments. A number sign (#) denotes a significant difference (P≤0.001) between Stx1 and LPS treatments.

Table 1. Estimated half-lives of TNF-α and IL-1β mRNA.

Treatment	Half-life (min)[a] of:	
	TNF-α mRNA	IL-1β mRNA
LPS	7.28 ± 5.12$^{*\#}$	114.39 ± 33.13
Stx1	75.86 ± 44.24$^{\#}$	175.60 ± 28.94
Stx1+LPS	101.63 ± 51.49*	ND[b]

[a] Significant differences ($P \leq 0.05$) between values for the different treatments with the same symbol are indicated by the * and # symbols.

[b] ND, not determined

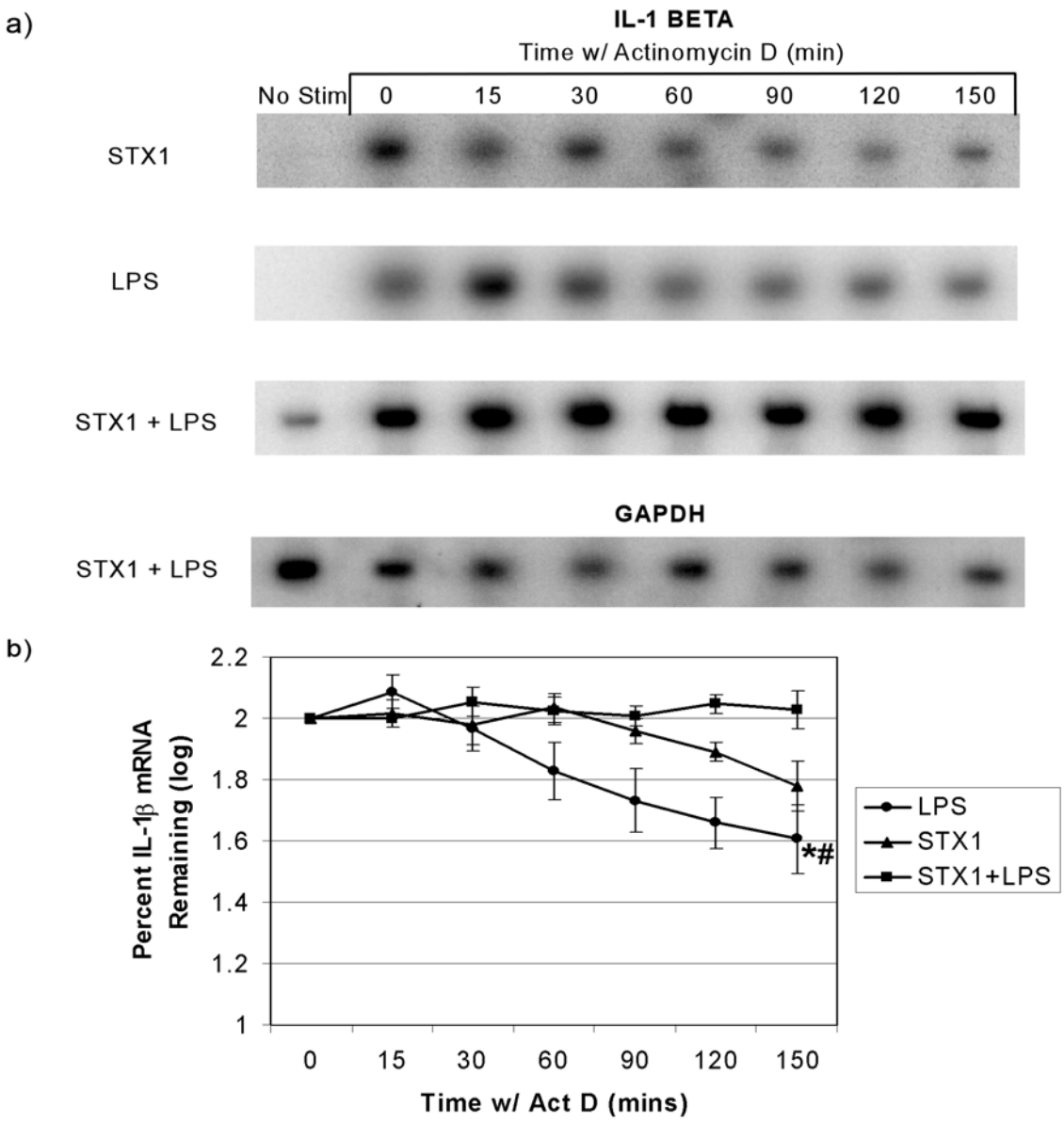

Figure 6. Effects of Stx1 and/or LPS on IL-1β mRNA stability in THP-1 cells. Differentiated THP-1 cells were treated and analyzed as in the figure legend to Figure 5 except that IL-1β and GAPDH specific probes were used. a) Representative Northern blots probed with ^{32}[P]-labeled IL-1β and GAPDH specific cDNA probes. b) Mean intensities of percentage IL-1β mRNA remaining (log) ± standard error of the means from three independent experiments. An asterisk (*) denotes a significant difference (P≤0.05) between Stx1+LPS and LPS treatments. A number sign (#) denotes a significant difference (P≤0.05) between Stx1 and LPS treatments.

Discussion

In addition to their critical roles in the innate host response and the induction of inflammation, TNF-α and IL-1β may also contribute to the pathogenesis of vascular damage that follows the systemic distribution of Stxs in the bloodstream. Our studies confirm earlier reports that LPS rapidly induce TNF-α and IL-1β transcripts in macrophages (11). In contrast to LPS, Stx1 is a less robust inducer of cytokine mRNA in terms of the kinetics of induction and total amount induced, although the transcripts remained elevated for a prolonged time (Figs. 1 and 2). Stx1 induction of maximal TNF-α and IL-1β mRNA expression was delayed (12 h and 24 h, respectively) compared to LPS-induced (0.5 h and 2 h) or Stx1 + LPS-induced (1 h and 4 h) maximal expression. The reason for the delay in induction of cytokine mRNAs by Stx1 is unknown, but may be attributable to the necessity for toxin internalization, retrograde transport, A-subunit processing, and translocation into the cytosol for toxin enzymatic activity. In contrast, LPS rapidly initiate transmembrane signaling events in macrophages through TLR4/MyD88 after binding to the cell surface receptor CD14 (12). When THP-1 cells were exposed to both the stimulants, we showed rapid mRNA induction characteristic of LPS treatment, and prolonged mRNA elevation characteristic of Stx1 treatment, suggesting that the bacterial

products may signal through separate pathways to elicit cytokine expression. The presence of both bacterial products in the bloodstream or inflammatory loci may optimize pro-inflammatory cytokine production. The kinetics data also suggest that TNF-α and IL-1β are differentially regulated. For all treatments, TNF-α mRNA reached maximal levels and returned to basal levels before IL-1β transcripts.

We previously showed that Stx1-induced TNF-α mRNA and protein expression were temporally correlated in that peak mRNA levels were reached at 2 h while peak protein levels were detected 3 h after toxin stimulation and remained elevated for up to 12 h. Compared to Stx1 stimulation, Stx1 + LPS treatment augmented TNF-α mRNA induction, resulting in 10-fold higher TNF-α protein levels detected in supernatants (105). We show here that the production of soluble IL-1β protein by THP-1 cells in response to Stx1 is very different. Although IL-1β mRNA was induced by Stx1 treatment, the levels of soluble IL-1β protein detected in cell supernatants (Fig. 3) were much less than predicted from the IL-1β transcript levels induced by Stx1 (Fig. 2b). IL-1β mRNA levels in THP-1 cells stimulated with Stx1 were roughly one half of the IL-1β mRNA levels in cells stimulated with LPS alone or Stx1+LPS. IL-1β protein levels, however, were 20-fold less in THP-1 cells treated with Stx1 compared to cells treated with LPS alone or Stx1 + LPS. The precise reason for the

discrepancy between Stx1-induced IL-1β mRNA and protein levels is unclear. An obvious explanation is that Stx1 inhibits protein synthesis. However, we have previously shown that, at the concentrations used in this study, Stx1 mediated a modest (≈ 10%) reduction in total protein synthesis in differentiated THP-1 cells (23). An alternative explanation is that Stx1 may affect post-translational processing and release mechanisms necessary for IL-1β expression that are not required for secretion of TNF-α. The 26 kDa membrane-associated form of TNF-α is cleaved to a 17 kDa form by the action of the metalloproteinase disintegrin (4,83). ProIL-1β, the 35 kDa precursor form of IL-1β, is cleaved to the active 17 kDa form by the cysteine-dependent aspartate-specific proteases caspase-1 and caspase-5 which form part of a high molecular weight complex called the inflammasome (76). Recently, Greenwell-Wild *et al.* (34) reported that infection of macrophages with *Mycobacterium avium* elicited IL-1β mRNA expression, but not IL-1β protein secretion. Failure to release soluble IL-1β was associated with reduced caspase-1 activity and reduced expression of inflammasome constituents. Whether Stxs similarly affect inflammasome function and post-translational processing mechanisms necessary for IL-1β secretion remain to be clarified. The presence of LPS, however, appears to restore IL-1β processing, as the levels of soluble IL-1β released in response to LPS *vs.* Stx1 + LPS are comparable. LPS signaling occurs earlier than Stx1

signaling, probably because Stx1 needs to be transported into the cell in order to elicit its effects. Thus, LPS-mediated signaling leading to the release of IL-1β may occur prior to Stx-mediated signaling events.

The contribution of Stx B-subunits in various biological activities may differ. For example, purified Stx1 B-subunits were reported to trigger apoptosis of Burkitt's lymphoma B-cell lines (75), while apoptosis induction of other cell types requires holotoxin. Earlier studies have suggested that Stx enzymatic activity is essential for IL-8 and TNF-α expression (23,137,147). Our data support a role for Stx1 A-subunit in IL-1β mRNA and protein production since no elevations in IL-1β mRNA or protein above unstimulated controls are detected when cells are treated with purified Stx1 B subunits (Fig. 4).

Excessive or prolonged expression of the cytokines TNF-α and IL-1β may lead to deleterious effects such as vascular leak syndrome and hypovolemic shock, coagulopathies, and the development of autoimmune diseases. Therefore, it is not surprising that TNF-α and IL-1β expression are tightly regulated at transcriptional, post-transcriptional and post-translational stages. We previously demonstrated that Stx1, like other protein synthesis inhibitors acting on the 28S rRNA (24,47), induces the ribotoxic stress response (24). Downstream substrates of JNK and p38 MAPK cascades are known to be transcriptional activators of TNF-α and IL-1β gene expression. Nuclear lysates prepared from Stx1-treated

THP-1 cells contained increased levels of proteins capable of binding oligonucleotides with NF-κB and AP-1 binding sites (105). Collectively, these data suggested that the Stxs regulate cytokine expression at a transcriptional level. The kinetic analyses in this study suggest that Stx1 has a regulatory effect on TNF-α and IL-1β mRNA stability since cytokine steady state transcripts from both Stx1- and Stx1 + LPS-treated cells remain elevated longer compared to LPS-induced transcripts. To determine whether Stx1 regulated TNF-α and IL-1β mRNA levels at a post-transcriptional stage, we determined the decay rates of transcripts induced by Stx1, LPS, or Stx1 + LPS (Figs. 5 and 6). The combined kinetics and mRNA stability data suggest that when Stxs and LPS are present following infection with Stx-producing bacteria, TNF-α transcript levels may be maximally increased, *i.e.,* superinduced, via alterations in transcriptional and post-transcriptional control mechanisms. Interestingly, this phenomenon has been described for chemokine mRNAs following treatment of the human intestinal epithelial cell line HCT-8 with Stx1 (137). Our studies on the regulation of IL-1β transcript expression produced different results. Treatment of cells with LPS or Stx1 + LPS resulted in similar levels of steady state transcripts, *i.e.*, IL-1β mRNA was not superinduced by Stx1 + LPS. However, the half-life of IL-1β transcripts induced by Stx1 + LPS appeared to be greater than that induced by LPS or Stx1 alone.

The precise mechanisms by which Stxs regulate cytokine transcript levels remain to be fully characterized, but it is known that many post-transcriptional control mechanisms map to the AU-rich elements (ARE) found within the 3'-UTRs of cytokine transcripts (6). Binding of proteins within the ARE may regulate transcript processing and translation in different ways. For example, binding of proteins within the TNF-α ARE may facilitate nuclear export of transcripts into the cytoplasm (13). Binding of the zinc finger proteins tristetraprolin or butyrate response factors to TNF-α ARE leads to increased mRNA deadenylation and degradation of the body of the transcript (7,61,62,123). Interaction of the RNA-binding proteins TIA-1 and TIAR with the TNF-α ARE results in translational silencing (36,95) via a mechanism which sequesters TNF-α mRNA in cytoplasmic ribonucleoprotein complexes called stress granules (57). Experiments to further characterize the mechanism(s) of Stx-mediated cytokine mRNA stabilization are planned.

Why some patients develop uncomplicated bloody diarrhea and others progress to life-threatening sequelae is not understood. Our data suggest that the presence of both Stxs and endotoxin in the bloodstream may be a predictor of progression to systemic disease.

CHAPTER III

CHEMOKINE EXPRESSION IN THE MONOCYTIC CELL LINE THP-1 IN RESPONSE TO PURIFIED SHIGA TOXIN 1 AND/OR LIPOPOLYSACCHARIDES

Overview

Infections with Shiga-toxin (Stx)-producing bacteria are associated with bloody diarrhea and post-diarrheal sequelae including the hemolytic uremic syndrome (HUS) and central nervous system (CNS) abnormalities. Stx-induced intestinal, renal, and CNS vascular lesions may involve localized production of proinflammatory cytokines in target organs, as tumor necrosis factor-α (TNF-α) and interleukin-1β (IL-1β) up-regulate Stx receptor globotriaosylceramide (Gb_3) expression on vascular endothelial cells. However, leukocyte recruitment to injured sites may also exacerbate vascular damage. Cytokine macroarray analysis of transcripts derived from macrophage-like THP-1 cells treated with Stx1, lipopolysaccharides (LPS), or both, demonstrated consistent up-regulation of *TNF-α*, *IL-1β*, and four genes encoding the chemokines interleukin-8 (IL-8), macrophage inflammatory protein-1α (MIP-1α), MIP-1β, and growth related oncogene-β (GRO-β). Real-time PCR analysis verified the macroarray results.

Northern blot analyses following addition of the transcriptional inhibitor actinomycin D revealed increased IL-8 mRNA stability in THP-1 cells treated with Stx1 or Stx1 + LPS. Finally, ELISA data from Stx1 + LPS-treated cells demonstrated a poor correlation between IL-8, MIP-1α, MIP-1β, and GRO-β mRNA levels and protein production, indicating a post-transcriptional regulatory effect. Our data suggest that in response to Stx1 and LPS, macrophages may be a source of chemokines that promote tissue damage through leukocyte recruitment and activation.

Introduction

Infections with *Shigella dysenteriae* serotype 1 and Shiga toxin (Stx)-producing *E. coli* (STEC) may result in bloody diarrhea and the subsequent development of life-threatening sequelae including acute renal failure and neurological abnormalities (92,97). The acute renal failure caused by Stxs is referred to as the hemolytic uremic syndrome (HUS) and is characterized by thrombotic microangiopathy with the swelling and detachment of glomerular endothelial cells from the basement membrane and the intraluminal deposition of platelet-fibrin thrombi within glomerular capillaries, hemolytic anemia with the formation of schistocytes (fragmented erythrocytes) and thrombocytopenia (82,104). Similar vascular lesions may occur in the brain, leading to lethargy,

disorientation, paralysis, seizures, coma and death (116). The pathogenesis of bloody diarrhea caused by Stx-producing bacteria is multifactoral. For example, *S. dysenteriae* serotype 1 are invasive organisms, and invasion of colonic epithelium is a critical virulence determinant (110). Fontaine *et al.* constructed a *S. dysenteriae* serotype 1 toxigenic/atoxigenic isogenic pair and showed that rhesus monkeys fed either one of the pair developed fulminant dysentery (21). However, the animals fed the toxin-producing strain had more blood in the stool and increased destruction of capillaries within the connective tissue of the colonic mucosa. Toxin mediated damage to intestinal blood vessels may create the means of access of Stxs and other bacterial constituents, such as bacterial lipopolysaccharides (LPS), into the bloodstream. Thus, Stxs appear to be important contributory virulence factors in prodromal hemorrhagic colitis. In contrast to intestinal disease, Stxs are essential for the development of HUS and neurological complications, as many of the histopathological features of renal and CNS vascular damage seen in humans can be reproduced in animals following the administration of purified Stxs (84).

Along with *E. coli* heat-labile enterotoxins, cholera toxin, and pertussis toxin, the Stxs are members of the AB_5 holotoxin family, all of which possess a single, enzymatically active A-subunit in non-covalent association with five B-subunits (18,25). The Stx family consists of the prototypical Shiga toxin expressed by *S. dysenteriae* serotype 1, and Shiga toxin 1 (Stx1) and Shiga toxin 2

(Stx2) produced by STEC. Stx1 is essentially identical to Shiga toxin, while Stx2 is only ≈56% homologous to Shiga toxin/Stx1 at the deduced amino acid sequence level (87). A number of Stx1 and Stx2 sequence variants have been characterized (79). The B-subunits form a pentameric ring and mediate toxin binding to the glycolipid receptor globotriaosylceramide (Gb_3; (65,49,68). Stxs enter cells through receptor-mediated endocytosis and undergo retrograde transport through the Golgi apparatus to reach the endoplasmic reticulum (ER) and nuclear membrane (49,67,107). During retrograde trafficking, the A-subunit is proteolytically cleaved by furin or a furin-like protease, but the two A-subunit fragments remain covalently attached through a disulfide bond (26,49). The ER membrane is thought to be the site of disulfide bond reduction and translocation of the 27 kDa A_1-fragment into the cytoplasm (49,108). The *N*-glycosidase activity of the A_1-fragment cleaves a specific adenine residue from the 28S rRNA of eukaryotic ribosomes, thereby blocking peptide elongation and inhibiting protein synthesis (16,111).

Studies utilizing human endothelial cells derived from large venous sources showed that Stxs possess minimal direct cytotoxicity for the cultured cells (88,134). In the presence of the proinflammatory cytokines TNF-α or IL-1β, however, Stx-mediated endothelial cell cytotoxicity increased significantly (71,134), and TNF-α and IL-1β were shown to up-regulate the expression of Gb_3

on endothelial cells (15,98,139,142). Endothelial cells do not appear to be a major source of TNF-α or IL-1β synthesized in response to Stxs (130). Our studies indicate that the innate immune response triggered by the interaction of Stxs with macrophages may play a key role in pathogenesis of HUS and CNS pathology by providing the cytokines necessary to sensitize vascular endothelial cells to the action of the toxins (99).

In addition to proinflammatory cytokines, chemokines may also play a role in the pathogenesis of disease caused by Stx-producing bacteria. Neutrophil migration into the intestinal lumen is a hallmark of many inflammatory diseases of the gastrointestinal tract, including those mediated by *Shigella dysenteriae* serotype 1 and STEC (119). Purified Stxs have been shown to directly induce the expression of the neutrophil chemoattractant interleukin-8 (IL-8 or CXCL8) by human intestinal epithelial cells (136,147). Studies using an *in vitro* model of basolateral-to-apical neutrophil transmigration across a polarized epithelial cell monolayer demonstrated increased paracellular permeability with a concomitant increase in apical-to-basolateral movement of Stxs across the monolayer (44). Treatment of intestinal epithelial cells with Stx1 results in stabilization of IL-8 mRNA, which may lead to prolonged IL-8 production and secretion, and increased neutrophil infiltration into the intestine (137). Finally, IL-8 and monocyte chemoattractant protein-1 (MCP-1 or CCL2) have been

detected in the urine and serum of some HUS patients (141), suggesting that chemokines are expressed following hematogenous dissemination of Stxs.

The role in pathogenesis of chemokines expressed by macrophages in response to Stxs and LPS has not been extensively studied. Non-adherent human blood monocytes were shown to express IL-8 in response to treatment with Stxs (140), but monocytes may not accurately represent the activities of tissue macrophages populating the lamina propria, kidneys and CNS. The human monocytic cell line THP-1 may be differentiated to a mature macrophage-like state, and possesses many of the physiological properties of primary monocyte-derived macrophages (2). In this study, we utilized macroarrays spotted with 268 cytokine and chemokine cDNAs to investigate the chemokine response of differentiated, macrophage-like THP-1 cells treated with purified Stx1, LPS or both. Real time PCR and Northern blot analyses were used to confirm the macroarray results and to examine the kinetics of IL-8 transcript expression, respectively. We examined the relative stabilities of IL-8 transcripts induced by Stx1, LPS, or both. Finally, we examined the synthesis and secretion of chemokines by Stx1 and/or LPS treated THP-1 cells.

Materials and Methods

Cells and toxins. The human myelogenous leukemia cell line THP-1 (138) was obtained from the American Type Culture Collection; Rockville, MD. The cells were maintained in RPMI 1640 (Invitrogen; Carlsbad, CA) supplemented with 10% fetal bovine serum (FBS; Hyclone Laboratories; Logan, UT), penicillin (100 U/ml) and streptomycin (100 μg/ml) at 37°C in 5% CO_2 in a humidified incubator. Stx1 was expressed from the recombinant *E. coli* DH5α(pCKS112) strain which harbors a plasmid containing the *stx1* operon under control of a thermoinducible promoter (131). Stx1 in bacterial lysates was purified by sequential ion-exchange, chromatofocusing, and immunoaffinity chromatography. Prior to use, Stx1 preparations were shown to contain < 0.1 ng endotoxin/ml by *Limulus* amoebocyte lysate assay. Purified lipopolysaccharides (LPS) derived from *E. coli* O111:B4 were purchased from Sigma Chemical Co. (St. Louis, MO).

Macrophage differentiation and stimulation. The mature macrophage-like state was induced by treating THP-1 cells (10^6 cells per ml) for 48 h with 50 ng/ml phorbol 12-myristate 13-acetate (PMA; Sigma Chem. Co., St. Louis, MO) in culture dishes. Differentiated, plastic-adherent cells were washed twice with cold, sterile Dulbecco's phosphate-buffered saline (PBS; Sigma) and incubated with fresh medium without PMA containing 10% FBS, penicillin (100 U/ml) and

streptomycin (100 μg/ml). The medium was changed every 24 h over the next three days. Experiments were performed on the fourth day following PMA removal. For all experiments, differentiated cells were treated with Stx1 (400 ng/ml), LPS (200 ng/ml), or Stx1 + LPS (400 ng/ml and 200 ng/ml, respectively) for varying times. We previously demonstrated that these stimulant doses produced maximal cytokine protein secretion in differentiated THP-1 cells *in vitro* (99).

Macroarrays. The Atlas Human Cytokine/Receptor cDNA expression arrays (Clontech; Palo Alto, CA), containing 268 immobilized human cDNAs, housekeeping controls, and negative controls in duplicate dots on nylon membranes were used to detect cytokine and chemokine genes regulated by Stx1 and/or LPS. Approximately 10 x 10^6 differentiated THP-1 cells were plated in 100 mm cell culture plates and treated with Stx1, LPS, or Stx1 + LPS for 2 or 6 h. Total RNA was isolated, DNase treated as *per* the manufacturer's instructions, and stored at -70°C until used. In accordance with the manufacturer's protocol, the Atlas arrays were pre-hybridized at 68°C for 1 h with continuous agitation in ExpressHyb pre-hybridization solution containing 100 μg/ml sheared salmon testes DNA (previously boiled for 5 min and chilled on ice prior to addition to the pre-hybridization solution). During the pre-hybridization step, 2-5 μg total RNA was converted to ^{32}P-labeled cDNA using

the Atlas Pure Total RNA labeling system (Amersham Pharmacia Biotech Inc., Piscataway, NJ). Unincorporated ^{32}P-labeled nucleotides were removed by column chromatography using the spin columns provided by the Atlas Pure Total RNA labeling system. C_0t-1 DNA was added to labeled probe to reduce background hybridization to repetitive DNA sequences prior to probe addition to the hybridization solution. The probe was allowed to hybridize overnight at 68°C with continuous agitation. Blots were then washed with 100 ml of pre-warmed wash solution I (2x SSC, 1% SDS) for 30 min at 68°C three times, followed by one wash with 100 ml of pre-warmed wash solution II (0.1x SSC, 0.5% SDS) at 68°C for 30 min. A final 5 min wash was performed with 100 ml wash solution III (2x SSC) at RT. The Atlas arrays were then removed, wrapped in plastic, and exposed to X-ray film at -70°C with an intensifying screen. Screens were scanned using a Phosphorimager (Molecular Dynamics, Sunnyvale, CA) to visualize up- or down-regulated genes. Data were quantitated using the ImageQuant Software (Molecular Dynamics). The experiments were performed in duplicate using GAPDH for normalization. The complete gene list for the Atlas Human Cytokine/Receptor cDNA Expression Array (#7744-1) may be viewed at www.bdbiosciences.com/clontech/atlas/genelists/index.shtml.

Real-time PCR. Total RNA was isolated using the RNeasy Mini Kit

(Qiagen; Valencia, CA) with an RNase-free DNase (Qiagen) treatment for 30 min. According to the manufacturer's instructions, RNA was reverse transcribed to cDNA using the TaqMan Reverse Transcription Reagents, and real-time PCR was performed on the resulting cDNAs using the SYBR Green I double-stranded DNA binding dye (Applied Biosystems; Foster City, CA). Real-time primers specific for MIP-1α (SICA3), MIP-1β (SICA4), GRO-β (GRO-2), IL-8, and GAPDH were designed using the Primer Express software (Applied Biosystems), and are listed in Table 2. The real-time reactions were carried out using 100 nM of forward and reverse primers in a total volume of 25 μl. In order to control for the presence of contaminating DNA in the real-time reactions, reverse transcriptase-negative reactions were run. Template-negative controls were also run in order to test for DNA-contaminated primers. Real-time reactions were run and analyzed using the ABI PRISM 7500 Sequence Detection System (Applied Biosystems). Dissociation curves for PCR samples were made through an additional denaturation step at 95°C for 15 s, annealing at 60°C for 20 s, and a slow increase in temperature back to 95°C with a ramp time of 19 min, 59 s to guarantee amplification of the correct genes. Fold induction of mRNA was determined from the threshold cycle values normalized for GAPDH expression and then normalized to the value derived from cells at time zero, prior to media change, or treatment.

Table 2. Real-time PCR primer sequences.[a]

mRNA	Primer[b]
MIP-1α	F, 5′ TTGTGATTGTTTGCTCTGAGAGTTC 3′
	R, 5′ CGGTCGTCACCAGACACACT 3′
MIP-1β	F, 5′ CCCTGGCCTTTCCTTTCAGT 3′
	R, 5′ AGCTTCCTCGCGGTGTAAGA 3′
GRO-β	F, 5′ CTGCCCTTACAGGAACAGAAGAG 3′
	R, 5′ CAAACACATTAGGCGCAATCC 3′
IL-8	F, 5′ AAGGAACCATCTCACTGTGTGTAAAC 3′
	R, 5′ ATCAGGAAGGCTGCCAAGAG 3′
GAPDH	F, 5′ CAACGGATTTGGTCGTATTGG 3′
	R, 5′ GGCAACAATATCCACTTTACCAGAGT 3′

[a] Primers were designed using the Primer Express software as described in Materials and Methods.

[b] F, forward; R, reverse.

Northern blot analysis. To determine IL-8 mRNA kinetics and decay rates, differentiated THP-1 cells were treated with stimulants in the presence or absence of the transcriptional inhibitor actinomycin D (act D, Sigma) using the protocol of Harrold *et al*. (39). Based on the IL-8 mRNA kinetics data in this study, 5.0 μg/ml act D were added to cells 1 h after treatment with LPS or Stx1 + LPS, or 6 h after Stx1 treatment. Two 1.0 ml aliquots of all cell supernatants were collected and stored at –20°C for use in ELISAs (see below). Total RNA from cells was extracted using the TRIzol Reagent (Invitrogen) protocol for cell monolayers. Following extraction, total RNA samples (up to 15 μg) were electrophoresed into 1.0% agarose-formaldehyde gels at 50 V for 1.5 h and then transferred to positively charged nylon membranes using the Turboblotter apparatus (Schleicher & Schuell, Keene, NH) for at least 3 h. Transferred RNA was cross-linked to membranes using a UV cross-linker (Bio-Rad; Hercules, CA). Membranes were washed in 2X SSC + 0.5% SDS for 30-60 min, and then pre-hybridized at 42°C for at least 3 h in a 10 ml hybridization solution containing 980 μg salmon testes DNA (9.8 mg/ml, Sigma), 2X SSC, 50% Formamide (Sigma), 10% SDS, 5X Denhardt's Solution (Invitrogen), in DEPC-treated water. The human IL-8 cDNA probe was the kind gift of Dr. Cheleste Thorpe, Division of Geographic Medicine and Infectious Diseases, Department of Medicine, Tufts – New England Medical Center, Boston, MA. Prior to pre-

hybridization, IL-8 plasmid DNA was digested with EcoRI (New England Biolabs, Beverly, MA) to yield a 500 bp fragment containing 365 bp of the IL-8 gene in addition to a portion of the polyA$^+$ tail. Restriction fragments were visualized following electrophoresis of the digests into 1.2% agarose gels containing ethidium bromide. The 500 bp fragment was excised and purified using the QIAquick Gel Extraction Kit (QIAGEN). During the last hour of pre-hybridization, the IL-8 cDNA fragment was resuspended in 10 mM Tris-1mM EDTA (TE) pH 8 to a total volume of 45 µl for use in [α^{32}P]-dCTP random prime labeling reactions employing the Rediprime II kit (Amersham Pharmacia Biotech Inc.; Piscataway, NJ). A 316 bp human glyceraldehyde-3-phosphate dehydrogenase (GAPDH) DNA probe (Ambion Inc.; Austin, TX) was random prime labeled using the Rediprime II kit to detect GAPDH mRNA that served as an mRNA stability control as well as a loading control. Following labeling, unincorporated [α^{32}P]-dCTP was removed using TE-Midi-Select D G-50 Sephadex columns (Shelton Scientific; Shelton, CT). The labeled probes were ready to use after boiling for 5 min. ^{32}P-labeled probes were added to the hybridization solution overnight at 42°C. After hybridization, blots were rinsed with 2X SSC, washed twice with 2X SSC + 1.0% SDS for 15 min at room temperature, and then washed once with 0.1X SSC + 1.0% SDS for 30 min at 60°C. Blots were dried briefly prior to exposure to a Phosphorimager screen and

analyzed using a Phosphorimager (Molecular Dynamics). Membranes were stripped by boiling in 0.1X SSC + 0.1% SDS twice for 15 min and sequentially re-probed with the GAPDH probe at 42°C. Quantitation of pixel intensities of the RNA bands was done using ImageQuant software (Molecular Dynamics). All of the RNA data were normalized by dividing the IL-8 band intensities by the corresponding GAPDH band intensities at each time point. Kinetics data were then expressed as percentage IL-8 mRNA above basal as determined by:

$$\frac{[\text{intensity stimulated cells} - \text{intensity unstimulated cells}]}{[\text{intensity unstimulated cells}]} \times 100$$

mRNA decay data were expressed as percent of IL-8 mRNA remaining as determined by:

$$\frac{[\text{intensity stimulated cells with actD for t=n}]}{[\text{intensity stimulated cells with actD for t=0}]} \times 100$$

where n equals time of actD exposure, so that when n=0, percent of IL-8 mRNA remaining equals 100.

Chemokine ELISAs. Quantitation of secreted IL-8, MIP-1α, and MIP-1β protein concentrations were carried out using the corresponding R&D Systems (Minneapolis, MN) Quantikine Colorimetric Sandwich ELISA Assay Kits. GRO-β protein concentrations were determined using the TiterZyme EIA human GRO-β Enzyme Immunometric Assay Kit from Assay Designs, Inc. (Ann Arbor, MI). Cellular debris was removed from the supernatants of treated cells by

centrifugation. Dilutions of Stx1, LPS, and Stx1 + LPS samples were made, when necessary, and the kit-specified volumes of each sample were added, in triplicate, to the ELISA plate wells. The manufacturer's protocol was followed, and A_{450} and A_{570} were measured on a microtiter plate reader (Dynatech MR5000; Dynatech Laboratories; Chantilly, VA). Chemokine protein concentrations were calculated based on a standard curve. The assay sensitivities were 4 pg/ml (IL-8), 10 pg/ml (MIP-1β), < 10 pg/ml (MIP-1α), and 20.5 pg/ml (GRO-β).

Statistics. Statistics for experiments were performed with the SAS statistics program (SAS Institute; Cary, NC) or Excel (Microsoft Corporation; Redmond, WA). Real-time PCR fold inductions and IL-8 mRNA kinetics were analyzed using two-way ANOVAs with the Duncan multiple range test for post-hoc comparisons. IL-8 mRNA levels in decay experiments, and IL-8, MIP-1α, MIP-1β, and GRO-β protein kinetics were analyzed using one-way ANOVAs with the Duncan multiple range test used for post-hoc analysis. For mRNA half-lives, the calculated half-lives were analyzed using the Student's t-test on Excel, to compare IL-8 mRNA half-lives in LPS and Stx1 treated cells. P values ≤ 0.05 were considered significant for the all analyses. All data are presented as means and standards errors of the means from a compilation of at least three independent experiments.

Results

Macroarray analysis of cytokine and chemokine gene expression in Stx1-, LPS-, and Stx1 + LPS-treated THP-1 cells. Cytokine gene expression analysis was performed on differentiated THP-1 cells following incubation with Stx1, LPS, and Stx1 + LPS for 2 or 6 hours. Total RNA isolated from treated and untreated cells were converted to ^{32}P-labeled cDNA probes and hybridized to identical arrays overnight (Fig. 7). Hybridization intensities were determined using a phosphorimager and normalized to the internal control GAPDH. Fold induction of genes from treated cells were calculated based on hybridization intensities from untreated cells. Using the protocol of Rosenberger *et al*., genes with fold inductions ≥2 were considered significantly up- or down-regulated (102). Changes in the expression of cytokine and chemokine transcripts following treatment of differentiated THP-1 cells with Stx1 and/or LPS are summarized in Table 3. Only six genes were consistently up-regulated at least 2-fold for most of the treatments. These genes encoded MIP-1α (SICA3 or CCL3), MIP-1β (SICA4 or CCL4), TNF-α, IL-1β, IL-8, and GRO-β (GRO-2 or CXCL2). The only exceptions were IL-1β and IL-8 expression for the 2 h Stx1 treatment where fold inductions were < 2. The up-regulated chemokines are classified as either CC or CXC chemokines, which primarily attract monocytes or neutrophils, respectively, to sites of infection. As previously noted for TNF-α

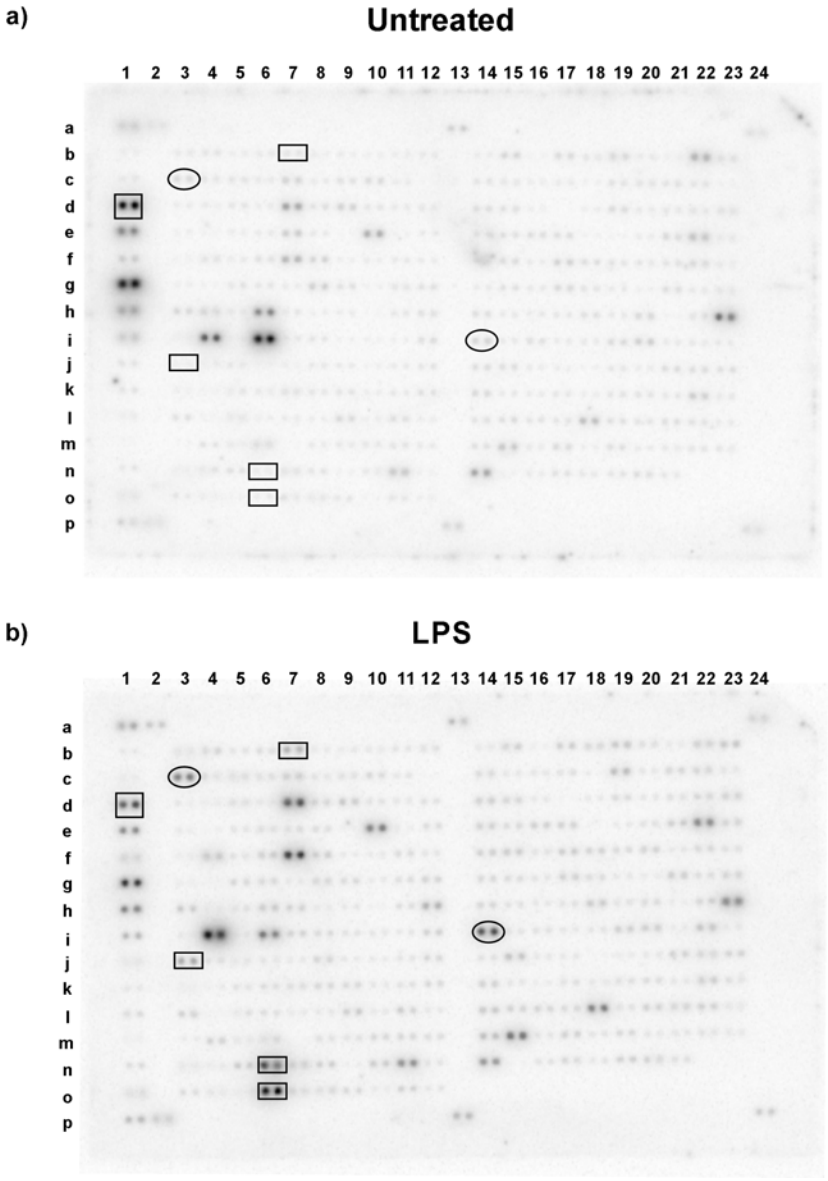

Figure 7. Differential gene expression by THP-1 cells following treatment with Stx1, LPS, or Stx1+LPS measured by gene arrays. Differentiated THP-1 cells were (a) unstimulated, (b) treated with 200 ng/ml LPS, (c) treated with 400 ng/ml Stx1, or (d) treated with Stx1+LPS for 6 h. Total RNA was isolated and converted into a ^{32}P-labeled cDNA probes using reverse transcriptase. Probes were hybridized to the membranes containing cDNAs derived from 268 cytokine and chemokine genes spotted in duplicate. Hybridization was detected using a phosphorimager. Paired spots within the squares correspond to the GAPDH internal control (position 1d on membranes). Pairs of spots identified by circles correspond to IL-1β (position 3c) and TNF-α (position 14j). Pairs of spots identified by rectangles correspond to MIP-1α (position 6n), MIP-1β (position 6o), GRO-β (position 7b), and IL-8 (position 3j).

Figure generated by Christel van den Hoogen.

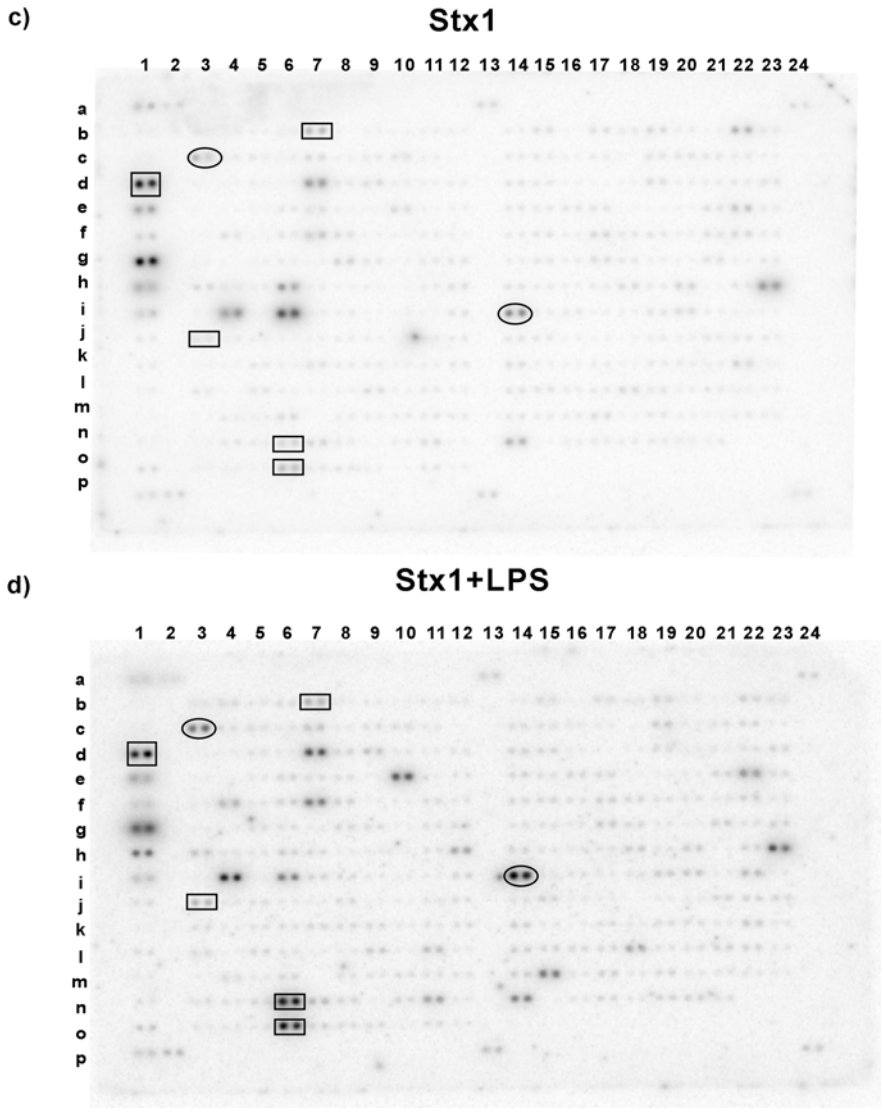

Figure 7 continued

Table 3. Fold inductions of up- or down-regulated genes from macroarrays.

			Fold Induction						
Functional category	Gene symbol	GB Acc. No.	Stx1 2h	Stx1 6h	LPS 2h	LPS 6h	Stx1+LPS 2h	Stx1+LPS 6h	Putative Function
Chemokine	SICA 3	M23452	2.2	3.9	27.5	33.8	48.2	91.1	Monocyte chemoattractant
Chemokine	SICA 4	J04130	3.4	6.8	8.5	81.6	155.1	55.5	Monocyte chemoattractant
Cytokine	TNF-α	X01394	7.9	6.6	25.1	31.8	40.1	37.7	Upregulate Gb_3 on vascular EC[a]
Cytokine	IL-1β	K02770	1.6	3.7	11	22	34.9	28.9	Upregulate Gb_3 on vascular EC[a]
Chemokine	IL-8	Y00787	1.6	2.4	6.4	12.2	14.8	11.7	Neutrophil chemoattractant
Chemokine	GRO 2	X53779	2.5	4.7	9.2	9.1	11.9	11.1	Neutrophil chemoattractant
Chemokine	SICA 2	M24545	1.7	1.4	-	7.9	-	8.9	Monocyte chemoattractant
Chemokine	SICA 5	M21121	-	-	3.2	5.4	3.4	8.6	T cell chemoattractant
Chemokine	ET-2	M65199	2.7	-	-	-	2.7	10.9	Affects CNS[b] and neuronal acitivity
Chemokine	BMP 4	D30751	-	-3	1.6	1.9	3.2	-1.6	Chemotactic growth factor
Chemokine	SCBPA 8	X06234	2.4	-1.2	-	2	-	-	Calcium-binding protein
Chemokine Receptor	CRHR 1	X72304	-	-	-	-	1.8	-2.4	Corticotropin releasing hormone receptor
Chemokine	FKTR 3	U04806	-	-	-	-	1.9	-2.5	Fms-related tyrosine kinase 3 ligand

[a] EC, endothelial cells.

[b] CNS, central nervous system.

and IL-1β expression (38), LPS and Stx1 + LPS treatments induced greater levels of chemokine gene expression compared to Stx1 treatment.

Real-time PCR confirmation of chemokine mRNA expression in THP-1 cells. THP-1 cells were examined by quantitative real-time PCR to verify the expression of MIP-1α, MIP-1β, GRO-β, and IL-8 transcripts above untreated controls, following treatment with Stx1, LPS, or both for 2 or 6 h (Fig. 8). At 2 h, treatment with LPS or Stx1 + LPS resulted in significant induction ($P \leq 0.05$) of MIP-1α and MIP-1β mRNAs above untreated controls, while GRO-β and IL-8 mRNA expression was significant ($P \leq 0.05$) following treatment with Stx1 + LPS only (Fig. 8b). Following 6 h, significant induction ($P \leq 0.05$) of MIP-1α, MIP-1β, and GRO-β mRNAs occurred only when cells were treated with Stx1 + LPS (Fig. 8b). IL-8 mRNA induction, however, was significantly ($P \leq 0.05$) above untreated controls following treatment with LPS or Stx1 + LPS (Fig. 8b). Furthermore, from 2 to 6 h, there was a significant ($P \leq 0.05$) increase in IL-8 mRNA levels for both LPS and Stx1 + LPS treatments (Fig. 8b). While MIP-1α and MIP-1β transcripts appeared to decrease from 2 to 6 h, these differences were not significant. In the case of GRO-β, the trend was similar to that of IL-8 in that transcript levels appeared to increase from 2 to 6 h, however, this difference was also not significant. Interestingly, Stx1 + LPS treatment induced significantly higher levels of IL-8 mRNA compared to LPS at 6 h ($P \leq 0.05$).

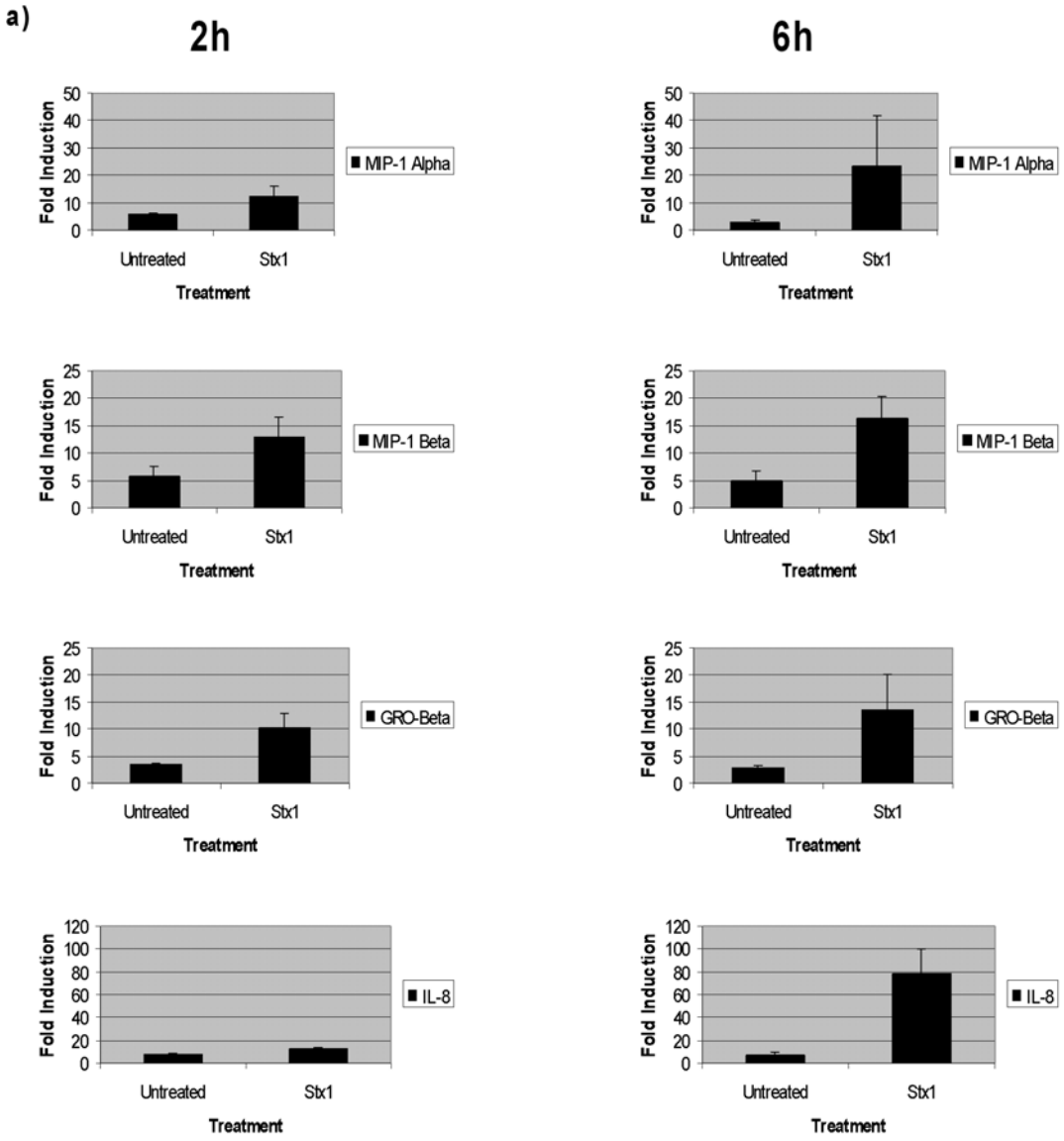

Figure 8. Real-time PCR verification of chemokine expression in Stx1- and/or LPS-treated THP-1 cells. Differentiated THP-1 cells (5 x 10^6 cells/ml) were incubated with (a) media alone (untreated) or 400 ng/ml Stx1, or (b) media alone, 200 ng/ml LPS, or both for 2 h (left panels) and 6 h (right panels). Threshold cycle values were normalized for GAPDH expression and fold inductions of MIP-1α, MIP-1β, GRO-β, and IL-8 expression were calculated above the 0 h untreated control. Data are expressed as means ± standard errors of means of three or four independent experiments. An asterisk (*) denotes a significant difference ($P \leq 0.05$) between treatments at each time point for each cytokine. A plus sign (+) denotes a significant difference ($P \leq 0.05$) between 2 and 6 h cytokine fold inductions within each treatment. A number sign (#) denotes a significant difference ($P \leq 0.05$) in cytokine fold induction between treatments within a time point.

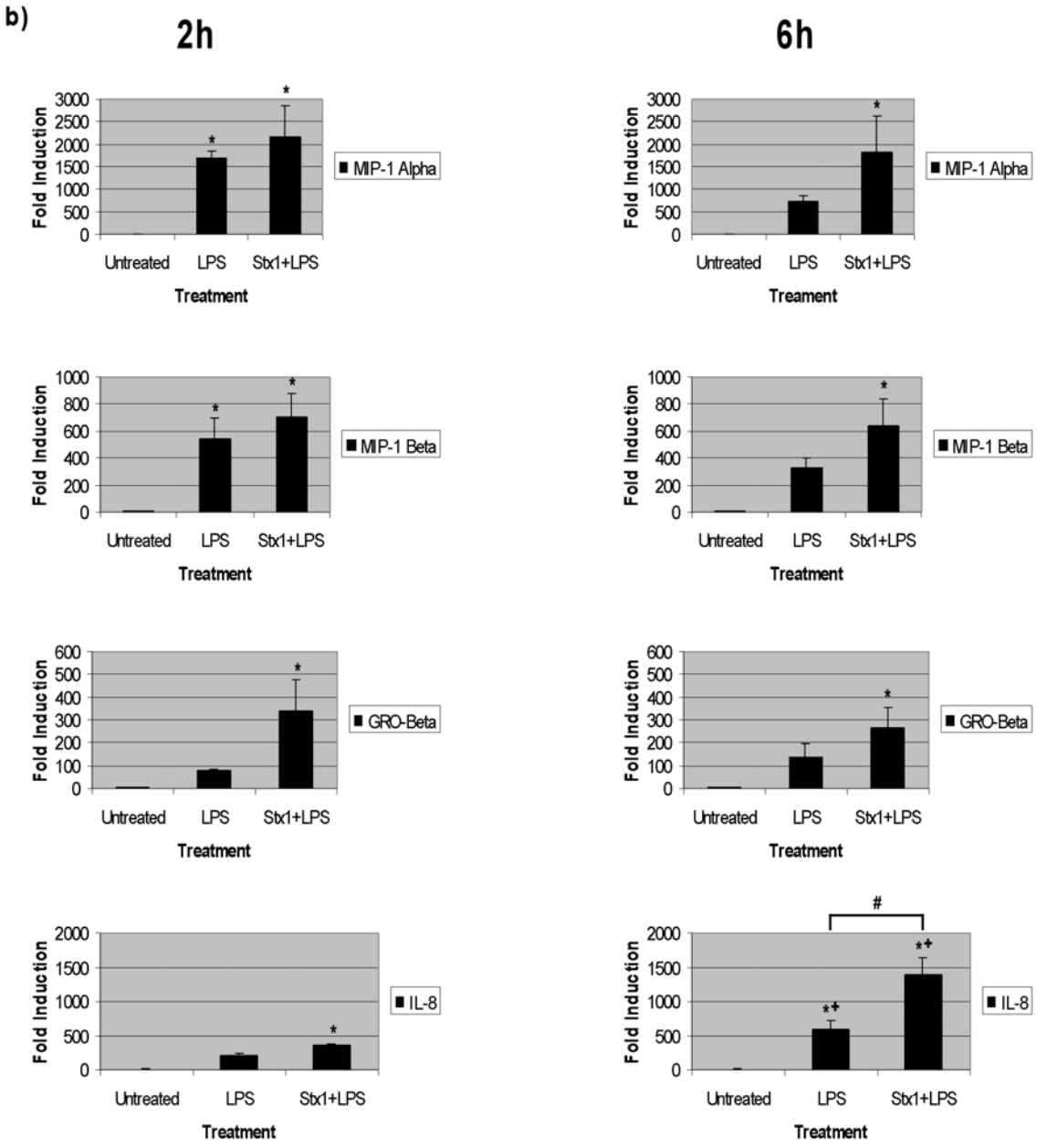

Figure 8 continued

Treatment with Stx1 alone did not appear to induce significant levels of any chemokine above untreated controls at 2 or 6 h (Fig. 8a).

IL-8 mRNA kinetics in THP-1 cells treated with Stx1, LPS, and Stx1 + LPS. Previous reports showed that Stx1 treatment of human intestinal epithelial cell lines resulted in the expression of IL-8 (136,147). However, our real time PCR studies suggested that Stx1 did not significantly activate IL-8 gene expression in macrophage-like THP-1 cells within 6 h of toxin treatment. Therefore, we used Northern blot analyses to more extensively characterize the IL-8 transcriptional response to Stx1 and/or LPS. When THP-1 cells were treated with LPS or Stx1 + LPS (Fig. 9a), IL-8 transcript induction occurred rapidly and with indistinguishable kinetics until 16 h and 24 h post treatment when Stx1 + LPS-induced IL-8 transcripts were significantly greater than LPS-induced transcripts ($P = 0.0014$ at 16 h and $P = 0.0005$ at 24 h). Due to the induction of apoptosis in Stx1 + LPS-treated THP-1 cells (See Chapter IV), we were unable to extract adequate RNA for Northern blots past the 24 h time point. Treatment of cells with Stx1 alone resulted in the relatively slow induction of IL-8 transcripts, with significantly elevated levels first reached at 12 h post treatment and peaking at 36 h (Fig. 9b). In terms of maximal IL-8 transcript levels above basal values, LPS induced approximately 5-times more, and Stx1 + LPS induced approximately 10-times more IL-8 mRNA compared to treatment with Stx1 alone.

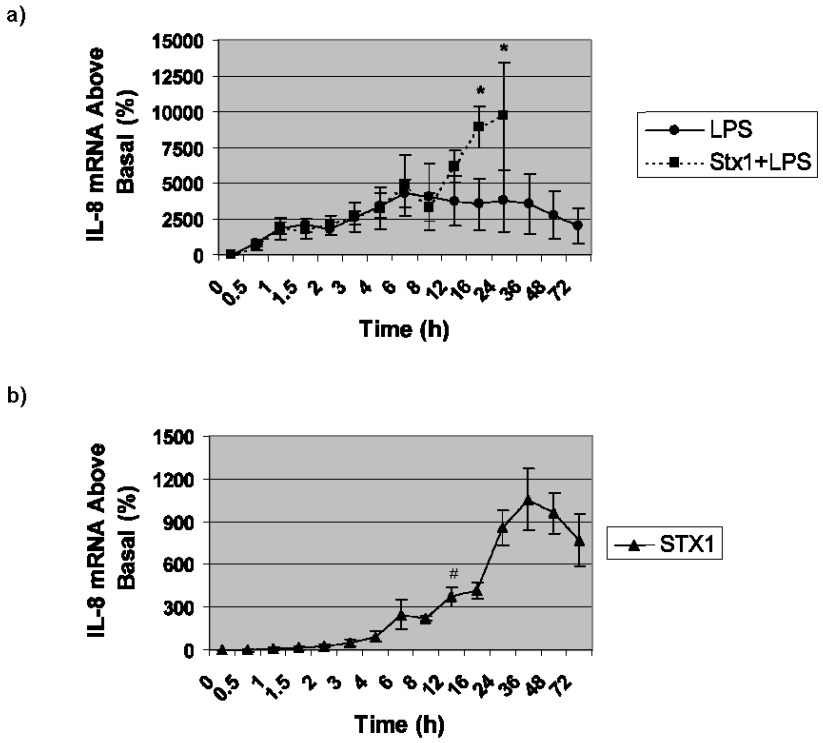

Figure 9. Comparison of IL-8 mRNA expression in THP-1 cells treated with Stx1, LPS, or Stx1+LPS. Differentiated THP-1 cells (5 x 10^6 cells/ml) were treated with 400 ng/ml Stx1, 200 ng/ml LPS, or both for 0 to 72 h. Total RNA (5-15 μg) was subjected to Northern blot analysis using ^{32}[P]-labeled IL-8 and GAPDH cDNA probes. Hybridization was detected and quantitated using a phosphorimager and expressed as percentage of IL-8 mRNA above basal (unstimulated) expression. Data are expressed as means ± standard errors of means from at least three independent experiments from (a) LPS- and Stx1+LPS-treated THP-1 cells and (b) Stx1-treated THP-1 cells. An asterisk (*) denotes a significant difference ($P \leq 0.05$) between LPS and Stx1+LPS treatments. A number sign (#) denotes the first point of significant induction for Stx1-induced IL-8 mRNA; all time points ≥ 12 h are significantly different from the zero time point.

Figure generated by Lisa Harrison and Ilona van Haaften.

Stx1 and Stx1 + LPS induce IL-8 transcripts with increased stabilities compared to the IL-8 transcript induced by LPS. We previously reported that increased TNF-α and IL-1β mRNA stabilities may be involved in the maintenance of elevated TNF-α and IL-1β transcript levels following treatment of THP-1 cells with Stx1 in the presence or absence of LPS (38). Increased IL-8 mRNA stability associated with Stx1 treatment of intestinal epithelial cells has also been reported (137). To determine whether Stx1 affects IL-8 transcript stability, we treated THP-1 cells with Stx1 for 6 h, and LPS or Stx1 + LPS for 1h, and then added the transcriptional inhibitor actinomycin D to measure mRNA decay rates by Northern blot analyses. LPS-induced transcripts were labile, with a calculated half-life of 1.2 h (Fig. 10a). Stx1- and Stx1 + LPS-induced IL-8 transcripts decayed more slowly (Fig. 10b). The calculated half-life for Stx1-induced IL-8 mRNA was 4.1 h, while the half-life for Stx1 + LPS-induced IL-8 mRNA was greater than the time course of the experiment (≥ 5 h). Statistical analysis revealed that IL-8 mRNA from cells treated with Stx1 had a significantly greater half-life than IL-8 mRNA from cells treated with LPS ($P = 0.02$). Although we did not determine a half-life for IL-8 transcripts induced by Stx1 + LPS, statistical analysis of IL-8 mRNA levels indicated that Stx1-induced IL-8 transcript levels were significantly lower than Stx1 + LPS-induced IL-8

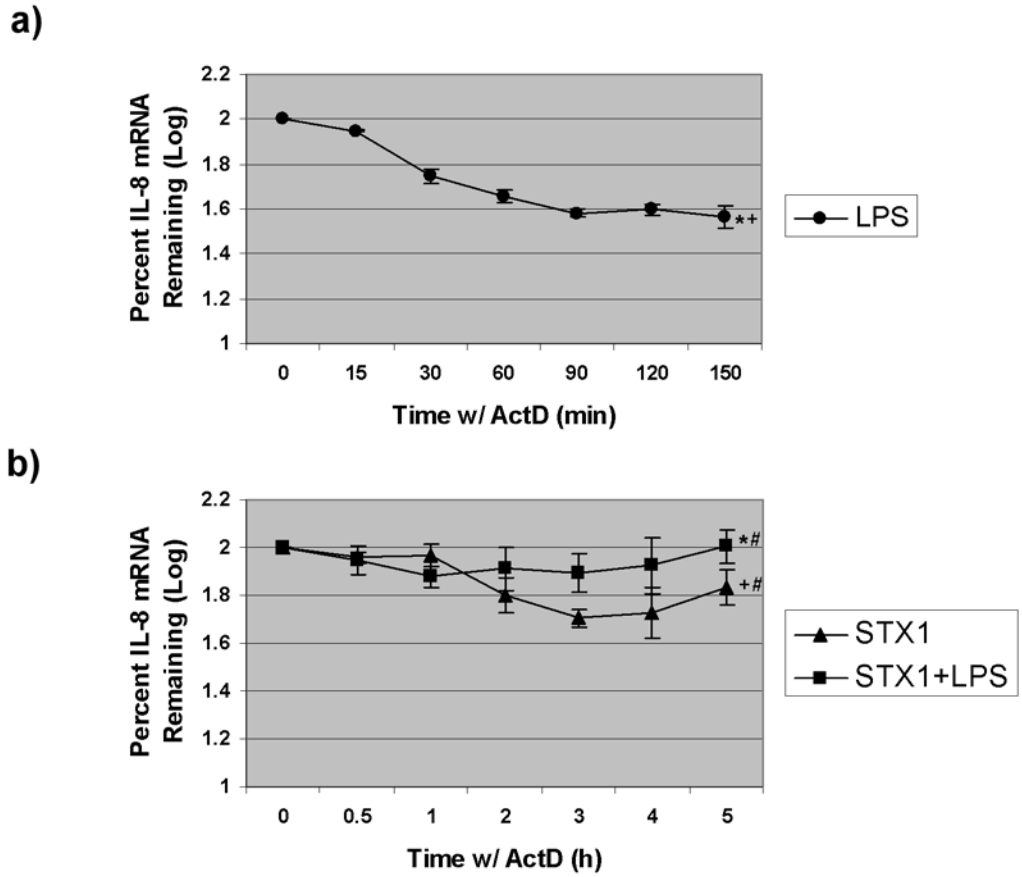

Figure 10. Effects of Stx1 and/or LPS on IL-8 mRNA stability in THP-1 cells. Differentiated THP-1 cells (5 x 10^6 cells/ml) were treated with (a) LPS (200 ng/ml) for 1 h, (b) Stx1 (400 ng/ml) for 6 h, or both for 1 h. Actinomycin D (actD) was then added to each plate at a final concentration of 5 μg/ml. Total RNA was isolated at each of the indicated time points after actD addition. Northern blot analysis was performed, and IL-8 mRNA was detected and quantitated using a phosphorimager. Data are expressed as means of percentage of IL-8 mRNA remaining (log) ± standard error of the means from at least three independent experiments. Treatments with the same symbol are significantly different ($P \leq 0.05$) from each other.

Figure generated by Lisa Harrison and Ilona van Haaften.

transcript levels over time, and thus, the half-life of Stx1 + LPS-induced IL-8 mRNA is also significantly greater than the half-life of LPS-induced mRNA.

Treatment of THP-1 cells with Stx1, LPS, and Stx1 + LPS results in IL-8 protein production. Figure 11 shows the induction of IL-8 protein, over time, from THP-1 cells treated with LPS, Stx1, and Stx1 + LPS. In general, IL-8 protein production correlated with IL-8 mRNA expression. For cells treated with LPS (Fig. 11a), IL-8 expression was significantly elevated ($P \leq 0.05$) 4 h post treatment, with peak concentrations of 151.8 ng/ml reached at 72 h. IL-8 protein levels from Stx1-treated cells (Fig. 11b) were not elevated above control cells until 8 h of treatment, with significant elevations occurring at 24 h ($P \leq 0.05$). Peak IL-8 protein expression by Stx1-treated cells was approximately 15-fold less than LPS-treated cells. This observation is consistent with previous reports showing that Stx1 is a less potent inducer of TNF-α and IL-1β compared to LPS (38,105). For cells treated with Stx1 + LPS (Fig. 11c), significantly elevated IL-8 expression was reached after 3 h. However, treatment of THP-1 cells with both stimulants resulted in less IL-8 protein than predicted based on levels of IL-8 mRNA induced by Stx1 + LPS. The "spike" of IL-8 mRNA we noted following 16 h of Stx1 + LPS exposure did not manifest as markedly increased IL-8 protein synthesis.

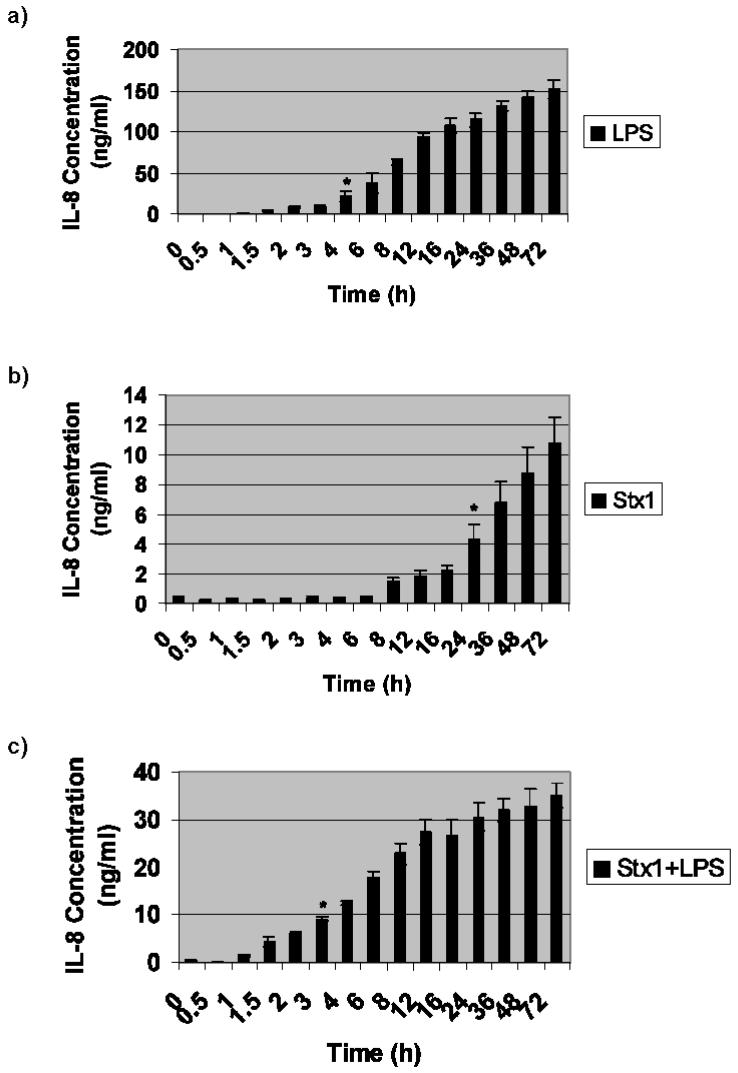

Figure 11. IL-8 protein production by THP-1 cells treated with Stx1, LPS, and Stx1+LPS. Cell-free supernatants from (a) LPS-, (b) Stx1-, and (c) Stx1+LPS-treated cells were collected and analyzed using human IL-8 specific ELISAs. Data shown are the means ± standard error of the means from at least three independent experiments. An asterisk (*) denotes the first significant expression difference ($P \leq 0.05$) between untreated and treated cells.

Figure generated by Lisa Harrison, Ilona van Haaften, and Christopher Thompson.

MIP-1α, MIP-1β, and GRO-β protein expression in THP-1 cells treated with Stx1, LPS, and Stx1 + LPS. We examined the pattern of expression of the monocyte chemoattractants MIP-1α, MIP-1β, and the neutrophil chemoattractant GRO-β following 24 h treatment of THP-1 cells with Stx1, LPS, and Stx1 + LPS. Within 4 h, relatively high levels of MIP-1α (Fig. 12a) and MIP-1β (Fig. 12b) were expressed by cells treated with all the stimulants, with concentrations of 20-40 ng/ml reached. LPS was the most significant ($P \leq 0.05$) stimulant of MIP-1α and MIP-1β expression, while Stx1 was the least robust inducer of these chemokines. MIP-1α and MIP-1β levels induced by LPS or Stx1 + LPS roughly doubled over the next 8 h of stimulation, and then remained constant for the remainder of the experiment. Levels of MIP-1α and MIP-1β induced by Stx1 did not appear to increase significantly beyond the 4 h time point. GRO-β expression (Fig. 12c) was slower and continued to rise for all treatments throughout the course of the experiments. As was the case for IL-8 protein, treatment of cells with Stx1 + LPS resulted in the synthesis or release of MIP-1α, MIP-1β, and GRO-β proteins at intermediate levels between those induced by treatment with Stx1 alone and LPS alone.

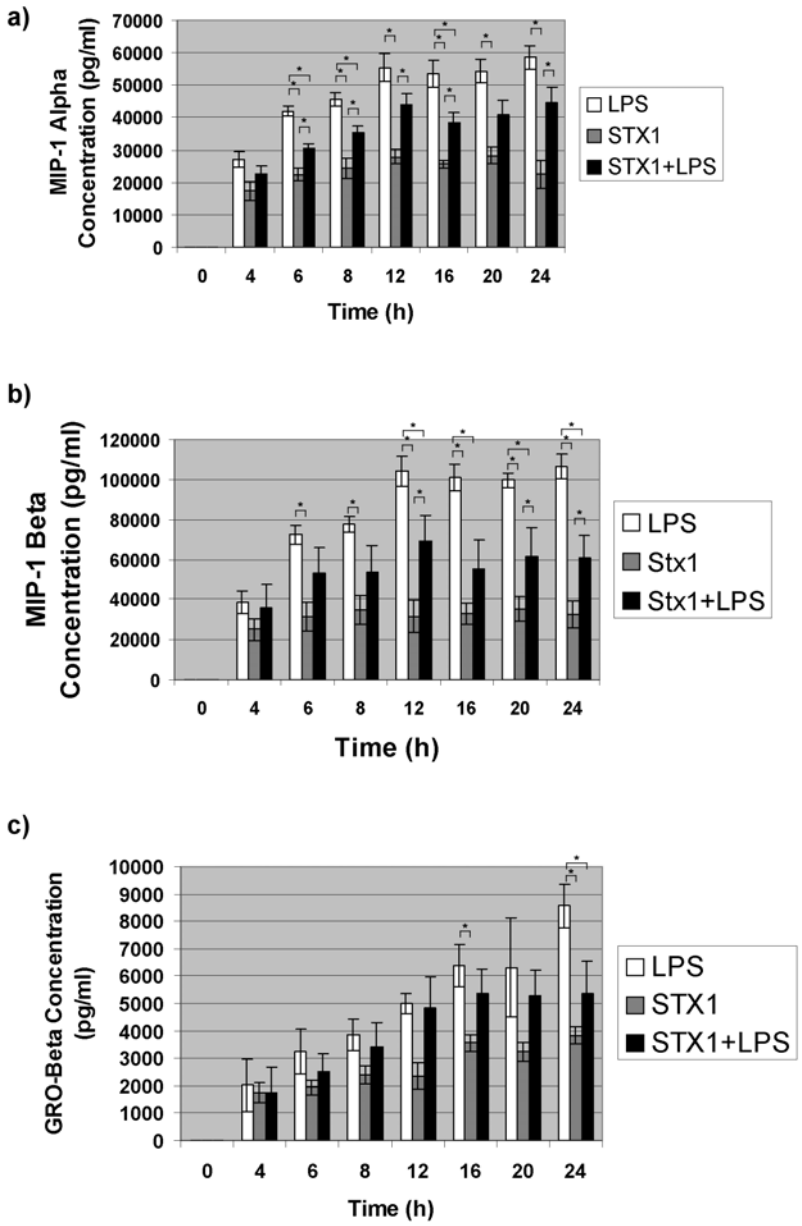

Figure 12. MIP-1α, MIP-1β, and GRO-β protein production by THP-1 cells treated with Stx1, LPS, and Stx1+LPS. Cell-free supernatants from LPS-, Stx1-, and Stx1+LPS-treated cells were collected and analyzed using human (a) MIP-1α-, (b) MIP-1β-, and (c) GRO-β-specific ELISAs. Data shown are means ± standard error of the means from at least three independent experiments. Significant differences between treatments are indicated by an asterisk (*).

Figure generated by Christel van den Hoogen and Lisa Harrison.

Discussion

Given the property of TNF-α and IL-1β to modulate toxin receptor expression on vascular endothelial cells, our earlier studies focused on the mechanisms by which Stxs signal proinflammatory cytokine expression by macrophages (24,38,105). In this study, we used commercially available macroarrays spotted with cytokine and chemokine cDNAs to obtain a more global view of the macrophage transcriptional response to Stx1 and/or LPS. We show that six genes were consistently up-regulated in response to these bacterial products: genes encoding the proinflammatory cytokines TNF-α and IL-1β, the CC chemokines MIP-1α and MIP-1β, and the CXC chemokines, IL-8 and GRO-β (Fig. 7 & Table 3). For four of the six genes, the levels of transcripts induced by treatment with Stx1 + LPS were greater than transcripts induced by either treatment alone at the 2 and 6 h time points. The exceptions were the chemokines IL-8 and MIP-1β, where treatment with LPS alone for 6 h induced greater increases than treatment with Stx1 + LPS. Other genes showed more complex patterns of induction. Monocyte chemotactic protein-1 (SICA2 or CCL2) was only up-regulated after 6 h treatments with LPS or Stx1 + LPS. RANTES (SICA5 or CCL5) was induced by LPS and its expression was increased by Stx1 + LPS. Endothelin-2 (ET2) was induced early (2 h) by Stx1 and Stx1 + LPS, and ET2 mRNA levels were increased by treatment with Stx1 + LPS at 6 h.

Bone morphogenetic protein-4 (BMP4) was induced early by Stx1 + LPS, but its levels were down-regulated by longer exposure to Stx1 or Stx1 + LPS. Corticotropin-releasing hormone receptor-1 (CRHR1) and fms-related tyrosine kinase 3 ligand (FKTR3) were modestly down-regulated by exposure to Stx1 + LPS. S100 calcium-binding protein A8 (SCBPA8) was the only transcript up-regulated early (2 h) in response to treatment with Stx1 alone.

We used chemokine-specific forward and reverse primers to conduct real-time PCR reactions to verify the chemokine expression patterns of Stx1-, LPS-, and Stx1 + LPS-treated THP-1 cells (Fig. 8). In accordance with the macroarray data, Stx1 treatment alone induced modest levels of chemokine transcripts at 2 and 6 h. At 2 h, LPS induced significant levels of the CC chemokines, MIP-1α and MIP-1β ($P \leq 0.05$), but did not induce significant levels of the CXC chemokines, IL-8 and GRO-β. Six hours after LPS treatment, the levels of MIP-1α and MIP-1β transcripts were not significant compared to untreated cells, suggesting that transcriptional activation may be transient or the mRNA transcripts are labile. LPS induced modest levels of GRO-β transcripts, while 6 h of LPS treatment produced a significant level ($P \leq 0.05$) of IL-8 mRNA expression. For both 2 and 6 h of Stx1 + LPS treatment, significant levels of all the observed chemokines were expressed ($P \leq 0.05$).

We noted some discrepancies between the macroarray and real time-PCR results. For example, the macroarray data suggested a slight decrease in IL-8 transcripts induced by Stx1 + LPS between 2 and 6 h, yet the real time PCR data showed an increase in IL-8 mRNA induced by Stx1 + LPS between the 2 and 6 h time points. To examine in more detail the kinetics of IL-8 mRNA expression by THP-1 cells treated with Stx1 and/or LPS, we utilized Northern blot analyses (Fig. 9). Treatment of cells with Stx1 alone resulted in the slow induction of IL-8 mRNA expression, with significant transcript elevation noted at 12 h after toxin treatment. In contrast, LPS and Stx1 + LPS treatments induced IL-8 transcripts with almost identical rapid kinetics until 16 to 24 h post treatment, when levels of IL-8 mRNA expressed by Stx1 + LPS-treated cells were significantly elevated compared to cells treated with LPS alone. We have previously shown that treatment of macrophage-like THP-1 cells with Stx1 + LPS results in programmed cell death (See Chapter IV), and at later time points, we were unable to extract adequate amounts of RNA to perform Northern blots. These data suggest that coincident with apoptotic signaling induced by Stx1 + LPS, the *IL*-8 gene may become transcriptionally active.

Thorpe *et al*. reported that Stx1 treatment of a human intestinal epithelial cell line stabilized IL-8 mRNA transcripts (137). To determine whether changes in mRNA stability were involved in the higher levels of IL-8 transcripts noted at later time points in Stx1 + LPS-treated THP-1 cells, we used the transcriptional

inhibitor actinomycin D to measure transcript decay rates (Fig. 10). LPS-induced IL-8 transcripts had a significantly shorter half-life (1.2 h; $P \leq 0.05$) compared to Stx1-, and Stx1 + LPS-induced IL-8 transcripts (4.1 and >5 h, respectively). Measurement of soluble IL-8 production suggested that IL-8 transcripts and protein induced by Stx1 or LPS treatments were correlated in that Stx1 induced the delayed expression of IL-8 mRNA and protein, while LPS induced an earlier, more robust IL-8 mRNA and protein response (Fig. 11a, 11b). This direct correlation between transcription and translation did not manifest in Stx1 + LPS-treated cells (Fig. 11c). Given the "spike" of IL-8 mRNA expression and the increased stability of IL-8 mRNA induced by Stx1 + LPS treatment, we predicted that soluble IL-8 protein levels induced by both stimulants would exceed that produced by cells treated with LPS alone. We found that IL-8 protein elicited by Stx1 + LPS treatment was five-fold less than that induced by LPS alone. This pattern of diminished protein expression in response to Stx1 + LPS treatment was also evident for MIP-1α, MIP-1β, and GRO-β expression (Fig. 12). Thus, in contrast to our earlier studies, where Stx1 + LPS treatment augments the production of soluble TNF-α (105), Stx1 appears to down-modulate the macrophage chemokine response to LPS.

Before Stxs elicit proinflammatory cytokine expression, they must traverse the intestinal epithelial cell barrier, and several studies have shown that

Stxs are transported in an apical-to-basolateral manner across polarized intestinal epithelial cell monolayers via energy-dependent transcytotic mechanisms (43,94). Neutrophil infiltration of the colonic submucosa and fecal leukocytosis are characteristics of the colitis caused by Stx-producing bacteria (119). Stxs have been shown to directly induce the expression of the neutrophil chemoattractants IL-8 and GRO-α from intestinal epithelial cells *in vitro* (136,137,147). These data suggest that Stxs not only possess the capacity to breach the intestinal epithelium, but may also contribute to the processes of neutrophil extravasation and migration into the lamina propria, and transmigration across the epithelium. Hurley *et al.* showed that the basolateral-to-apical migration of neutrophils across intestinal epithelial cell monolayers resulted in the enhanced paracellular transport of Stxs across the monolayers (44). Thus, the localized production of IL-8 and other chemokines in response to Stxs may establish an amplification loop in which the gut is made markedly more permeable to Stxs and other bacterial constituents such as LPS.

It has proven to be difficult to detect circulating Stxs in the blood and the precise means of systemic toxin transport remain to be fully characterized. Following translocation into the lamina propria, or destruction of the colonic epithelium, Stxs may be in an environment rich in neutrophils and macrophages. The toxins may delay the onset of apoptosis of neutrophils, thereby extending the lifespan of these short-lived cells (70). te Loo *et al.* have

reported that Stx1 binds to neutrophils in blood plasma via a relatively low affinity interaction with a non-Gb_3 receptor (129). Furthermore, functional Stx1 can be transferred from neutrophils to endothelial cells *in vitro*. These findings raise the possibility that the elicitation of a neutrophil infiltrate into the lamina propria may provide the cells to which Stxs "piggyback" for distribution to the microvasculature of target organs.

In addition to acting as chemoattractants for cells that increase intestinal permeability and serve to disseminate the toxins, IL-8 and the GRO proteins are known to activate phagocytic and respiratory burst activities of neutrophils and basophils (30,146). All three GRO proteins are expressed by macrophages in response to LPS treatment, and GRO-α protein is expressed by Stx1-treated intestinal epithelial cells (31,137). We show here that Stx1 and LPS induce the expression of the GRO-β protein from THP-1 cells (Fig. 12). By activating neutrophils, IL-8 and GRO-β production may contribute to the development of extraintestinal disease triggered by Stxs. Neutrophils isolated from HUS patients are more adherent to endothelial cell monolayers and mediate greater destruction of underlying fibronectin substrates compared to neutrophils isolated from healthy controls (22). Levels of urinary IL-8 and MCP-1 are frequently elevated in HUS patients and correlate with neutrophil and monocyte infiltration into the kidneys (46,141). Levels of plasma IL-8 in HUS

patients positively correlate with leukocytosis and plasma elastase levels (a marker of neutrophil activation; (20)). Finally, chemokines produced in response to Stxs may facilitate platelet activation and aggregation (29).

MIP-1α and MIP-1β are powerful monocyte chemoattracts that activate the cells by increasing $[Ca^{2+}]_i$ and releasing arachidonic acid (80). MIP-1α production by macrophages is increased following engagement with intercellular adhesion molecule-1 expressed on the surface of endothelial cells (73). Renal biopsies from patients with inflammatory glomerulonephritis revealed elevated MIP-1α and MIP-1β mRNAs levels in glomerular leukocyte infiltrates (9). IL-1β-treated human astrocytes release MIP-1α proteins, and human brain microvascular endothelial cells release MIP-1β in response to treatment with LPS, TNF-α, IFN-γ, or IL-1β (81,115). Collectively, these data suggest that the localized production of MIP-1α and MIP-1β in the kidneys and brain in response to Stxs and/or LPS, particularly at sites of monocyte-endothelial cell adherence, may further exacerbate vascular damage.

CHAPTER IV

COMPARATIVE EVALUATION OF APOPTOSIS INDUCED BY SHIGA TOXIN 1 AND/OR LIPOPOLYSACCHARIDES IN THE HUMAN MONOCYTIC CELL LINE THP-1

Overview

The enteric pathogens *Shigella dysenteriae s*erotype 1 and Shiga toxin-producing *E. coli* share the property of expressing the structurally and functionally related cytotoxins that comprise the Shiga toxin (Stx) family. Stx-producing bacteria are causative agents of bloody diarrheal diseases that may progress to life threatening complications primarily involving the destruction of blood vessels in the kidneys and the central nervous system (CNS). The precise mechanisms of toxin transport across the gut epithelial barrier, and the role of the toxins in the development of systemic complications, remain to be fully characterized. Our earlier studies suggested that Stxs and lipopolysaccharides (LPS) induce the expression of proinflammatory cytokines from differentiated (macrophage-like) THP-1 cells. These cytokines may exacerbate vascular damage by up-regulating the expression of toxin receptors on endothelial cells. Purified Stxs have also been shown to induce apoptosis of epithelial and

endothelial cells *in vitro.* Here, we used FACS, TUNEL, and DNA laddering analyses to show that both Shiga toxin-1 (Stx1) and LPS induce apoptosis in undifferentiated and differentiated THP-1 cells, although the kinetics and extent of apoptosis induction differ between monocytic and macrophage-like cells. Stx1-induced apoptosis is A-subunit-dependent. Both Stx1 and LPS trigger apoptosis, possibly through caspase-3 activation, as evidenced by the cleavage of poly(ADP-ribose) polymerase (PARP). Induction of apoptosis in response to Stx1 and/or LPS treatment occurs without the widespread transcriptional activation of apoptosis-related genes. Finally, we present a model of the role of macrophages and monocytes in the pathogenesis of disease caused by Stxs.

Introduction

Shiga toxins (Stxs; alternatively called verotoxins) are potent cytotoxins produced by the enteric pathogens *Shigella dysenteriae* serotype 1 and certain serotypes of *Escherichia coli*. Infections with *S. dysenteriae* serotype 1 and Stx-producing *E. coli* (STEC) cause bloody diarrhea that may further progress to post-diarrheal sequelae such as the hemolytic uremic syndrome (HUS) and/or CNS complications (92,97). Although the pathogenesis of disease caused by Stx-producing bacteria remains to be fully characterized, it is thought that Stxs damage microvascular endothelial cells serving the colon, kidneys and CNS,

leading to the deposition of microthrombi within affected blood vessels and resulting in acute renal failure, seizures, paralysis, coma, and death. The vascular lesions characteristic of post-diarrheal sequelae can be reproduced in several animal models following the administration of purified Stxs (14,41,101,128). Stxs consist of a single A-subunit in non-covalent association with a pentameric ring of B-subunits (25). The B-subunits mediate toxin binding to susceptible cells through interaction with the neutral glycolipid globotriaosylceramide (Gb_3; (49,68,65)). Following binding, toxins are internalized and undergo retrograde transport through the trans-Golgi network and Golgi apparatus to reach the lumen of the endoplasmic reticulum (ER) and nuclear membrane (1,107). During retrograde transport, the A-subunit is proteolytically cleaved and reduced to form the enzymatically active A_1-fragment. The ER is thought to be the site of translocation of the A_1-fragment into the cytosol, where the toxins subsequently inhibit protein synthesis by cleaving a single adenine residue from a prominent loop structure of the 28S rRNA of the 60S ribosomal subunit (16,111).

While the cytotoxic activity of Stxs for many cell types has been well defined, previous work in our laboratory revealed that the human monocytic cell line THP-1 manifested different responses to the toxins based on the maturation state of the cells (99). Treatment of undifferentiated, monocyte-like THP-1 cells with Stxs resulted in rapid cell death, whereas treatment of

differentiated, macrophage-like THP-1 cells with Stxs or bacterial lipopolysaccharides (LPS) induced the production of the proinflammatory cytokines tumor necrosis factor-α (TNF-α) and interleukin-1β (IL-1β). Production of these cytokines was augmented when both Stxs and LPS were present (38). Pre- or co-treatment of human vascular endothelial cells with TNF-α or IL-1β promotes Gb_3 expression (98,139), resulting in increased sensitivity to Stxs *in vitro* (71,98,142). Elevated cytokine levels are occasionally detected in the sera, and frequently detected in the urine, of HUS patients (130). Taken together, these data suggest that the presence of Stxs and LPS elicits an innate immune response that may, in turn, exacerbate vascular damage by sensitizing target endothelial cells to the cytotoxic action of the toxins.

In the course of experiments to measure the decay rates of TNF-α and IL-1β transcripts induced by treatment of differentiated THP-1 cells with Shiga toxin type 1 (Stx1) and/or LPS, we noted that as the toxin exposure times increased, total yields of RNA diminished and cell detachment from culture plates increased (38). These observations suggested that macrophage-like THP-1 cells may be susceptible to the cytotoxic action of Stxs, and that cell killing is delayed compared to the rapid killing of monocytic cells. To establish that cell detachment was due to cytotoxicity mediated by Stx1 and/or LPS, we measured cell viability using the tetrazolium salt MTT. There are two main mechanisms of

cell death: necrosis and apoptosis. Necrosis is usually thought of as "accidental cell death" and involves cell swelling, lysis, and the subsequent release of cytoplasmic and nuclear contents resulting in inflammation. Apoptosis, in contrast, is "programmed cell death" and involves shrinkage of cells with loss of intercellular contacts, chromatin condensation, nuclear DNA fragmentation, and cytoplasmic blebbing (149). Phagocytic cells recognize and ingest remnants of apoptotic cells, sparing the host an inflammatory response. Stxs have been shown to induce apoptosis in numerous cell types. We used several assays that specifically measure the induction of apoptosis to examine cell death caused by Stx1 and LPS in undifferentiated and differentiated THP-1 cells. The role of purified Stx1 B-subunits *versus* the holotoxin in apoptosis was also examined. A preliminary characterization of apoptosis induction by both Stx1 and LPS through caspase-3 activation, and the transcriptional activation of apoptosis-related genes in response to Stx1 and/or LPS treatment are presented. Finally, we present a model of the role of macrophages and monocytes in the pathogenesis of disease caused by Stxs.

Materials and Methods

Cells. The human myelogenous leukemia cell line THP-1 (138) was purchased from American Type Culture Collection (ATCC; Rockville, MD). Cell

cultures were maintained in RPMI 1640 (GibcoBRL; Grand Island, NY) supplemented with 10% fetal bovine serum (FBS; Hyclone Laboratories; Logan, UT), penicillin (100 U/ml) and streptomycin (100 μg/ml) at 37°C in 5% CO_2 in a humidified incubator.

Toxins. Stx1 was expressed from *Escherichia coli* DH5α(pCKS112), a recombinant strain containing a plasmid encoding the *stx1* operon (131). Stx1 in crude bacterial lysates was purified by sequential ion-exchange, chromatofocusing, and immunoaffinity chromatography. Toxin purity was assessed by sodium dodecyl sulfate-polyacrylamide gel electrophoresis (SDS-PAGE) with silver staining and by Western blots using bovine polyclonal Stx1 specific antisera (kind gift of Dr. James Samuel, Texas A&M University System Health Science Center, College Station, TX). Toxin preparations were passed through ActiClean Etox columns (Sterogene Bioseparations; Carlsbad, CA) to remove trace endotoxin contaminants, and were determined to contain <0.1 ng of endotoxin *per* ml by the *Limulus* amoebocyte lysate assay (Associates of Cape Cod, East Falmouth, MA). Purified Stx1 B-subunits were the kind gift of Dr. Cheleste Thorpe, Tufts University School of Medicine, Boston, MA. Purified lipopolysaccharides (LPS) derived from *E. coli* O111:B4 were purchased from Sigma Chemical Co. (St. Louis, MO).

Macrophage differentiation and stimulation. The mature macrophage-like state was induced by treating THP-1 cells (10^6 cells per ml) for 48 h with phorbol 12-myristate 13-acetate (PMA; Sigma) at 50 ng/ml. Plastic-adherent cells were washed twice with cold, sterile Dulbecco's phosphate-buffered saline (PBS; Sigma) and incubated with fresh RPMI-1640 lacking PMA, but containing 10% FBS, penicillin (100 U/ml) and streptomycin (100 μg/ml). The medium was then changed every 24 h for 3 additional days. Experiments were performed on the fourth day after removal of PMA. For all experiments, cells were treated with Stx1 or LPS using concentrations we previously demonstrated produced maximal TNF-α protein secretion in differentiated THP-1 cells (99).

MTT assay for cell death. Differentiated and undifferentiated THP-1 cells (1 X 10^5 cells per well) were plated in 96-well plates. Cells were stimulated with Stx1 (400 ng/ml), LPS (200 ng/ml), or Stx1 + LPS (400 ng/ml and 200 ng/ml, respectively) for 0.5, 1.5, 3, 6, 12, 24, 48, and 72 h. Following treatment, 25 μl of MTT (3-(4,5-dimethylthiazol-2-yl)-2,5-diphenyltetrazolium bromide) solution (5.0 μg/μl) were added to each well and incubated at 37°C in humidified 5% CO_2 for 2 h. After incubation, the plates were centrifuged at 1000 rpm for 5 min. The supernatants were removed and 100 μl of lysis buffer (20% SDS, 50% 2-2 dimethylformamide [pH 4.7]) were added to each well. Plates were incubated at 37°C without CO_2 for 3 hours. Optical densities were

measured in an automated plate reader (Dynatech MR5000, Molecular Dynamics, Chantilly, VA). The percentage of cell death was calculated as follows:

$$\% \text{ cell death} = \frac{[\text{avg. } OD_{570} \text{ treated cells} - \text{avg. } OD_{570} \text{ control cells}]}{[\text{avg. } OD_{570} \text{ control cells}]} \times 100$$

Annexin V and propidium iodide staining. Differentiated and undifferentiated THP-1 cells (1 X 10^6 cells per well) were plated in 6-well plates. Cells were stimulated with medium alone, Stx1 B-subunit (800 ng/ml), Stx1 (400 ng/ml), LPS (200 ng/ml), or Stx1 + LPS (400 ng/ml and 200 ng/ml, respectively) for 4, 12, and 24 h. Cells were then stained with Annexin V and Propidium Iodide (PI) using the Annexin-V-FLUOS Staining Kit (Roche Diagnostics Corp., Indianapolis, IN) according to the manufacturer's protocol. Briefly, undifferentiated cells were transferred to 15 ml conical tubes and centrifuged at 200 x *g* for 5 min. Supernatants were removed and cells were washed twice with cold, sterile 1X PBS. Cells were then resuspended in the provided incubation buffer containing Annexin V and/or PI and incubated for 10-15 min at room temperature. Cells were centrifuged at 200 x *g* for 5 min and resuspended in 500 µl incubation buffer and transferred to FACS tubes. For differentiated THP-1 cells, the media containing the stimuli were transferred to 15 ml conical tubes, the adherent cells were washed once with 2.0 ml cold, sterile 1X PBS, and the PBS washes were transferred to the same 15 ml conical tubes.

One milliliter of 0.05% trypsin-0.53 mM EDTA (Invitrogen Life Technologies; Carlsbad, CA) was added to the adherent cells and incubated at 37°C for approximately 5 min. The plates were then tapped under each well to loosen any remaining adherent cells and 1.0 ml RPMI 1640 with 10% FBS, and penicillin-streptomycin was added to deactivate the trypsin. Cells were transferred to the same 15 ml conical tubes containing the media and PBS washes to be spun at 200 x *g* for 5 min. The cells were then washed twice with cold, sterile 1X PBS and processed as described above. Fluorescence was detected using a fluorescence-activated cell sorter (FACSCalibur, Becton-Dickinson, Palo Alto, CA). Fluorescence parameters were gated using unstained and single-stained untreated control cells, and 10,000 cells were counted for each treatment. Data shown are expressed as percentages of Annexin V positive cells plus Annexin V and PI double positive cells for quantitation of total apoptosis.

***In Situ* cell death detection.** THP-1 cells (2 x 10^5 cells *per* well) were differentiated on 16-well Lab-Tek chamber slides (Nalge-Nunc International, Naperville, IL), resulting in approximately 1 x 10^5 cells *per* well. Eight wells were treated in RPMI 1640 containing 0.5% FBS (to reduce background signaling), and the other 8 wells were treated in RPMI 1640 containing 10% FBS. Cells were stimulated with media alone, Stx1 (400 ng/ml), LPS (200 ng/ml), or both, in duplicate, for 4, 12, and 24 hours. DNA strand breaks were then labeled using the *In Situ* Cell Death Detection Kit - Fluorescein (Roche) as *per* the

manufacturer's protocol. Briefly, the media were removed, the wells were detached, and the adherent cells were allowed to air dry. Cells were then fixed with freshly prepared 4% paraformaldehyde in PBS (pH 7.4) for 1 h at room temperature. Slides were rinsed with PBS and cells were incubated with freshly prepared permeabilization solution (0.1% Triton X-100 in 0.1% sodium citrate) for 2 min on ice. Slides were rinsed twice with PBS and dried. Fifty microliters of Label Solution (negative control) or TUNEL reaction mixture (1:10 mixture of Enzyme Solution to Label Solution) were added to each sample, and incubated for 1 h in a humidified atmosphere at 37°C in the dark. Slides were then rinsed three times with PBS and analyzed directly by fluorescence microscopy. The total number of TUNEL positive cells was determined by counting fluorescent cells from ten different 20X fields for each treatment.

DNA fragmentation analysis. Detection of DNA fragmentation was done using the Apoptotic DNA ladder kit (Roche). Genomic DNA was isolated according to the manufacturer's instructions. Briefly, THP-1 cells (differentiated and undifferentiated) were treated with Stx1 (400 ng/ml), LPS (200 ng/ml), or both for 12 h in RPMI 1640 medium containing 10% FBS, in the presence or absence of the general caspase inhibitor *N*-benzyl-oxycarbonyl-Val-Ala-Asp (OMe)-fluoro-methylketone (zVAD-fmk; Calbiochem, San Diego, CA) at 25 μM or 50 μM. Following treatment, cells were lysed using the provided lysis buffer.

Lysates were passed through DNA binding columns, after which the DNA was eluted using the provided elution buffer. Equal amounts of DNA (2-4 μg) were run on 1.2% agarose gels. Gels were stained with ethidium bromide. DNA bands were visualized by ultraviolet light and photographed using the BioRad Gel Imager (Bio-Rad; Hercules, CA). The data shown are representative of at least two independent experiments.

Preparation of cellular lysates for detection of PARP cleavage. Eighteen hours prior to stimulation, THP-1 cells ($5x10^6$ cells *per* well) were washed twice in cold Dulbecco's PBS, and RPMI-1640 with penicillin/streptomycin and 0.5% FBS was added to reduce endogenous kinase activity. Cells were stimulated with Stx1 (400 ng/ml), LPS (200 ng/ml), or both for 1, 2, 4, 8, 20, or 24 h. The cells were lysed with modified radioimmunoprecipitation assay (RIPA) buffer (1.0% Nonidet P-40, 1.0% Na-deoxycholate, 150 mM NaCl, 50 mM Tris-HCl [pH 7.5], 0.25 mM Na-pyrophosphate, 2.0 mM sodium vanadate, 2.0 mM sodium fluoride, 10 μg/ml aprotinin, 1.0 μg/ml leupeptin, 1.0 μg/ml pepstatin, and 200 mM phenylmethylsulfonyl fluoride) at 4°C. Extracts were collected and cleared by centrifugation at 15,000 x *g* for 10 min. Cleared extracts were stored at -80°C until further use in Western blot analysis.

Western blot analysis for detection of PARP cleavage. Protein concentrations in cell extracts prepared from stimulated THP-1 cells were determined using the Micro BCA Protein Assay Kit (Pierce, Rockford, IL). Equal

amounts of proteins (60–80 μg protein per gel lane) were separated by 8% Tris-glycine SDS-PAGE and transferred to nitrocellulose membranes. Membranes were blocked with 5% milk (Fat free dry milk powder) prepared in TBST (20 mM Tris [pH 7.6], 137 mM NaCl, containing 0.1% Tween 20) overnight at 4°C. Membranes were then incubated with a primary antibody specific for PARP (New England Biolabs, Beverly, MA) in 5% BSA in TBST overnight at 4°C. The PARP-specific antibody recognizes full length PARP (116 kD) as well as a cleaved PARP fragment (89 kD). Membranes were washed twice with TBST for 5 min at room temperature and then incubated with a horseradish peroxidase-coupled goat anti-rabbit IgG (New England Biolabs) for 2 h at room temperature. The bands were visualized using the Western Lightning Chemiluminescence System (NEN, Perkin Elmer, Boston, MA). Data shown are representative of at least two independent experiments.

Macroarrays. Atlas Human Apoptosis cDNA expression arrays (Clontech; Palo Alto, CA), containing 205 immobilized human cDNAs, housekeeping controls, and negative controls in duplicate spots on nylon membranes, were used to examine the regulation of apoptosis-related genes in response to treatment with Stx1, LPS or both. Differentiated THP-1 cells (20 ml at 1.0 X 10^6 cells/ml) were plated in 100 mm cell culture plates and treated with Stx1, LPS, or Stx1 + LPS for 6 or 12 h. Total RNA was isolated and DNase treated as *per* the manufacturer's instructions, and stored at -70°C until use. Total RNA

was ^{32}[P]-labeled using the Atlas Pure Total RNA labeling system (Amersham Pharmacia Biotech Inc.; Piscataway, NJ), and unincorporated nucleotides were removed by column chromatography. C_0t-1 DNA was added to labeled probes to reduce background hybridization to repetitive DNA sequences. The arrays were pre-hybridized for 1 h with continuous agitation at 68°C in ExpressHyb solution containing sheared salmon testes DNA. Probes were then allowed to hybridize overnight at 68°C with continuous agitation. Arrays were washed four times with 100 ml of pre-warmed wash solution I (2X SSC, 1% SDS) for 30 min at 68°C with continuous agitation. The blots were washed with 100 ml of pre-warmed wash solution II (0.1X SSC, 0.5% SDS) at 68°C with continuous agitation for 30 min. A final 5 min wash was performed with 100 ml wash solution III (2X SSC) with continuous agitation at room temperature. The arrays were exposed to X-ray film at -70°C with an intensifying screen. Screens were scanned using a Phosphorimager (Molecular Dynamics) to visualize up- or down-regulated genes. Data were quantitated using ImageQuant Software (Molecular Dynamics). The experiments were performed in duplicate using GAPDH cDNA spots for normalization. A complete listing of cDNAs spotted on the Atlas Human Apoptosis cDNA Expression Array (# 7743-1) may be viewed at www.bdbiosciences.com/clontech/atlas/genelists/index.shtml.

Statistics. Statistical analyses of experiments were performed with the SAS statistics program (SAS Institute; Cary, NC), the SPSS statistics program (SPSS, Inc.; Chicago, IL), or Excel (Microsoft, Corp., Redmond, WA). Differences in time points in the MTT cell viability assays were analyzed using the Student's *t*-test. All FACS data were analyzed using two-way ANOVAs with the Duncan multiple range test for post-hoc comparisons. TUNEL data were analyzed using one-way ANOVAs with the Tukey post-hoc test. P values ≤ 0.05 were considered significant for all analyses. All data are presented as means and standard errors of the means from a compilation of at least three independent experiments, except the Stx1 B-subunit FACS data, which is from at least two independent experiments.

Results

Decreased cell viability of undifferentiated (monocytic) and differentiated (macrophage-like) THP-1 cells treated with Stx1 and/or LPS. In earlier studies, we noted that prolonged treatment of macrophage-like THP-1 cells with Stx1 + LPS resulted in cell detachment from plastic surfaces (38). To determine if cell detachment was due to a decrease in cell viability, undifferentiated and differentiated THP-1 cells (approx. 1 X 10^5/well) were incubated with Stx1, LPS, or both for 0.5, 1.5, 3, 6, 12, 24, 48, and 72 h. Using the

cell viability indicator MTT (3-(4,5-dimethylthiazol-2-yl)-2,5-diphenyltetrazolium bromide), percentages of cell death following treatments were calculated in comparison to untreated control cells. We noted differences in both the kinetics and extent of cell death caused by Stx1 and/or LPS between undifferentiated and differentiated THP-1 cells. In undifferentiated (monocyte-like) THP-1 cells (Fig. 13a), treatment with Stx1 or Stx1 + LPS resulted in the rapid onset of cell death compared to LPS treatment, with 83.7% and 88.1% of cells dying following 12 h of treatment with Stx1 and Stx1+LPS, respectively, compared to 12.6% cell death following LPS treatment for the same time period. However, by 72 h of treatment with LPS, 52.5% of undifferentiated THP-1 cells were dead. Cell death induced by Stx1 alone did not appear to be greatly augmented by the addition of LPS. However, statistical analysis revealed that at 3, 6, and 12 h post-treatment, Stx1+LPS induced greater levels of cell death compared to Stx1 alone, indicating a slightly faster induction of cell death in Stx1+LPS-treated cells ($P \leq 0.05$).

The response of differentiated (macrophage-like) THP-1 cells to treatment with Stx1 appeared to differ compared to undifferentiated cells, with only 10.7% cell death noted at 12 h and peak levels of cell death (36.4%) occurring after 48 h of toxin exposure (Fig. 13b). Thus, differentiation was associated with the partial loss of susceptibility to killing mediated by Stx1. Although over the 72 h time course of the experiments, LPS caused roughly equivalent levels of cell death

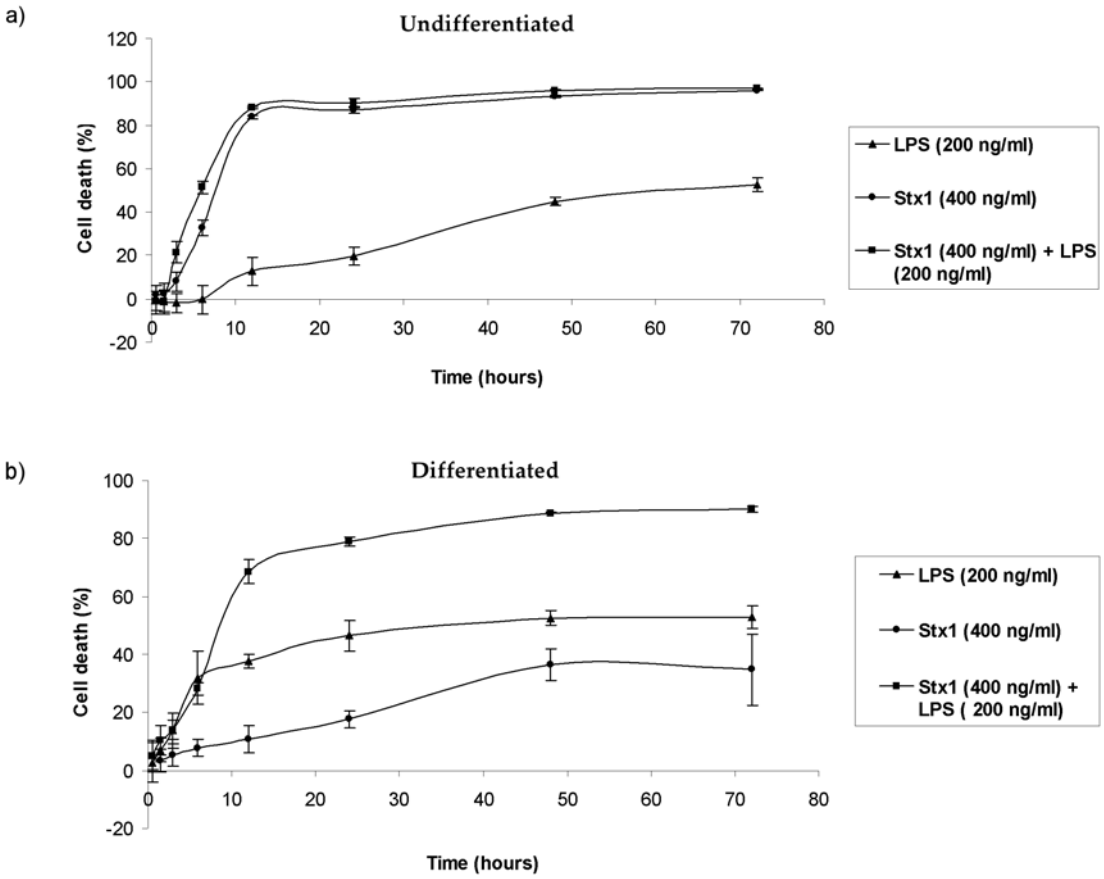

Figure 13. Cell death of undifferentiated and differentiated THP-1 cells following treatment with Stx1, LPS, and Stx1 + LPS. (a) Undifferentiated (monocytic) and (b) differentiated (macrophage-like) THP-1 cells were treated with Stx1 (400 ng/ml), LPS (200 ng/ml), or both for varying times. Cells viability was measured spectrophotometrically after addition of the tetrazolium salt MTT. Cell death percentages were calculated as described in Materials and Methods. Data shown are the means ± standard deviations derived from six replicates for each time point from at least three independent experiments.

Figure generated by Ilona van Haaften and Christel van den Hoogen.

(52.9% cell death in differentiated cells *vs.* 52.5% cell death in undifferentiated cells), the induction of cell death by LPS appeared to be faster in differentiated THP-1 cells, with 37.6% cell death reached after 12 h, compared to 12.6% cell death induced in undifferentiated cells at the same time point. Treatment with both stimulants clearly maximized the extent of cell killing in differentiated cells with 68.6% cell death at 12 h, and a maximum of 90.1% cell death occurring at 72 h. In contrast, treatment with Stx1 alone or LPS alone reached maximum cell death percentages of 36.4% and 52%, respectively, by 48 h.

Stx1 and LPS induce apoptosis in undifferentiated (monocytic) THP-1 cells in a time-dependent manner. To examine the mechanism(s) of cell death in Stx1-, LPS- and Stx1 + LPS-treated THP-1 cells, we used the apoptosis- and necrosis-specific markers Annexin V and propidium iodide (PI) in FACS analyses. The percentage of cells in gates defined as Annexin V positive (apoptosis) and Annexin V/PI double positive (apoptosis and secondary necrosis) were determined following 4, 12, and 24 h of treatment (Fig. 14a). Since many signaling assays utilize cells grown in low serum conditions to reduce endogenous kinase activities, these experiments were conducted using cells in media containing 10% or 0.5% FBS. Over the 24 h time course of the experiments, we did not note significant differences in apoptosis in unstimulated cells maintained in media containing 10% or 0.5% FBS (data not shown). Background fluorescence of control (unstimulated) cells was subtracted

from each time point in order to calculate the percentage of apoptotic cells above basal levels, and total apoptosis was determined (Annexin V positive plus Annexin V/PI double positive cells; Fig 14 b). In accordance with the cell viability data, LPS treatment produced the lowest percentages of apoptosis in undifferentiated cells, ranging from 1.2 ± 0.3% at 4 h to 12.4 ± 2.3% at 24 h in 0.5% FBS (Fig. 14b, top panel), and from 2.7 ± 0.2% at 4 h to 11.3 ± 4.0% at 24 h in 10% FBS (Fig. 14b, bottom panel). Stx1 and Stx1 + LPS treatments induced apoptosis, with Stx1 + LPS inducing significantly more apoptosis than treatment with LPS alone at 4 h (30.3 ± 10.5% *vs*. 1.2 ± 0.3% in 0.5% FBS, and 34.1 ± 3.3% *vs*. 2.7 ± 0.3% in 10% FBS; $P \leq 0.05$). Stx1 induced an intermediate percentage of apoptosis at 4 h (16.3 ± 2.5% in 0.5% FBS, and 17.5 ± 3.4% in 10% FBS), without being significantly different from either LPS- or Stx1+LPS-induced apoptosis. By 12 h, Stx1-induced apoptosis was significantly different from both LPS- and Stx1+LPS-induced apoptosis ($P \leq 0.05$). However, at 24 h, Stx1-induced apoptosis was no longer significantly different from Stx1 + LPS-induced apoptosis since most of the cells displayed the Annexin V^+ or Annexin V^+/PI^+ phenotype by this time. These data indicate a faster induction of apoptosis by treatment with Stx1 + LPS compared to that of Stx1 or LPS alone. Furthermore, Stx1-induced apoptosis occurred more rapidly compared to LPS-induced apoptosis.

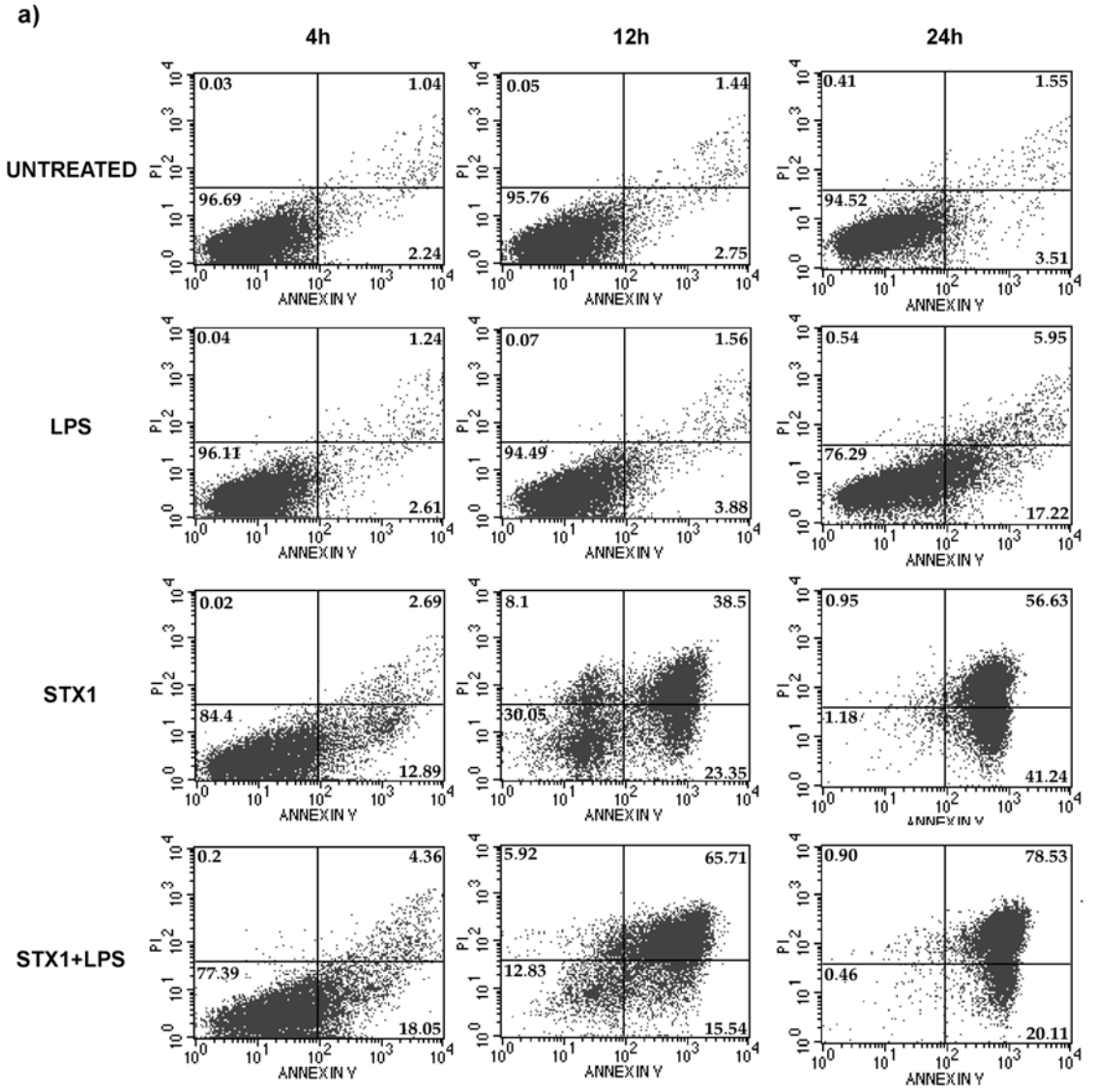

Figure 14. Apoptosis in undifferentiated THP-1 cells treated with Stx1, LPS, and Stx1 + LPS. Undifferentiated (monocytic) THP-1 cells were treated with Stx1 (400 ng/ml), LPS, (200 ng/ml), or both for 4, 12, or 24 h in media containing 0.5% or 10% FBS. Cells were stained with Annexin V and PI and subjected to FACS analysis to determine percentages of apoptotic cells. a) Representative FACS histograms of undifferentiated THP-1 cells treated with the stimulants in media containing 0.5% FBS. b) Percentages of total apoptosis (Annexin V positive plus Annexin V/PI double positive cells) of undifferentiated THP-1 cells in media containing 0.5% FBS (top panel) or 10% FBS (bottom panel). Data shown are the means ± standard errors from at least three independent experiments. An asterisk (*) denotes a significant difference ($P \leq 0.05$) between treatments within each time point.

Figure generated by Lisa Harrison and Ilona van Haaften.

b)

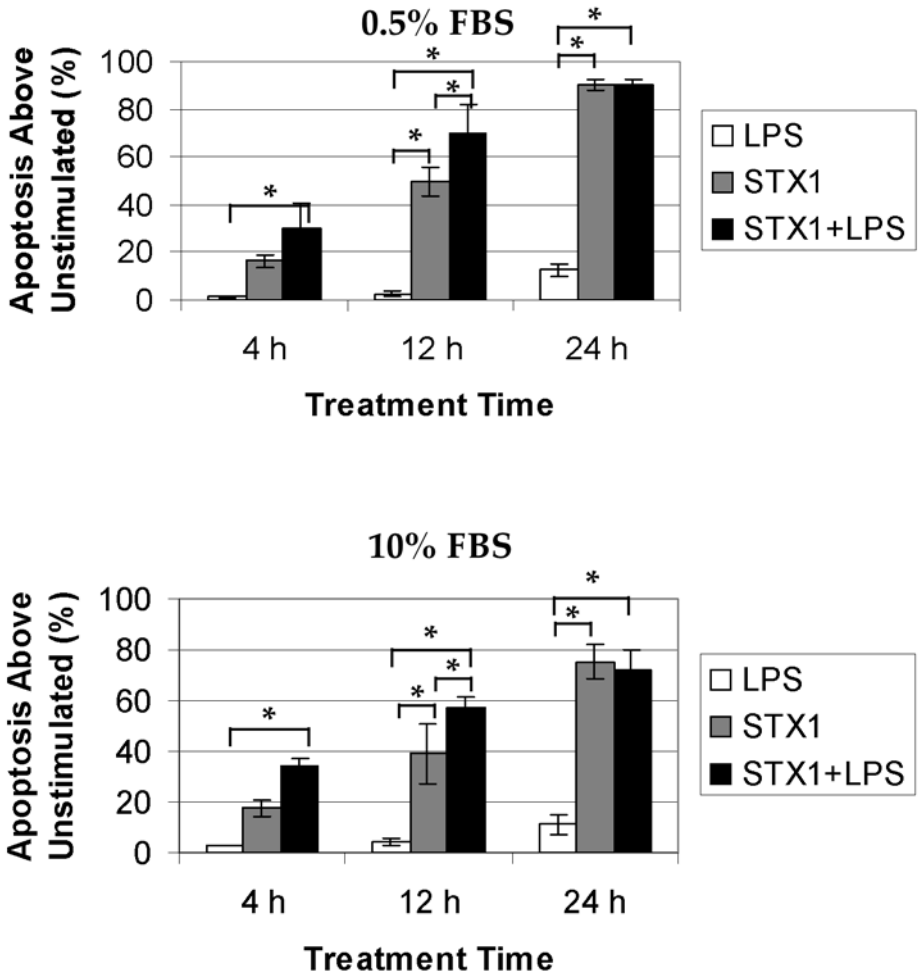

Figure 14 continued

Stx1 and LPS induce apoptosis in differentiated (macrophage-like) THP-1 cells in a time-dependent manner. In contrast to non-adherent undifferentiated cells, FACS analysis of Annexin V and PI stained adherent differentiated THP-1 cells produced variable results with high background apoptosis percentages in unstimulated cells ranging from 12.6 to 71.8%, possibly due to the use of trypsin to detach cells for analysis by flow cytometry. Because of this intra-assay variability, we chose to examine the kinetics and extent of apoptotic cell death of differentiated THP-1 cells using the TUNEL assay which measures levels of nicked DNA as an indicator of apoptosis (28) and does not require the detachment of adherent cells from plastic surfaces. Figure 15a shows representative 20X fields of untreated, differentiated THP-1 cells, and differentiated THP-1 cells treated with Stx1, LPS, and Stx1 + LPS for 4, 12, and 24 h. Very few apoptotic cells were detected in any of the unstimulated controls, suggesting that trypsinization of adherent cells may have contributed to the high background apoptosis seen in the FACS data. While treatment with either Stx1 or LPS alone induced apoptosis, it is clear that treatment with both stimulants clearly enhanced apoptosis of differentiated THP-1 cells. For each treatment in 0.5% or 10% FBS, we counted the total number of TUNEL positive cells from 10 different 20X fields from three independent experiments (Fig. 15b). While untreated cells showed the lowest levels of apoptosis, treatment of cells with LPS, Stx1, or Stx1+LPS showed significantly elevated levels of apoptosis

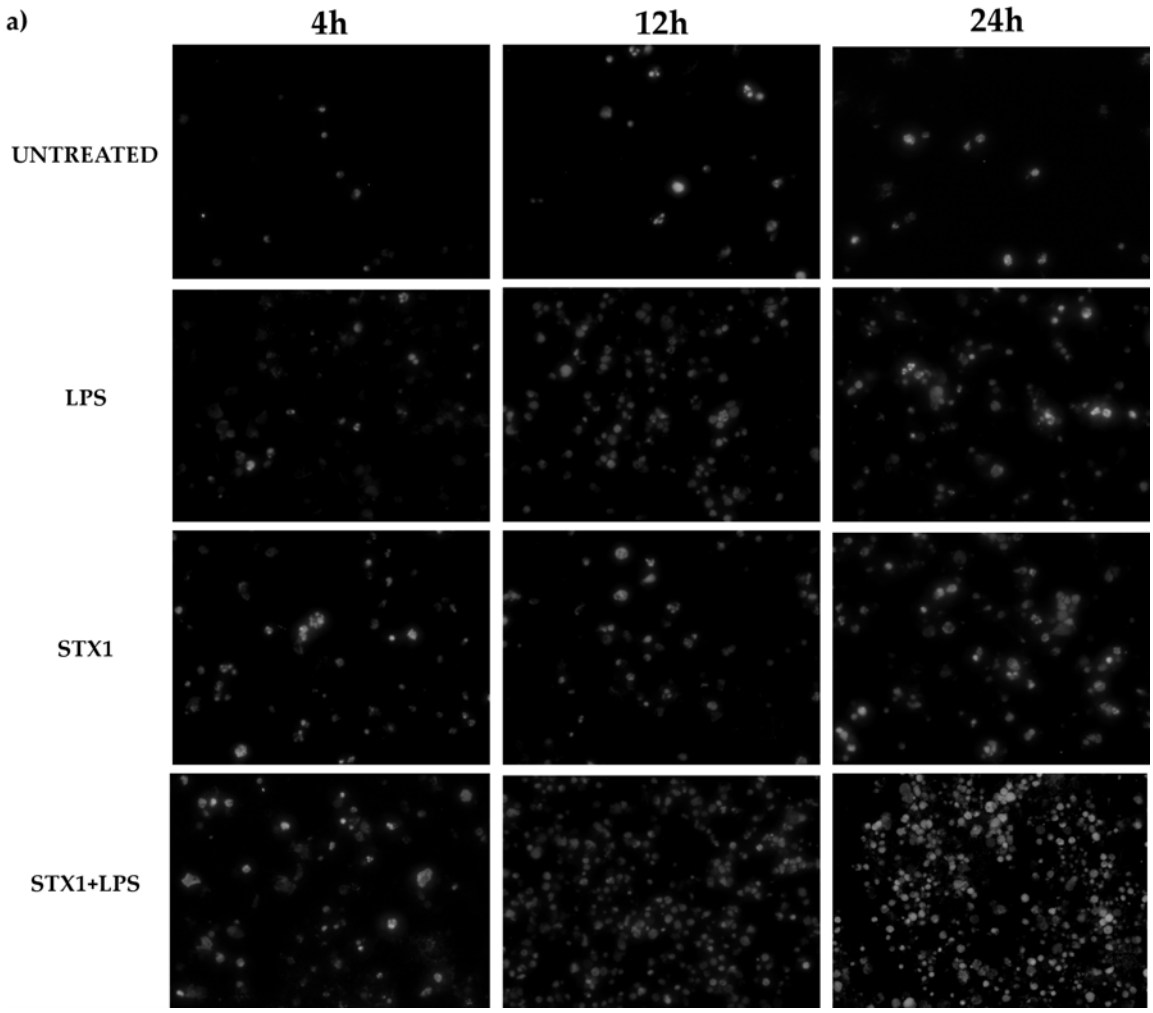

Figure 15. Apoptosis in differentiated THP-1 cells treated with Stx1, LPS, and Stx1 + LPS. Differentiated (macrophage-like) THP-1 cells grown on chamber slides were treated with Stx1 (400 ng/ml), LPS (200 ng/ml), or both for 4, 12, or 24 h in media containing 0.5% or 10% FBS. Cells were fixed, permeabilized, and incubated with TUNEL reaction solution. TUNEL positive cells were visualized by fluorescence microscopy, and 10 different 20X fields for each treatment were used to count total numbers of TUNEL positive cells. a) Representative 20X fields showing TUNEL positive cells from each treatment in 10% FBS. b) Numbers of TUNEL positive cells *per* 20X field for each treatment of differentiated THP-1 cells in media containing 0.5% FBS (top panel) or 10% FBS (bottom panel). Data shown are the means ± standard errors from at least three independent experiments. Significant differences ($p \leq 0.05$) between treatments at each time point occur for all data except where denoted by NS.

b)

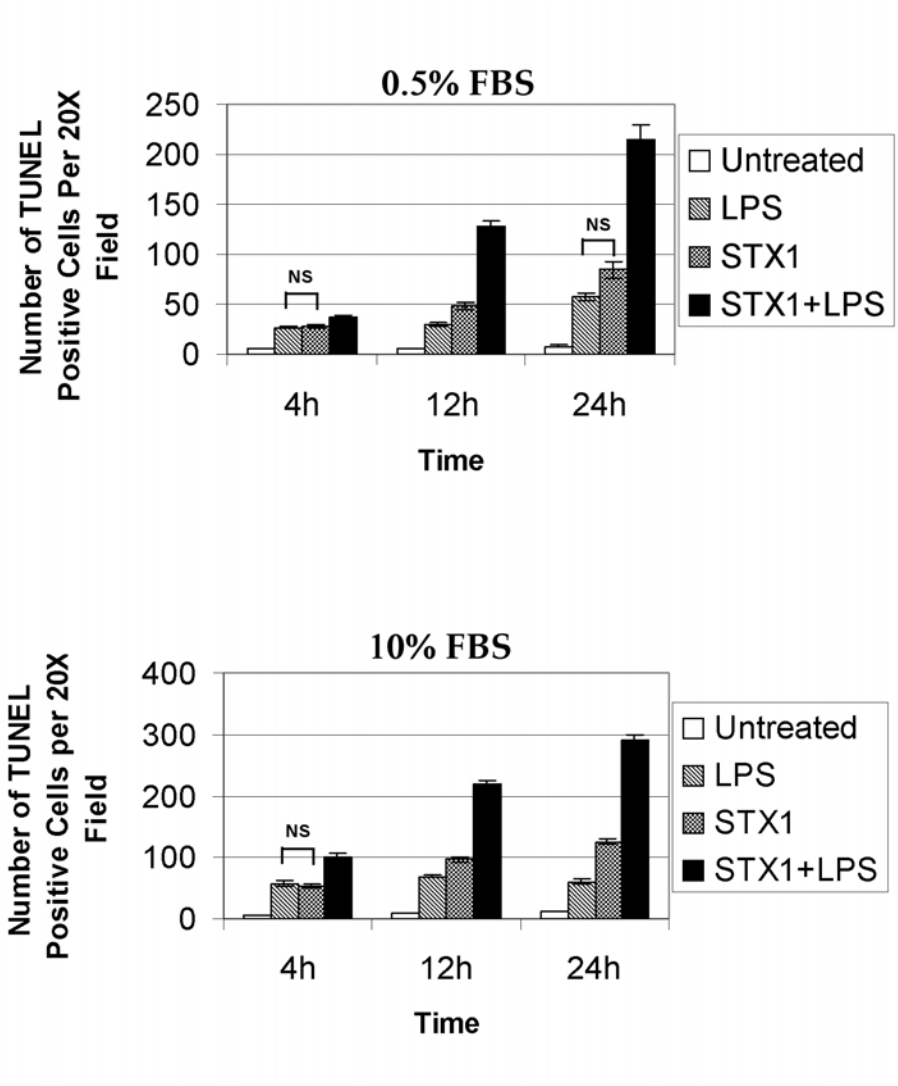

Figure 15 continued

above untreated cells. For two of the three time points in cells cultured in 0.5% FBS, and one of the three time points in cells cultured in 10% FBS, differences in apoptosis between Stx1 *vs.* LPS treatments were not significant (indicated by NS in Fig. 15b). These data suggest that both Stx1 and LPS are individually capable of inducing intermediate levels of apoptosis of differentiated THP-1 cells. However, comparisons between treatment with Stx1 + LPS and treatments with either stimulant alone resulted in significant differences in apoptosis, with Stx1 + LPS treatment yielding the highest levels of apoptosis at all the time points.

Stx1-induced apoptosis occurs in a dose-dependent manner and is inhibited by a general caspase inhibitor. A general feature of apoptosis is the cleavage of chromosomal DNA into 180-200 bp internucleosomal fragments (85). We visualized DNA fragmentation in THP-1 cells treated with Stx1, LPS, and Stx1 + LPS for 12 h. Stx1 triggered DNA fragmentation in a dose-dependent manner in undifferentiated (Fig. 16a) and differentiated THP-1 cells (Fig. 16c). Stx1-induced DNA fragmentation was inhibited in both undifferentiated and differentiated cells by the general caspase inhibitor, zVAD-fmk (50 μM) (Figs. 16a-c). Additionally, DNA fragmentation caused by LPS or Stx1 + LPS was also inhibited by zVAD-fmk (Figs. 16b, d). Collectively, these data suggest the involvement of caspases in signaling for Stx1-, LPS-, and Stx1 + LPS-induced apoptosis in THP-1 cells.

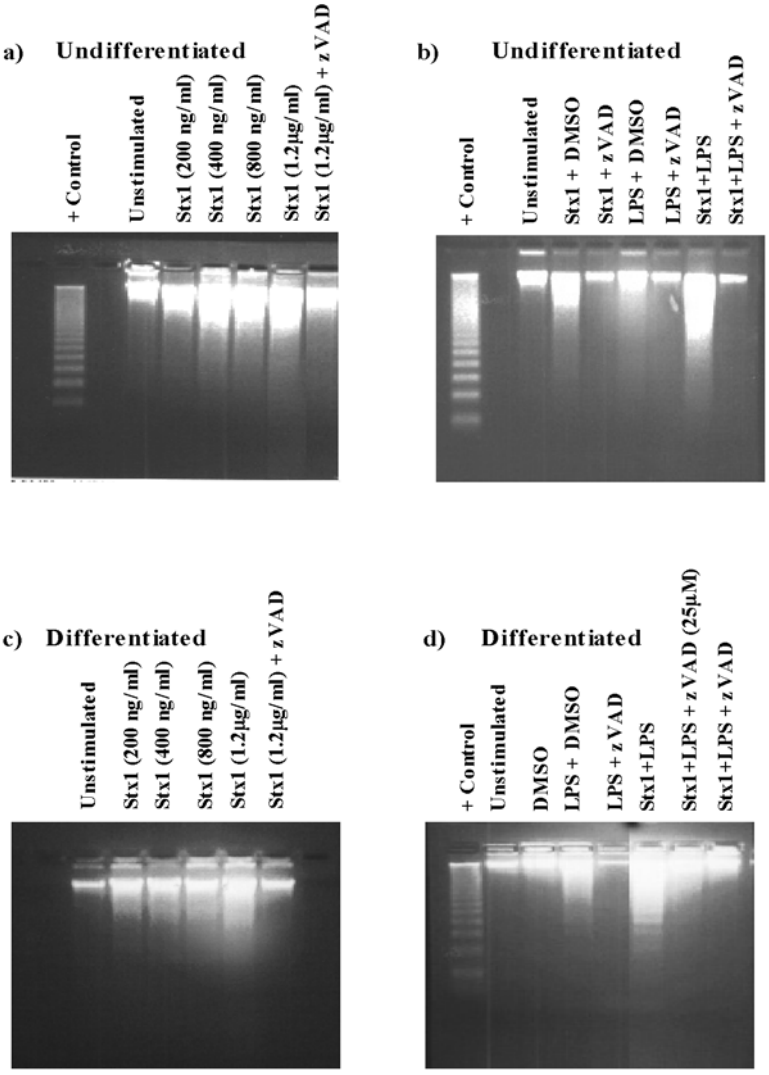

Figure 16. Stx1, LPS, and Stx1 + LPS induce DNA fragmentation which is inhibited by the general caspase inhibitor zVAD-fmk. Undifferentiated (monocytic) and differentiated (macrophage-like) THP-1 cells were treated with Stx1 (400 ng/ml), LPS (200 ng/ml), or both in media containing 10% FBS in the presence or absence of 50 µM (except where indicated) zVAD-fmk for 12 h at 37°C. DNA was extracted, and 2-4 µg of DNA from each treatment was electrophoresed into 1.2% agarose gels. DNA laddering was visualized using ethidium bromide under uv light. a) Dose response of apoptosis induction by Stx1 and zVAD inhibition of Stx1-induced apoptosis in undifferentiated THP-1 cells. b) zVAD inhibition of apoptosis induced by Stx1, LPS, and Stx1 + LPS in undifferentiated THP-1 cells. c) Dose response of apoptosis induction by Stx1 and zVAD inhibiton of Stx1-induced apoptosis in differentiated THP-1 cells. d) zVAD inhibition of apoptosis induced by LPS and Stx1 + LPS in differentiated THP-1 cells. Data shown are representative gels from at least three independent experiments.

Figure generated by Rama P. Cherla and Sang-Yun Lee.

Stx1, LPS, and Stx1+LPS induce the cleavage of PARP in both differentiated and undifferentiated THP-1 cells. Western blots were performed using cell lysates prepared from both differentiated and undifferentiated THP-1 cells that were treated with Stx 1, LPS or both to determine if the caspase-3 substrate, poly(ADP-ribose) polymerase (PARP) is cleaved. In accordance with the cell viability data and FACS analysis which showed that LPS was the least effective inducer of cell death and apoptosis in undifferentiated THP-1 cells, treatment of the monocytic cells with LPS showed low levels of the 89 kD PARP cleavage product, even after 20 h of stimulation (Fig. 17a, top panel). However, when cells were stimulated with Stx1 alone or Stx1 + LPS, PARP cleavage was apparent by 4 and 2 h, respectively (Fig. 17a, middle and bottom panels). In contrast to monocytic cells where LPS was not an effective inducer of PARP cleavage, treatment of macrophage-like THP-1 cells with LPS alone resulted in PARP cleavage that was detectable 1 h after stimulation (Fig. 17b, top panel). For macrophage-like cells treated with Stx1 or Stx1 + LPS, the 89kD PARP fragment can be seen 2 h after stimulation (Fig. 17b, bottom panel).

Apoptosis induction in THP-1 cells requires the presence of the Stx1 A -subunit. To determine if purified Stx1 B-subunits alone can induce apoptosis in monocytic and macrophage-like cells, we treated both undifferentiated and differentiated THP-1 cells with 800 ng/mL purified Stx1 B-subunit or 400 ng/ml

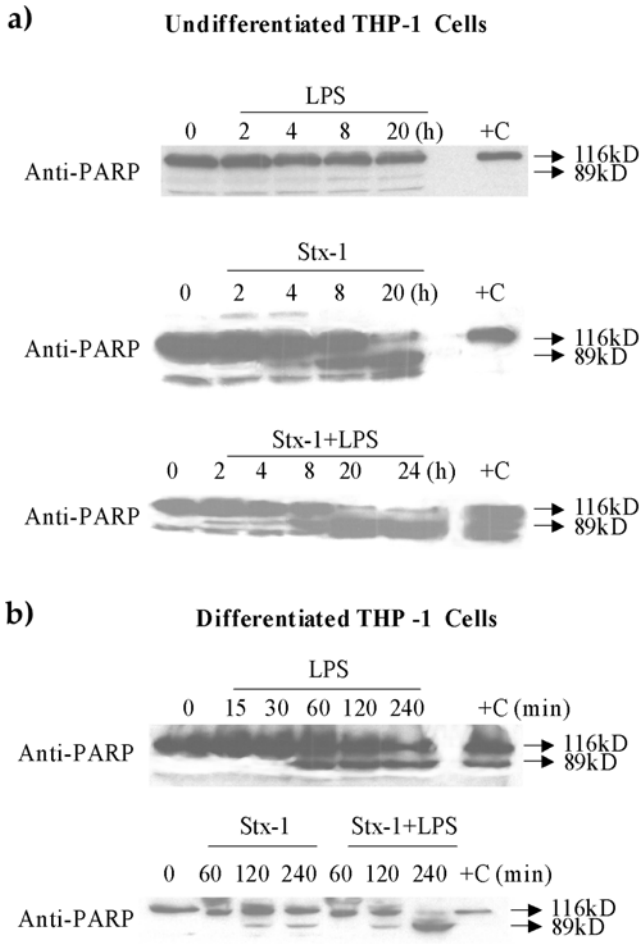

Figure 17. Treatment of undifferentiated and differentiated THP-1 cells with Stx1, LPS, and Stx1 + LPS induces PARP cleavage. Undifferentiated (monocytic) and differentiated (macrophage-like) THP-1 cells were treated for the indicated times with Stx1 (400 ng/ml), LPS (200 ng/ml), or both in media containing 0.5% FBS. Cells were lysed and total protein concentrations were determined from cellular extracts. Equal amounts of total proteins (60-80 μg) were separated by 8% Tris-glycine SDS-PAGE and transferred onto nitrocellulose membranes for detection of cleaved PARP using a PARP-specific antibody. a) PARP cleavage in undifferentiated THP-1 cells treated with LPS (top panel), Stx1 (middle panel), or Stx1 + LPS (bottom panel). b) PARP cleavage in differentiated THP-1 cells treated with Stx1 or Stx1+LPS (top panel), or LPS (bottom panel). Data shown are representative blots from at least two independent experiments.

Figure generated by Rama P. Cherla and Sang-Yun Lee.

Stx1 for 4, 12, and 24 h. Cells were stained with Annexin V and PI, and percentages of apoptotic cell death calculated by FACS analysis. Despite the variability associated with the use of trypsin to detach adherent differentiated cells, neither undifferentiated nor differentiated cells treated with Stx1 B-subunits showed statistically significant induction of apoptosis above unstimulated control cells at any time point (Fig. 18). These data suggest that the Stx1 B-subunit alone is incapable of inducing apoptosis in THP-1 cells, and that the holotoxin is required for apoptosis induction.

Apoptosis macroarrays for differentiated THP-1 cells. We have shown that Stxs and LPS up-regulate TNF-α and IL-1β expression by differentiated THP-1 cells *in vitro* (99). To examine the role, if any, of Stx1 and LPS in the regulation of expression of apoptosis-related genes, we utilized commercially available macroarray membranes spotted in duplicate with 205 cDNAs derived from apoptosis-related genes. cDNAs were prepared from total RNA extracted from differentiated THP-1 cells treated with Stx1, LPS, or Stx1 + LPS for 6 and 12 h. Radiolabeled cDNAs were hybridized to apoptosis-related gene macroarrays, hybridization intensity was quantitated using a Phosphorimager (Molecular

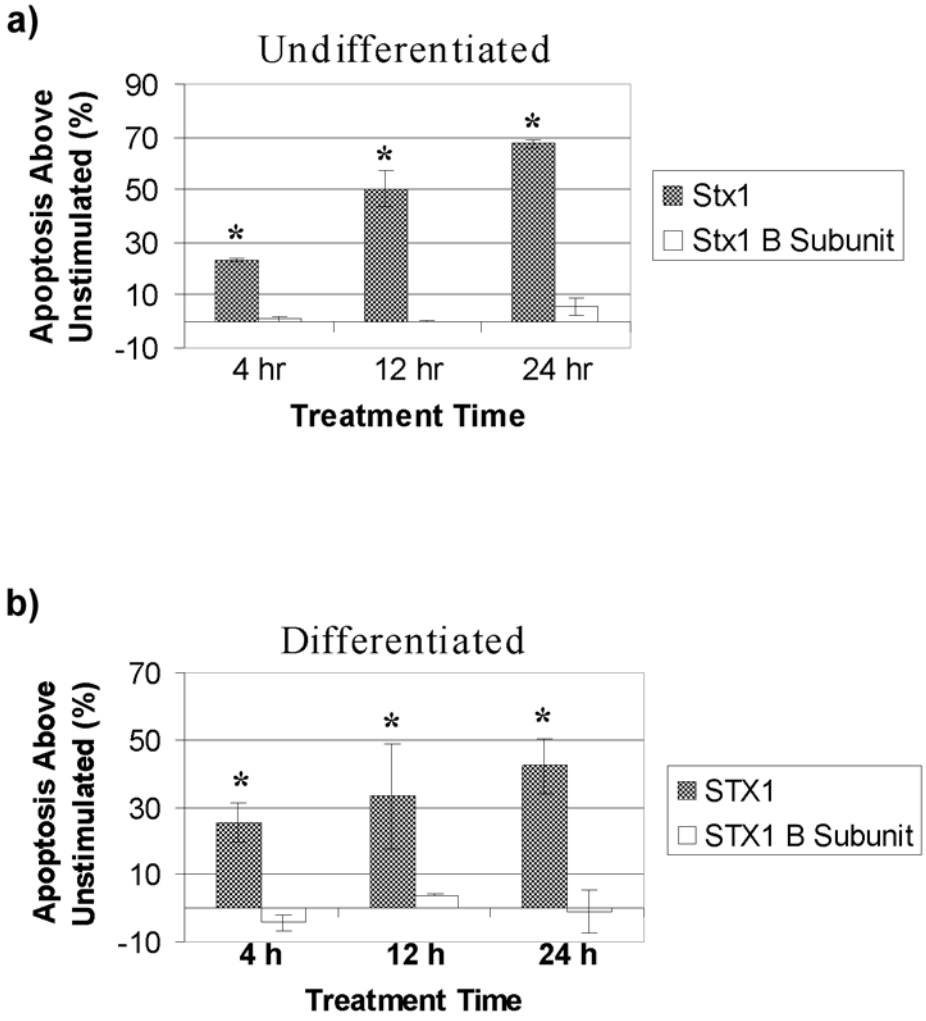

Figure 18. Purified Stx1 B-subunits do not induce apoptosis of undifferentiated or differentiated THP-1 cells. Undifferentiated (monocytic) or differentiated (macrophage-like) THP-1 cells were treated with purified Stx1 B-subunits (800 ng/ml), or Stx1 (400 ng/ml) in media containing 10% FBS for 4, 12, and 24 h. Cells were stained with Annexin-V and PI, and were subjected to FACS analysis. a) Percentage of apoptosis induction by Stx1 or Stx1 B-subunits above unstimulated controls in undifferentiated THP-1 cells. b) Percentage of apoptosis induction by Stx1 or Stx1 B-subunits above unstimulated controls in differentiated THP-1 cells. Data shown are means ± standard errors from at least two independent experiments. An asterisk (*) denotes a significant difference ($P \leq 0.05$) between Stx1- and Stx1 B-subunit-induced apoptosis.

Dynamics), and significant up- and down-regulation of expression was established as 2-times the hybridization signal generated by cDNAs derived from unstimulated cells. Using this assay, we determined that only two genes were up-regulated, and no genes were down-regulated, in response to stimulation with Stx1, LPS, or both. The genes up-regulated in response to the stimulants encoded TNF-α and TNF ligand superfamily member 7 (TNFSF7 or CD70). Optimal fold induction occurred following treatment with Stx1 and/or LPS for 6 h. Maximum fold inductions for TNF-α induced by Stx1, LPS, or both were 9.9, 33.6, and 84.1, respectively. Fold induction maxima for TNFSF7 induced by Stx1, LPS, or both were < 2, 6.1, and 8.4, respectively. By 12 h of treatment, all fold-induction values were < 2-fold (data not shown). These data suggest that the induction of apoptosis by Stx1 and/or LPS does not require the extensive expression of apoptosis-related genes.

Discussion

We previously showed that undifferentiated, monocytic THP-1 cells express the Stx receptor Gb_3 and are killed by treatment with purified Stxs. In contrast, differentiated, macrophage-like THP-1 cells express lower levels of Gb_3, express increased levels of membrane CD14, and rapidly respond to toxin challenge by secreting the proinflammatory cytokines TNF-α and IL-1β (99). Based on these findings, we employed differentiated THP-1 cells treated with Stx1 and/or LPS for short time periods (< 4 h) to study the expression and regulation of proinflammatory cytokine genes, the activation of transcriptional factors NF-κB and AP-1, and the activation of the ribotoxic stress response through the stress-activated protein kinase cascades JNK and p38 (24,38,105). When we extended our time course studies to examine the stabilities of TNF-α and IL-1β mRNA transcripts induced by Stxs, we noted that prolonged exposure of differentiated THP-1 cells to Stx1 and/or LPS resulted in decreasing yields of extractable RNA and increased detachment of cells from culture plates. These observations suggested that macrophage-like THP-1 cells may indeed be susceptible to killing by Stx1, but that killing may be delayed in comparison to killing of undifferentiated cells. We used the cell viability stain MTT to show that treatment of THP-1 cells with Stx1 and LPS resulted in cell death, although

the kinetics and extent of cell death differed based on the maturation state of the cells. Undifferentiated THP-1 cells were relatively refractory to killing mediated by LPS (Fig. 13a). However, treatment of monocytic cells with Stx1, in the presence or absence of LPS, resulted in the rapid onset of cell death that reached maximal levels within 12 h. Macrophage-like THP-1 cells manifested a different pattern of cell death in response to the stimulants (Fig. 13b). Differentiated cells were less sensitive to killing by Stx1 alone and showed a more rapid onset of cell death when treated with LPS alone. Treatment of cells with Stx1 + LPS resulted in maximal cell death for both undifferentiated and differentiated THP-1 cells, although the kinetics of cell death appeared to be slightly different between macrophage-like cells (68.6% at 12 h) compared to monocytic cells (88.1% at 12 h).

Stxs have been shown to induce apoptosis in numerous cells types (8). Kojio *et al*. showed that Stxs induce apoptosis in undifferentiated THP-1 cells (59). We used Annexin V/PI double-labeling, TUNEL staining, and DNA laddering assays to extend on these studies to show that both Stx1 and LPS trigger apoptosis in undifferentiated and differentiated THP-1 cells. In accordance with the cell viability assays, monocytic cells undergo apoptosis in a similar manner when cells are treated with Stx1 in the absence or presence of LPS, while LPS alone is the least potent inducer of apoptosis (Fig. 14). In macrophage-like cells, apoptosis induction by Stx1 or LPS alone is significantly

elevated compared to untreated cells, and the combination of both stimulants markedly increased the numbers of TUNEL positive cells detected *per* microscopic field (Fig. 15). A similar macrophage cell death enhancement phenomenon was recently reported using 12-*O*-tetradecanoylphorbol 13-acetate treated human leukemic U937 cells treated with LPS derived from the periodontal pathogen *Actinobacillus actinomycetemcomitans* and the protein synthesis inhibitor cycloheximide (125). While neither LPS nor cycloheximide alone effectively induced apoptosis, the combination of the two induced apoptosis characterized by DNA laddering, increased release of cytochrome c into the cytoplasm, and the activation of caspase-3. These data suggest that anti-apoptotic pathways normally activated by LPS may be compromised in the face of protein synthesis inhibition, leading to enhanced programmed cell death.

It is tempting to speculate that sensitivity of the cells to apoptosis by Stx1 or LPS is directly correlated with expression of the Stx receptor Gb_3 and the LPS receptor CD14, although a number of issues confound this speculation. For example, it has been shown that Stx binding and intracellular trafficking are dependent upon the isoform of Gb_3 synthesized (1,93) and the expression of Gb_3 within glycolipid-enriched microdomains in the membrane (17). LPS has been reported to delay apoptosis of primary human blood monocytes *in vitro* (74). We showed that treatment of THP-1 cells with PMA or other differentiative agents modestly increased membrane CD14 expression (99), and Suzuki *et al.* (125)

showed that apoptosis induced by LPS treatment of cycloheximide-treated U937 cells was blocked by pre-treatment with antibodies directed against CD14 or toll-like receptor 4. The precise mechanisms contributing to enhanced cytotoxicity caused by Stx1 + LPS treatment, and the rapid (within 6 h) onset of cell death that we noted in approximately one-third of PMA-differentiated THP-1 cells treated with LPS alone, remain to be explored.

Apoptosis may be induced through the sequential activation of a family of cysteine-dependent, aspartate-specific proteases called caspases. Procaspases are precursors that are constitutively expressed as cytosolic single-chain proteins. Activation of caspase cascades usually involves proteolytic cleavage of procaspases to form heterodimers that then assemble into tetramers that possess proteolytic activity (122). There are two major pathways of caspase activation: extrinsic activation which is triggered through the engagement of membrane-bound "death receptors" (*e.g.*, Fas-FasL engagement), and intrinsic activation which is triggered by cell stressors that alter mitochondrial transmembrane potential (33). Although there may be additional pathways of apoptosis induction, both major activation pathways converge on caspase-3. Caspase-3 is referred to as an "executioner" caspase since its downstream substrates are directly involved in morphological and biochemical processes leading to apoptosis. In the presence of DNA strand breaks, PARP binds the damaged strands, and using NAD as an ADP-ribose donor, initiates the process of

autocrine poly-ADP-ribosylation. Subsequently, the modified PARP molecule dissociates from DNA and the repair process begins. Following activation of apoptosis, caspase-3 and caspase-7 may cleave PARP so that the DNA-binding and catalytic domains of PARP are separated. A fragment of PARP remains associated with DNA and repair does not proceed (121). We show here that caspases are involved in Stx1-, LPS-, and Stx1 + LPS-induced apoptosis of monocytic and macrophage-like THP-1 cells, as the general caspase inhibitor Z-VAD-fmk inhibits DNA fragmentation induced by the stimulants (Fig. 16). Just as LPS treatment of undifferentiated cells was the least effective inducer of cell death and apoptosis, LPS treatment of monocytic cells had the least effect on PARP cleavage (Fig. 17a). In contrast, treatment of undifferentiated cells with Stx1 or Stx1 + LPS induced PARP cleavage. The kinetics of PARP cleavage appeared to be slower in undifferentiated cells compared to differentiated cells, where all the stimulants induced PARP cleavage within 1 to 2 h of stimulation (Fig. 17b). Cleavage of PARP following treatment with Stx1 and/or LPS may be due, in part, to the activation of caspase-3. Experiments are ongoing in our laboratory to characterize caspase cascades activated in both undifferentiated and differentiated THP-1 cells following treatment with Stx1 in the presence or absence of LPS.

A number of studies demonstrated that treating B-lymphoma cells with purified B-subunits or anti-Gb_3 antibodies was sufficient to induce apoptosis

(75,126,135), possibly through cross-linking Gb_3 on the cell membrane (66). We show here that purified Stx1 B-subunits are unable to induce apoptosis in monocytic or macrophage-like THP-1 cells (Fig. 18) suggesting that the presence or the action of the Stx1 A-subunit may be necessary for apoptosis induction. Treatment of undifferentiated THP-1 cells with brefeldin A, a compound that disrupts toxin retrograde transport, also inhibited apoptosis induced by Stxs (59). Collectively, these data suggest that the A-subunit must be internalized and routed to ER or nuclear membranes for apoptosis to occur. Macroarray analysis suggested that apoptosis was induced without the need for extensive *de novo* transcription, as out of 205 apoptosis related genes, only TNF-α and TNFSF7 (CD70) mRNA expression were up-regulated in response to treatment with Stx1 and/or LPS. TNF-α is a well-characterized initiator of apoptosis, acting through TNF receptors to promote death signals through the assembly of TNFR-associated death domain protein, Fas-associated death domain protein, and caspase-8 (143). TNF-α is capable of inducing apoptosis in monocyte-derived macrophages, particularly when anti-apoptotic signaling pathways are blocked (69). CD70 is a type II transmembrane glycoprotein with homology to TNF-α that is primarily expressed by activated lymphocytes (64). CD70 acts as a co-stimulatory molecule for enhancement of proliferation by $CD45RA^+$ (naïve) $CD4^+$ T-cells, cytotoxicity mediated by $CD8^+$ T-cells, and immunoglobulin

synthesis by B-cells. Ramos and Raji B-lymphoma cell lines express both CD70 and CD27, and the cells undergo apoptosis when CD70 molecules are overexpressed on the cell surface (96). Human NK cells constitutively express CD70 and other TNF ligand superfamily members, and are capable of rapidly killing solid tumor cell targets via a non-secretory apoptotic mechanism (56). The role of CD70-CD27 interaction in the induction of macrophage apoptosis is less well understood. Goodwin *et al.* (32) detected CD70 mRNA in THP-1 cells by Northern blot analysis, but Hintzen *et al.* (42) failed to detect membrane CD70 expression by PMA- or IFN-γ-treated U937 cells, or by resting or activated monocytes. We have previously shown that levels of soluble TNF-α proteins are increased by Stx and LPS treatment of macrophages (99). Whether or not macrophages will express membrane CD70 after Stx or LPS treatment, and the role CD70 in apoptosis induction, await further analysis.

The monocyte/macrophage represents a first line of defense against microbial invaders. We have used our results on proinflammatory cytokine production by, and apoptosis of, THP-1 cells in response to treatment with Stx1 and LPS to derive a model of the role of these sentinel cells in the pathogenesis of disease caused by Stx-producing bacteria (Fig. 19). Following the invasion of

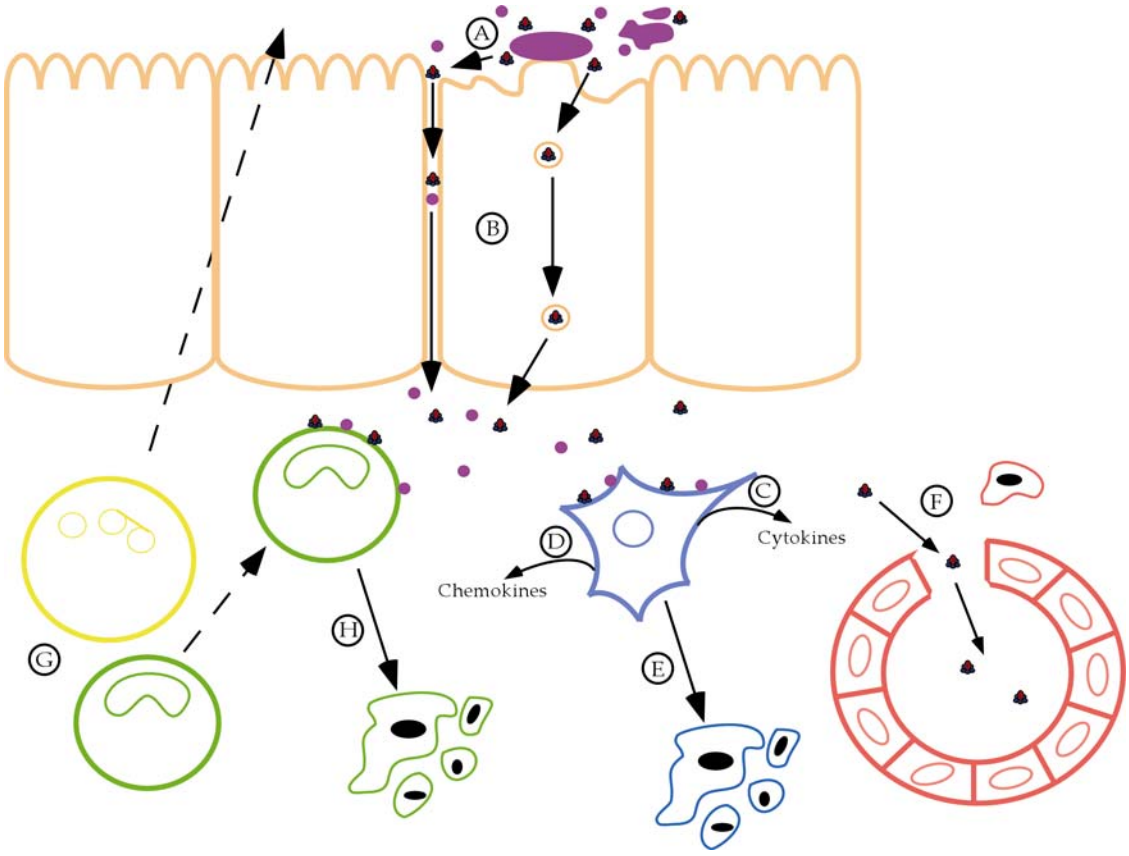

Figure 19. Potential roles of Stxs and LPS in the pathogenesis of disease caused by Stx-producing bacteria. A. *S. dysenteriae* serotype 1 invade (not shown), or STEC intimately adhere to, the colonic epithelium. B. The bacteria produce and release Stxs and LPS, which may gain access to the submucosa via transcytotic or paracellular mechanisms. C, D) Stxs and LPS are internalized by resident tissue macrophages, rapidly inducing the production and secretion of proinflammatory cytokines and chemokines. E) Macrophages then are induced to undergo apoptosis. F) TNF-α and IL-1β upregulate expression of the Stx receptor on endothelial cells, resulting in increased vascular destruction and systemic transport of Stxs and LPS in the blood. G) Chemokines recruit PMNs and blood monocytes into the submucosa. H) Monocytes rapidly undergo apoptosis following exposure to Stxs and LPS.

colonic epithelial cells by *S. dysenteriae* serotype 1 (not shown), or intimate adherence to epithelial cells by STEC, the bacteria produce Stxs (Fig 19, A). The mechanism of transepithelial transport of Stxs across the colonic epithelial barrier (Fig. 19, B) is an area of active research, with energy-dependent transcytotic and paracellular toxin transport mechanisms described (43,44,94). LPS from Stx-producing bacteria or from other intestinal flora, may also gain access to the submucosa, as patients with *S. dysenteriae* serotype 1 infections may be endotoxemic (60), and patients with STEC infections frequently possess elevated anti-STEC O-antigen antibody titers (97). Once within the lamina propria, the toxins encounter resident tissue macrophages. The toxins are internalized, eliciting the rapid expression and
secretion of proinflammatory cytokines and chemokines (Fig. 19, C, D). Coincident with signaling for cytokine production, Stxs and LPS also signal apoptosis induction in macrophages (Fig. 19, E). The cytokines TNF-α and IL-1β may exacerbate Stx-induced damage to colonic capillaries, releasing blood into the lumen of the intestine and creating a portal of entry for Stxs and LPS into the bloodstream (Fig. 19, F). Simultaneously, chemokines expressed by tissue macrophages and intestinal epithelial cells (137) trigger the extravasation and directed migration of peripheral blood monocytes and neutrophils from the bloodstream into the submucosa (Fig. 19, G). Our data suggest that newly extravasated monocytes may rapidly undergo apoptosis in response to Stxs and

LPS. In this way, a potentially beneficial cell type capable of phagocytosis, and with the appropriate stimulation, antigen processing and presentation, may be eliminated from the submucosa (Fig. 19, H). In contrast to monocytes, studies examining the interaction of Stxs with human neutrophils suggest that the toxins delay the onset of apoptosis (70). Thus, neutrophils may migrate into the submucosa and pass through the epithelial cell barrier, thereby increasing paracellular "leakiness" leading to fecal leukocytosis and increased paracellular transport of Stxs and LPS into the lamina propria.

The risk factors for progression from bloody diarrhea to the life-threatening systemic complications following infection with Stx-producing bacteria are not well understood. Our data suggest that the perturbation of normal colonic epithelial barrier function, allowing both Stxs and LPS to access the submucosa and bloodstream, may be an important factor in progression of disease. The presence of both bacterial products may maximize signaling for macrophage cytokine expression and monocyte/macrophage apoptotic cell death. Stxs clearly modulate the host innate immune response. Further study will be necessary to devise interventional therapeutic strategies to overcome the capacity of Stxs to eliminate a critical cell type, the monocyte/macrophage, in the establishment of an effective immune response.

CHAPTER V

CONCLUSIONS

Children infected with *Shigella dysenteriae* type 1 or Stx-producing bacteria may develop severe bloody diarrhea, and possibly serious post-diarrheal complications in the form of HUS or CNS disorders (92,97). The development of such life-threatening sequelae is associated with the production of potent cytotoxins known as Shiga toxins (Stxs) (53). Stxs promote disease in the kidneys and CNS by injuring the microvascular endothelial cells of these organs. Once internalized through receptor-mediated endocytosis (1,109), via binding to Gb_3 (49,65), Stxs inhibit protein synthesis by cleaving a single adenine residue on ribosomes, blocking peptide elongation (16,45,89,111). Damage to intestinal microvascular endothelial cells results in endothelial cell swelling and subsequent detachment of cells from the basement membrane, allowing Stx access to the bloodstream (117). Even though Stxs are known to have pathological effects on endothelial cells, *in vitro* studies have indicated that many endothelial cell types are not sensitive to the cytotoxic actions of Stxs (88,134), suggesting the involvement of additional factors. These factors may possibly be proinflammatory cytokines such as tumor necrosis factor-alpha (TNF-α) and interleukin-1 beta (IL-1β), since some patients with HUS have elevated levels of both cytokines in their sera and urine (130). Furthermore, both

of these cytokines have also been shown to increase sensitivity to Stxs by up-regulating the Stx receptor, Gb_3, on the surface of different endothelial cell types, *in vitro* (15,72,88,98,139,142). While the actual sources of these cytokines is not known, it is possible that tissue macrophages are involved in cytokine production. In 1996, van Setten et al (140) reported that nonadherent human monocytes were able to produce both TNF-α and IL-1β following treatment with Stx1. However, in the tissues, it seems more likely that mature macrophages would encounter Stxs. Therefore, our lab has concentrated on developing a model system using the human monocytic cell line THP-1, which we differentiate into adherent, mature, macrophage-like cells, giving them the properties more representative of the resident tissue macrophages (2). Previous work in our lab has demonstrated that differentiated THP-1 cells treated with purified Stx1 were able to produce both TNF-α and IL-1β (99). In addition to Stxs, LPS is also known to be a potent inducer of cytokine expression. Patients infected with *S. dysenteriae* are frequently endotoxemic (60), while some patients infected with EHEC present with elevated antibody titers directed against EHEC O-antigens (52,97), suggesting that LPS may play a role in exacerbating the diseases caused by Stxs. Previous experiments examining TNF-α mRNA and protein kinetics in differentiated THP-1 cells, following treatment Stx1 and/or LPS, revealed prolonged mRNA expression over time in Stx1- and Stx1+LPS-

treated cells, in addition to higher levels of both TNF-α mRNA and protein when cells were treated with Stx1+LPS compared to either stimulant alone (105). Prolonged expression of proinflammatory cytokines could be detrimental to the integrity of host tissues, and the extended presence of TNF-α and IL-1β could further promote the up-regulation of Gb_3 expression on endothelial cells, thus increasing microvascular damage in the tissues. One possible contributor to the prolonged transcript elevation is increased mRNA stability.

A time course extension of the TNF-α mRNA kinetics study revealed that treatment of THP-1 cells with Stx1 or Stx1+LPS resulted in a similar transcript profile as previous experiments, showing extended expression over time compared to treatment with LPS alone (Figure 1, Chapter II). Treatment with Stx1+LPS also resulted in significantly higher TNF-α message compared to treatment with LPS. Interestingly, the combination of Stx1 and LPS induced rapid TNF-α transcription, as with treatment with LPS alone, but displayed the same prolonged elevation of transcripts as Stx1-induced transcripts. These data suggest a difference in signaling pathways elicited by Stx1 and LPS, and that the combination of the two stimulants leads to optimal TNF-α expression. As previously noted, Stx1 treatment alone is a less potent inducer of TNF-α message or protein compared to LPS or Stx1+LPS treatment. Production and secretion of TNF-α protein, up to 12 h, was previously determined by Sakiri et al

in 1998, and showed a pattern that correlated with mRNA production, with Stx1+LPS yielding the greatest level of TNF-α protein (105).

The prolonged TNF-α mRNA and protein levels appear to be due, in part, to an increase in Stx1-induced mRNA stability (Figure 5, Chapter II). The levels of Stx1- and Stx1+LPS-induced TNF-α transcripts are not only significantly higher compared to LPS-induced transcripts (Figure 5b, Chapter II), but the calculated half-lives of TNF-α transcripts from cells treated with Stx1 or Stx1+LPS are also significantly greater than transcripts from cells treated with LPS alone (Table 1, Chapter II). Based on these observations, Stx1 appears play a role in regulating TNF-α expression in human macrophages, at a post-transcriptional level. A similar mRNA stabilization phenomenon has been described for IL-8 regulation in the human intestinal epithelial cell line, HCT-8, following treatment with purified Stx1 (137). The mechanisms controlling the stability of cytokine transcripts have not been completely characterized, however, the AU-rich elements (ARE) within the 3' untranslated regions (3' UTRs) of cytokine transcripts appear to be involved (6). Proteins that bind to the ARE can result in interactions that either promote or prevent degradation of RNA transcripts. For instance, binding of tristetraprolin or butyrate to TNF-α ARE can result in increased deadenylation and degradation of the transcript (7,61,62,123). In contrast, binding of TIA-1 or TIAR to TNF-α ARE results in

cytoplasmic ribonucleoprotein complexes, which sequester TNF-α mRNA, resulting in translational silencing (36,57,95). The effects of such ARE-binding proteins on Stx-induced TNF-α mRNA stability is not known, although we suspect that it is more likely that TIA-1 or TIAR would be involved. In addition to post-transcriptional regulation, it has been reported that Stx1 may also regulate TNF-α expression at the transcriptional level, based on experiments demonstrating that the transcription factors nuclear factor-κB (NF-κB) and activator protein-1 (AP-1) translocate into the nucleus following treatment with Stx1 (105). Direct evidence for the roles of NF-κB and AP-1 in the activation of TNF-α expression has not yet been determined due to the difficulty of stably transfecting differentiated THP-1 cells.

In comparison to TNF-α, experiments conducted to examine the kinetics of IL-1β mRNA and protein, as well as the role of mRNA stability in Stx-induced pathogenesis, revealed some differences. First of all, IL-1β mRNA kinetics differed from that of TNF-α, in that IL-1β induction was not significantly different between treatments with Stx1, LPS, and Stx1+LPS (Figure 2, Chapter II). Secondly, treatment with Stx1 alone resulted in greater levels of IL-1β transcripts compared to TNF-α transcripts, suggesting a difference in the effect of Stx1 on the transcriptional regulation of the two cytokines. Also, the kinetics of IL-1β transcripts indicate a dominant role of LPS in inducing IL-1β

transcription since co-treatment with Stx1 fails to significantly augment IL-1β transcript levels above those in cells treated solely with LPS. The lack of IL-1β superinduction has been described previously, in human peripheral blood mononuclear cells (PBMCs), following treatment with a combination of LPS and the protein synthesis inhibitor cycloheximide (112). In the same report, the authors observed superinduction of TNF-α mRNA when PBMCs were treated with LPS and cycloheximide. Another report, involving plastic-adherent THP-1 cells, showed that IL-1β mRNA was superinduced following treatment with LPS+cycloheximide (19). Although this differs from our results, which do not suggest superinduction following treatment with LPS plus a protein synthesis inhibitor, it is possible that the differences in inhibitor concentrations, or differences in the mechanisms of protein synthesis inhibition may alter the outcome. Previous work in our lab indicated, however, that very low levels of protein synthesis inhibition (≈ 10%) were detected in Stx1-treated differentiated THP-1 cells (23).

Despite the lack of a significant synergistic effect by treatment with both Stx1 and LPS, the higher levels of IL-1β mRNA compared to TNF-α mRNA led us to believe that IL-1β production could still contribute to Stx1-induced pathogenesis, possibly through an increase in transcript stability. As with TNF-α transcripts, IL-1β transcripts levels were significantly greater in cells treated

with Stx1 or Stx1+LPS (Figure 6b, Chapter II), however, the half-life of IL-1β mRNA from Stx1-treated cells was not significantly greater than that from LPS-treated cells (Table 1, Chapter II). Although the half-life of IL-1β mRNA in cells treated with Stx1+LPS was greater than 150 mins, the parameters of our experiment did not allow for an exact half-life calculation. In contrast to TNF-α, Stx1 alone did not appear to play a significant role in increasing IL-1β mRNA stability.

At the protein level, IL-1β expression, again, differed from TNF-α expression (Figure 3, Chapter II). Treatment with Stx1+LPS did not result in significantly greater levels of IL-1β protein production compared to treatment with LPS or Stx1 alone. Furthermore, based on IL-1β mRNA levels from Stx1-treated THP-1 cells, which were approximately 2-fold less than in LPS-treated cells, we anticipated the same levels of IL-1β protein. Instead, Stx1-treated cells yielded 20-fold less IL-1β protein compared to LPS-treated cells. IL-1β mRNA and protein production appears to require the presence of the Stx1 holotoxin, as purified Stx1 B-subunits are unable to initiate IL-1β expression (Figure 4, Chapter II). The dissociation between IL-1β mRNA and protein levels is unclear, and we were initially tempted to attribute this disconnect to the fact that Stx1 is a protein synthesis inhibitor. However, as stated above, protein synthesis is only slightly inhibited (≈ 10%) in differentiated THP-1 cells

following treatment with Stx1, up to 4 h (23). Another possible explanation may lie in the mechanisms involved in the post-translational processing and release of IL-1β. Following transcription, IL-1β mRNA is translated into Pro-IL-1β (35 kDa), and stored until it is cleaved, by a complex of proteases and proteins called an inflammasome, into active IL-1β (17 kDa) (76). In an abstract by Greenwell-Wild et al (34), macrophages are described to produce IL-1β mRNA, but, due to a decrease in caspase-1 activity, are not able to secrete IL-1β protein after infection with *Mycobacterium avium*. Another disconnect has been described between IL-1β mRNA and protein production in human PBMCs (112), although this was attributed to the process of adherence. Subsequent LPS, *S. epidermidis*, or cycloheximide treatment of the human PBMCs resulted in IL-1β protein production in addition to IL-1β mRNA production. Lastly, in order to determine if some of the IL-1β protein detected in our experiments included ProIL-1β, cell supernatants from Stx1-treated THP-1 cells were tested using ProIL-1β-specific ELISAs. The levels of ProIL-1β protein (Figure 20) detected were almost identical to the levels of IL-1β protein (Figure 3, Chapter II) suggesting that the IL-1β protein detected initially from Stx1-treated THP-1 cells may be in the form of ProIL-1β. Therefore, in actuality, Stx1 treatment of THP-1 cells does not appear to induce IL-1β protein production, despite the induction of large amounts of IL-1β mRNA. It is still feasible that Stx1 may be affecting

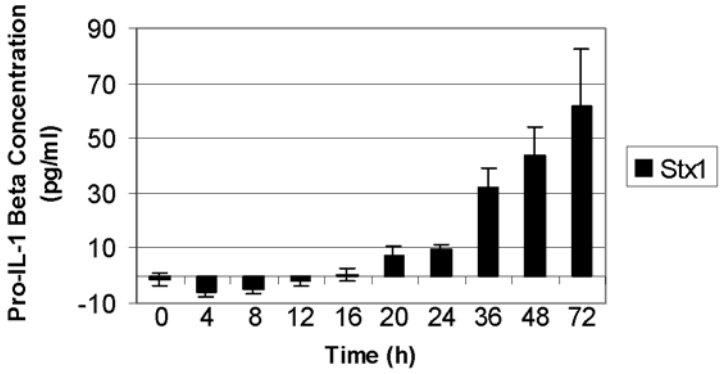

Figure 20. Pro-IL-1β protein production by THP-1 cells treated with Stx1. Cell-free supernatants from Stx1-treated cells were collected and analyzed using human Pro-IL-1β-specific ELISAs. Data shown are the means ± standard error of the means from triplicate determinations of three independent experiments.

the post-translational processing and secretion of IL-1β protein through the alteration of inflammasome function, possibly by preventing caspase-1 or caspase-5 activity. However, the role for IL-1β in the macrophage model of Stx pathogenesis remains uncertain. At least in differentiated THP-1 cells, IL-1β is not secreted following Stx treatment, and therefore, suggests that IL-1β would not be involved in up-regulating Gb_3 on target endothelial cell surfaces for increased Stx sensitivity. The treatment of other macrophage-like cells lines and primary macrophages with Stxs would be useful in resolving this issue, since the lack of IL-1β secretion THP-1 cells may be a consequence of the differentiation process. Determining the presence of intracellular stores of IL-1β protein as well as the status of caspase-1 activation would provide further insight on the level of IL-1β regulation affected by Stx1 treatment.

In addition to the possible roles of TNF-α and IL-1β in Stx-induced pathogenesis, other proinflammatory mediators may contribute to the extensive tissue damage seen in infections with Stx-producing bacteria. Neutrophil infiltration was detected in the colons of patients infected with Stx-producing bacteria (119), and the kidneys of baboons who were injected with Stx1 plus LPS (118). Both humans and baboons with HUS had elevated sera and urinary concentrations of IL-8 (20,141), which indicated that the production of chemokines, such as IL-8, in tissues exposed to Stxs and LPS, may be partially

responsible for the extensive tissue pathology seen in HUS patients. *In vitro* experiments, using intestinal epithelial cell lines, have indicated that Stxs may be able to actively translocate across the mucosal barrier, as well as induce IL-8 expression, which can promote neutrophil migration, and thus compromise the monolayer and increase Stx paracellular transport (44,94,136).

Besides epithelial cells, other cell types such as the macrophage may also contribute to the localized inflammatory response through the elicitation of chemokines. Monocytes have been shown to produce IL-8 following exposure to Stx1 (140), however as previously mentioned, resident tissue macrophages may be more likely to encounter Stxs in target organs. By using differentiated THP-1 cells, we were able to show that mature macrophage-like cells were able to express IL-8 mRNA and protein in response to treatment with Stx1, LPS, and Stx1+LPS (Figures 9 & 11, Chapter III). These data suggest that macrophages could be a possible source of IL-8 in the intestines and kidneys following infection with Stx-producing bacteria. Also, treatment with Stx1+LPS appeared to induce significantly greater levels of IL-8 transcripts compared to treatment with LPS. Experiments to determine the role of mRNA stability in elevated IL-8 transcript levels revealed that treatment of cells with Stx1 or Stx1+LPS resulted in significantly more stable IL-8 transcripts compared to treatment with LPS (Figure 10, Chapter III). The calculated half-life for IL-8 mRNA induced by LPS alone was 1.2 h, which was significantly lower than the 4.1 h IL-8 mRNA half-

life from cells treated with Stx1. Stx1+LPS treatment resulted in IL-8 mRNA levels that showed no signs of decay over 5 h. The ability of Stx1+ LPS to induce greater and stable IL-8 transcripts led us to anticipate a greater level of IL-8 protein production, as in the case of TNF-α expression (105). Unexpectedly, treatment with Stx1+LPS did not result in greater IL-8 protein levels compared to treatment with LPS alone (Figure 11, Chapter III). Conversely, Stx1+LPS treatment resulted in less IL-8 protein compared to treatment with LPS alone, but still more compared to treatment with Stx1 alone, leading us to believe that Stx1 affects the expression of IL-8 at the translational level.

Interestingly, IL-8 mRNA and protein induction in Stx1-treated cells were delayed compared to induction in cells treated with LPS or Stx1+LPS, similar to the kinetics of IL-1β induction (Figures 2 & 3, Chapter II). In contrast to IL-1β protein levels expressed by cells treated with Stx1, IL-8 protein levels were much greater, although still lower compared to LPS- or Stx1+LPS-treated cells. These results were not surprising since mechanisms for IL-8 expression and secretion are less complicated than those for IL-1β, involving *de novo* protein synthesis and leader sequence-mediated secretion following stimulation.

Aside from IL-8 induction, macroarray analysis of Stx1-, LPS-, and Stx1+LPS-treated THP-1 cells indicated the possible induction of additional chemokines, including MIP-1α, MIP-1β, and GRO-β (Figure 7 & Table 3, Chapter

III). Real-time experiments verified significant expression of MIP-1α, MIP-1β, and GRO-β in LPS- and LPS+Stx1-treated cells (Figure 8, Chapter III). Induction by Stx1 was not significant at either 2 or 6 h post-treatment, although, in order for Stx1 to elicit a response, it needs to be internalized prior to the initiation of signaling events for gene expression. This is verified by the kinetics of IL-8 mRNA expression in cells treated with Stx1 (Figure 9, Chapter III). ELISAs indicated that Stx1, in the presence or absence of LPS, induced MIP-1α, MIP-1β, and GRO-β protein expression (Figure 12, Chapter III) in a similar pattern to IL-8 expression (Figure 11, Chapter III). Stx1+LPS treatment, again, resulted in lower MIP-1α, MIP-1β, and GRO-β protein levels compared to LPS treatment alone, suggesting that the combination of the two toxins affects chemokine production at the translational level.

Collectively, the cytokine and chemokine data showed that the expression of cytokines and chemokines do not occur in identical patterns, suggesting that Stxs may regulate the expression of different genes in different cell types in different ways by acting at many levels. The normal, controlled regulation of cytokine and chemokine production is important in limiting the harmful effects of an extended inflammatory response, in the host, during an infection. By understanding the mechanisms by which Stxs affect the regulation of cellular biochemical processes, such as transcription, translation, secretion,

and homeostasis, we can better determine more effective ways of thwarting Stx-mediated diseases.

During the experiments to elucidate the regulatory mechanisms of cytokine and chemokine production in response to Stxs and/or LPS, it was noted that as treatment times were extended, the yield of total RNA extracted decreased and the ELISA supernatants contained larger cell pellets, suggesting that fewer cells were remaining on the plates during RNA extraction. One possible explanation for these observations was that the cells were dying. MTT assays performed to detect cell viability revealed that in addition to inducing rapid cell death in undifferentiated THP-1 cells, Stx1, LPS, or Stx1+LPS were able to induce cell death in differentiated THP-1 cells as well (Figure 13, Chapter IV). Even though treatment of differentiated THP-1 cells with Stx1 or LPS alone resulted in cell death, it was clear that their ability to induce cell death was nowhere near the magnitude of cell death induced when both toxins were given in combination. Furthermore, the biggest difference seen between undifferentiated THP-1 cells and differentiated THP-1 cells following treatment with Stx1 and/or LPS was that undifferentiated THP-1 cells were almost as sensitive to treatment with Stx1 alone as it was to treatment with Stx1+LPS, while this was not the case for differentiated THP-1 cells. Experiments conducted to determine the mechanism involved in Stx- and/or LPS-induced cell death indicated that the differentiated (Figure 14, Chapter IV) and

undifferentiated (Figure 15, Chapter IV) cells were undergoing programmed cell death, or apoptosis. Stx-induced apoptosis of undifferentiated THP-1 cells has been demonstrated previously by Kojio et al (59), however apoptosis of Stx-treated differentiated THP-1 cells has not been reported. Due to the nature of previous experiments conducted in our lab, looking at the signaling events, early cytokine production, and protein synthesis inhibition in THP-1 cells in response to Stxs, the notion of cell death was not a concern (23,24,99,105). Furthermore, susceptibility of differentiated THP-1 cells to Stxs was not anticipated due to the decrease in the expression of the toxin receptor, Gb_3 on their surfaces (99). Upon extension of time course experiments, we can now see that even though differentiated THP-1 cells express less toxin receptor, they may still be susceptible to apoptosis induction, although not to the same extent, as undifferentiated THP-1 cells. These data suggest that differentiation of THP-1 cells alters their susceptibility to Stx1, and this alteration is partially bypassed by the addition of LPS. In support of this, Suzuki et al recently reported that when the macrophage cell line U-937 was differentiated using 12-*O*-tetradecanoylphorbol 13-acetate, and subsequently treated with LPS and the protein synthesis inhibitor cycloheximide, a similar cell death phenomenon was observed, while treatment with either LPS or cycloheximide alone were ineffective in inducing apoptosis (125). The actual initiation signal of Stx1+LPS-

induced apoptosis in differentiated THP-1 cells is still not known, but one possible mechanism may involve the production of TNF-α.

The involvement of caspase activation in Stx1-, LPS-, and Stx1+LPS-induced differentiated THP-1 cell death was shown in experiments using the pan-caspase inhibitor zVAD-fmk (Figure 16, Chapter IV) and further verified by the demonstration of poly-ADP-ribose polymerase (PARP) cleavage (Figure 17, Chapter IV), which leads to the loss of PARP activity. PARP inactivation results in the loss of DNA repair, and is a good indicator of apoptosis, as well as caspase activity, since caspase-3 and caspase-7 have been shown to be involved in PARP cleavage (121). Kojio et al previously demonstrated the activation of caspase-3 in undifferentiated THP-1 cells following treatment with Stx1 or Stx2 (59). Surprisingly, results of our apoptotic gene array analysis did not demonstrate the activation of numerous apoptosis-related genes, showing only up-regulation of TNF-α and a type II transmembrane glycoprotein, CD70, whose role in macrophage-induced apoptosis is still unknown. The lack of extensive up-regulation of apoptotic genes suggests that Stx- and/or LPS-induced apoptosis may not require transcriptional activation of apoptosis-related genes.

As with cytokine production, purified Stx1 B-subunit is unable to induce apoptosis in differentiated THP-1 cells (Figure 18, Chapter IV), despite reports

that purified B-subunits or anti-Gb_3 antibodies were able to induce apoptosis in B-lymphoma cells (75,126,135). The transport of Stxs within THP-1 cells may be necessary for apoptosis induction, since treatment with brefeldin A, a toxin that disrupts retrograde transport, inhibits the induction of apoptosis in undifferentiated THP-1 cells (59). An important caveat in interpreting this data may be that in addition to affecting Stx retrograde transport through the cell, brefeldin A may also disrupt the normal transport of cellular proteins, resulting in cellular stress, and thus resulting in the induction of cytokine production, as well as apoptosis.

The work presented here was based on the idea that cytokines may have a role in Stx pathogenesis by rendering target endothelial cells more susceptible, and that a possible source of these cytokines were the resident tissue macrophages in target organs. In addition to showing that Stxs, in the presence or absence of LPS, were able to alter the state of cytokine mRNA stability, we were able to demonstrate their ability to induce apoptosis in cells that were formerly thought to be resistant to the cytotoxic effects of Stxs. The increased mRNA stability seen in TNF-α transcripts produced by differentiated THP-1 cells may be a factor in increased TNF-α production, leading to a prolonged inflammatory response, as well as increased Gb_3 upregulation on target endothelial cells. The apoptosis of differentiated THP-1 cells following

treatment with Stx1, or even more so following treatment with Stx1+LPS, reveals a possible additional complication to Stx-induced pathogenesis, namely the elimination of the very cells involved in clearing toxins and toxin-producing bacteria. Together, these findings were incorporated into a model of the macrophage in pathogenesis (Figure 19, Chapter IV), and indicate the potential complexity of Stx pathogenesis through the involvement of numerous cell types of the immune system in enhancing, rather than ameliorating the outcome of infection with Stx-producing bacteria. Furthermore, these findings support the need to elucidate the multifaceted effects of Stx-producing bacteria and their main virulence factors in order to treat or prevent the life-threatening diseases that are caused by these organisms.

REFERENCES

1. **Arab, S. and C. A. Lingwood.** 1998. Intracellular targeting of the endoplasmic reticulum/nuclear envelope by retrograde transport may determine cell hypersensitivity to verotoxin via globotriaosylceramide fatty acid isoform traffic. Journal of Cellular Physiology **177**:646-660.

2. **Auwerx, J.** 1991. The human leukemia cell line THP-1: a multifacetted model for the study of monocyte-macrophage differentiation. Experentia **44**:22-31.

3. **Beebakhee, G., M. Louie, J. De Azavedo, and J. Brunton.** 1992. Cloning and nucleotide sequence of the eae gene homologue from enterohemorrhagic *Escherichia coli* serotype O157:H7. FEMS Microbiol.Lett. **70**:63-68.

4. **Black, R. A., C. T. Rauch, C. J. Kozlosky, J. J. Peschon, J. L. Slack, M. F. Wolfson, B. J. Castner, K. L. Stocking, P. Reddy, S. Srinivasan, N. Nelson, N. Boiani, K. A. Schooley, M. Gerhart, R. Davis, J. N. Fitzner, R. S. Johnson, R. J. Paxton, C. J. March, and D. P. Cerretti.** 1997. A metalloproteinase disintegrin that releases tumour-necrosis factor-alpha from cells. Nature **385**:729-733.

5. **Boyd, B. and C. Lingwood.** 1989. Verotoxin receptor glycolipid in human renal tissue. Nephron **51**:207-210.

6. **Caput, D., B. Beutler, K. Hartog, R. Thayer, S. Brown-Shimer, and A. Cerami.** 1986. Identification of a common nucleotide sequence in the 3'-untranslated region of mRNA molecules specifying inflammatory mediators. Proc.Natl.Acad.Sci.USA **83**:1670-1674.

7. **Chen, C. Y., R. Gherzi, S. E. Ong, E. L. Chan, R. Raijmakers, G. J. Pruijn, G. Stoecklin, C. Moroni, M. Mann, and M. Karin.** 2001. AU binding proteins recruit the exosome to degrade ARE-containing mRNAs. Cell **107**:451-464.

8. **Cherla, R. P., S. Y. Lee, and V. L. Tesh.** 2003. Shiga toxins and apoptosis. FEMS Microbiol.Lett. **228**:159-166.

9. **Cockwell, P., A. J. Howie, D. Adu, and C. O. Savage.** 1998. *In situ* analysis of C-C chemokine mRNA in human glomerulonephritis. Kidney Int. **54**:827-836.

10. **Degrandis, S., H. Law, J. Brunton, C. Gyles, and C. A. Lingwood.** 1989. Globotetraosylceramide is recognized by the pig edema disease toxin. J.Biol.Chem. **264**:12520-12525.

11. **Dinarello, C. A.** 1999. Immediate cytokine responses to endotoxin: tumor necrosis factor-α and interleukin-1 family. 549-560.

12. **Dobrovolskaia, M. A. and S. N. Vogel.** 2002. Toll receptors, CD14, and macrophage activation and deactivation by LPS. Microbes.Infect. **4**:903-914.

13. **Dumitru, C. D., J. D. Ceci, C. Tsatsanis, D. Kontoyiannis, K. Stamatakis, J. H. Lin, C. Patriotis, N. A. Jenkins, N. G. Copeland, G. Kollias, and P. N. Tsichlis.** 2000. TNF-alpha induction by LPS is regulated posttranscriptionally via a Tpl2/ERK-dependent pathway. Cell **103**:1071-1083.

14. **Dykstra, S. A., R. A. Moxley, B. H. Janke, E. A. Nelson, and D. H. Francis.** 1993. Clinical signs and lesions in gnotobiotic pigs inoculated with Shiga-like toxin I from *Escherichia coli*. Vet.Pathol. **30**:410-417.

15. **Eisenhauer, P. B., P. Chaturvedi, R. E. Fine, A. J. Ritchie, J. S. Pober, T. G. Cleary, and D. S. Newburg.** 2001. Tumor necrosis factor alpha increases human cerebral endothelial cell Gb3 and sensitivity to Shiga toxin. Infect.Immun. **69**:1889-1894.

16. **Endo, Y., K. Tsurugi, T. Yutsudo, Y. Takeda, T. Ogasawara, and K. Igarashi.** 1988. Site of action of a Vero toxin (VT2) from *Escherichia coli* O157:H7 and of Shiga toxin on eukaryotic ribosomes. RNA N-glycosidase activity of the toxins. Eur.J.Biochem. **171**:45-50.

17. **Falguieres, T., F. Mallard, C. Baron, D. Hanau, C. Lingwood, B. Goud, J. Salamero, and L. Johannes.** 2001. Targeting of Shiga toxin B-subunit to retrograde transport route in association with detergent-resistant membranes. Mol.Biol.Cell **12**:2453-2468.

18. **Fan, E., E. A. Merritt, C. L. Verlinde, and W. G. Hol.** 2000. AB(5) toxins: structures and inhibitor design. Curr.Opin.Struct.Biol. **10**:680-686.

19. **Fenton, M. J., B. D. Clark, K. L. Collins, A. C. Webb, A. Rich, and P. E. Auron.** 1987. Transcriptional regulation of the human prointerleukin 1 beta gene. J.Immunol. **138**:3972-3979.

20. **Fitzpatrick, M. M., V. Shah, R. S. Trompeter, M. J. Dillon, and T. M. Barratt.** 1992. Interleukin-8 and polymorphoneutrophil leucocyte activation in hemolytic uremic syndrome of childhood. Kidney Int. **42**:951-956.

21. **Fontaine, A., J. Arondel, and P. J. Sansonetti.** 1988. Role of Shiga toxin in the pathogenesis of bacillary dysentery, studied by using a Tox- mutant of *Shigella dysenteriae* 1. Infect.Immun. **56**:3099-3109.

22. **Forsyth, K. D., A. C. Simpson, M. M. Fitzpatrick, T. M. Barratt, and R. J. Levinsky.** 1989. Neutrophil-mediated endothelial injury in haemolytic uraemic syndrome. Lancet **2**:411-414.

23. **Foster, G. H., C. S. Armstrong, R. Sakiri, and V. L. Tesh.** 2000. Shiga toxin-induced tumor necrosis factor alpha expression: requirement for toxin enzymatic activity and monocyte protein kinase C and protein tyrosine kinases. Infect.Immun. **68**:5183-5189.

24. **Foster, G. H. and V. L. Tesh.** 2002. Shiga toxin 1-induced activation of c-Jun NH(2)-terminal kinase and p38 in the human monocytic cell line THP-1: possible involvement in the production of TNF-alpha. J.Leukoc.Biol. **71**:107-114.

25. **Fraser, M. E., M. M. Chernaia, Y. V. Kozlov, and M. N. James.** 1994. Crystal structure of the holotoxin from *Shigella dysenteriae* at 2.5 A resolution. Nat.Struct.Biol. **1**:59-64.

26. **Garred, O., B. van Deurs, and K. Sandvig.** 1995. Furin-induced cleavage and activation of Shiga toxin. J.Biol.Chem. **270**:10817-10821.

27. **Gasser, C., E. Gautier, A. Steck, R. E. Siebenmann, and R. Oechslin.** 1955. Hemolytic-uremic syndrome: bilateral necrosis of the renal cortex in acute acquired hemolytic anemia. Schweiz.Med.Wochenschr. **85**:905-909.

28. **Gavrieli, Y., Y. Sherman, and S. A. Ben Sasson.** 1992. Identification of programmed cell death *in situ* via specific labeling of nuclear DNA fragmentation. J.Cell Biol. **119**:493-501.

29. **Gear, A. R., S. Suttitanamongkol, D. Viisoreanu, R. K. Polanowska-Grabowska, S. Raha, and D. Camerini.** 2001. Adenosine diphosphate strongly potentiates the ability of the chemokines MDC, TARC, and SDF-1 to stimulate platelet function. Blood **97**:937-945.

30. **Geiser, T., B. Dewald, M. U. Ehrengruber, I. Clark-Lewis, and M. Baggiolini.** 1993. The interleukin-8-related chemotactic cytokines GRO alpha, GRO beta, and GRO gamma activate human neutrophil and basophil leukocytes. J.Biol.Chem. **268**:15419-15424.

31. **Goodman, R. B., R. M. Strieter, C. W. Frevert, C. J. Cummings, P. Tekamp-Olson, S. L. Kunkel, A. Walz, and T. R. Martin.** 1998. Quantitative comparison of C-X-C chemokines produced by endotoxin-stimulated human alveolar macrophages. Am.J.Physiol **275**:L87-L95.

32. **Goodwin, R. G., M. R. Alderson, C. A. Smith, R. J. Armitage, T. VandenBos, R. Jerzy, T. W. Tough, M. A. Schoenborn, T. Davis-Smith, K. Hennen, and .** 1993. Molecular and biological characterization of a ligand for CD27 defines a new family of cytokines with homology to tumor necrosis factor. Cell **73**:447-456.

33. **Green, D. R.** 1998. Apoptotic pathways: the roads to ruin. Cell **94**:695-698.

34. **Greenwell-Wild, T., G. Peng, N. Vazquez, W. Jin, K. Lei, J. M. Orenstein, and S. M. Wahl.** 2003. *Mycobacterium avium* targets the inflammasome to suppress caspase-1-dependent production of IL-1β. J.Leukocyte Biol. [Abst.]**74**:38-

35. **Grisham, M. B. and D. N. Granger.** 1988. Neutrophil-mediated mucosal injury. Role of reactive oxygen metabolites. Dig.Dis.Sci. **33**:6S-15S.

36. **Gueydan, C., L. Droogmans, P. Chalon, G. Huez, D. Caput, and V. Kruys.** 1999. Identification of TIAR as a protein binding to the translational regulatory AU-rich element of tumor necrosis factor alpha mRNA. J.Biol.Chem. **274**:2322-2326.

37. **Harel, Y., M. Silva, B. Giroir, A. Weinberg, T. B. Cleary, and B. Beutler.** 1993. A reporter transgene indicates renal-specific induction of tumor necrosis factor (TNF) by Shiga-like toxin. Possible involvement of TNF in hemolytic uremic syndrome. J.Clin.Invest **92**:2110-2116.

38. **Harrison, L. M., W. C. van Haaften, and V. L. Tesh.** 2004. Regulation of proinflammatory cytokine expression by Shiga toxin 1 and/or lipopolysaccharides in the human monocytic cell line THP-1. Infect.Immun. **72**:2618-2627.

39. **Harrold, S., C. Genovese, B. Kobrin, S. L. Morrison, and C. Milcarek.** 1991. A comparison of apparent mRNA half-life using kinetic labeling techniques *vs* decay following administration of transcriptional inhibitors. Anal.Biochem. **198**:19-29.

40. **Hensold, J. O., D. Barth-Baus, and C. A. Stratton.** 1996. Inducers of erythroleukemic differentiation cause messenger RNAs that lack poly(A)-binding protein to accumulate in translationally inactive, salt-labile 80 S ribosomal complexes. J.Biol.Chem. **271**:23246-23254.

41. **Hertzke, D. M., L. A. Cowan, P. Schoning, and B. W. Fenwick.** 1995. Glomerular ultrastructural lesions of idiopathic cutaneous and renal glomerular vasculopathy of greyhounds. Vet.Pathol. **32**:451-459.

42. **Hintzen, R. Q., S. M. Lens, M. P. Beckmann, R. G. Goodwin, D. Lynch, and R. A. van Lier.** 1994. Characterization of the human CD27 ligand, a novel member of the TNF gene family. J.Immunol. **152**:1762-1773.

43. **Hurley, B. P., M. Jacewicz, C. M. Thorpe, L. L. Lincicome, A. J. King, G. T. Keusch, and D. W. Acheson.** 1999. Shiga toxins 1 and 2 translocate differently across polarized intestinal epithelial cells. Infect.Immun. **67**:6670-6677.

44. **Hurley, B. P., C. M. Thorpe, and D. W. Acheson.** 2001. Shiga toxin translocation across intestinal epithelial cells is enhanced by neutrophil transmigration. Infect.Immun. **69**:6148-6155.

45. **Igarashi, K., T. Ogasawara, K. Ito, T. Yutsudo, and Y. Takeda.** 1987. Inhibition of elongation factor 1-dependent aminoacyl-tRNA binding to ribosomes by Shiga-like toxin I (VT1) from *Escherichia coli* O157: H7 and by Shiga toxin. FEMS Microbiol.Lett. **44**:91-94.

46. **Inward, C. D., A. J. Howie, M. M. Fitzpatrick, F. Rafaat, D. V. Milford, and C. M. Taylor.** 1997. Renal histopathology in fatal cases of diarrhoea-associated haemolytic uraemic syndrome. British Association for Paediatric Nephrology. Pediatr.Nephrol. **11**:556-559.

47. **Iordanov, M. S., D. Pribnow, J. L. Magun, T. H. Dinh, J. A. Pearson, S. L. Chen, and B. E. Magun.** 1997. Ribotoxic stress response: activation of the stress-activated protein kinase JNK1 by inhibitors of the peptidyl transferase reaction and by sequence-specific RNA damage to the alpha-sarcin/ricin loop in the 28S rRNA. Mol.Cell Biol. **17**:3373-3381.

48. **Isogai, E., H. Isogai, K. Kimura, S. Hayashi, T. Kubota, N. Fujii, and K. Takeshi.** 1998. Role of tumor necrosis factor alpha in gnotobiotic mice infected with an *Escherichia coli* O157:H7 strain. Infect.Immun. **66**:197-202.

49. **Jacewicz, M., H. Clausen, E. Nudelman, A. Donohue-Rolfe, and G. T. Keusch.** 1986. Pathogenesis of *Shigella* diarrhea. XI. Isolation of a *Shigella* toxin-binding glycolipid from rabbit jejunum and HeLa cells and its identification as globotriaosylceramide. J.Exp.Med. **163**:1391-1404.

50. **Jackson, M. P., J. W. Newland, R. K. Holmes, and A. D. O'Brien.** 1987. Nucleotide sequence analysis of the structural genes for Shiga-like toxin I encoded by bacteriophage 933J from *Escherichia coli*. Microb.Pathog. **2**:147-153.

51. **Jones, N. L., A. Islur, R. Haq, M. Mascarenhas, M. A. Karmali, M. H. Perdue, B. W. Zanke, and P. M. Sherman.** 2000. *Escherichia coli* Shiga toxins induce apoptosis in epithelial cells that is regulated by the Bcl-2 family. Am.J.Physiol Gastrointest.Liver Physiol **278**:G811-G819.

52. **Karmali, M. A.** 1998. Human immune response and immunity to Shiga toxin (verotoxin)-producing *Escherichia coli* infection. 236-248.

53. **Karmali, M. A., M. Petric, C. Lim, P. C. Fleming, G. S. Arbus, and H. Lior.** 1985. The association between idiopathic hemolytic uremic syndrome and infection by verotoxin-producing *Escherichia coli*. J.Infect.Dis. **189**:556-563.

54. **Karmali, M. A., B. T. Steele, M. Petric, and C. Lim.** 1983. Sporadic cases of haemolytic-uraemic syndrome associated with faecal cytotoxin and cytotoxin-producing *Escherichia coli* in stools. Lancet **1**:619-620.

55. **Karpman, D., A. Hakansson, M. T. Perez, C. Isaksson, E. Carlemalm, A. Caprioli, and C. Svanborg.** 1998. Apoptosis of renal cortical cells in the hemolytic-uremic syndrome: *in vivo* and *in vitro* studies. Infect.Immun. **66**:636-644.

56. **Kashii, Y., R. Giorda, R. B. Herberman, T. L. Whiteside, and N. L. Vujanovic.** 1999. Constitutive expression and role of the TNF family ligands in apoptotic killing of tumor cells by human NK cells. J.Immunol. **163**:5358-5366.

57. **Kedersha, N. L., M. Gupta, W. Li, I. Miller, and P. Anderson.** 1999. RNA-binding proteins TIA-1 and TIAR link the phosphorylation of eIF-2 alpha to the assembly of mammalian stress granules. J.Cell Biol. **147**:1431-1442.

58. **Kiyokawa, N., T. Taguchi, T. Mori, H. Uchida, N. Sato, T. Takeda, and J. Fujimoto.** 1998. Induction of apoptosis in normal human renal tubular epithelial cells by *Escherichia coli* Shiga toxins 1 and 2. J.Infect.Dis. **178**:178-184.

59. **Kojio, S., H. Zhang, M. Ohmura, F. Gondaira, N. Kobayashi, and T. Yamamoto.** 2000. Caspase-3 activation and apoptosis induction coupled with the retrograde transport of shiga toxin: inhibition by brefeldin A. FEMS Immunol.Med.Microbiol. **29**:275-281.

60. **Koster, F., J. Levin, L. Walker, K. S. Tung, R. H. Gilman, M. M. Rahaman, M. A. Majid, S. Islam, and R. C. Williams, Jr.** 1978. Hemolytic-uremic syndrome after shigellosis. Relation to endotoxemia and circulating immune complexes. N.Engl.J.Med. **298**:927-933.

61. **Lai, W. S., E. Carballo, J. R. Strum, E. A. Kennington, R. S. Phillips, and P. J. Blackshear.** 1999. Evidence that tristetraprolin binds to AU-rich elements and promotes the deadenylation and destabilization of tumor necrosis factor alpha mRNA. Mol.Cell Biol. **19**:4311-4323.

62. **Lai, W. S., E. Carballo, J. M. Thorn, E. A. Kennington, and P. J. Blackshear.** 2000. Interactions of CCCH zinc finger proteins with mRNA. Binding of tristetraprolin-related zinc finger proteins to AU-rich elements and destabilization of mRNA. J.Biol.Chem. **275**:17827-17837.

63. **LeBlanc, J. J.** 2003. Implication of virulence factors in *Escherichia coli* O157:H7 pathogenesis. Crit Rev.Microbiol. **29**:277-296.

64. **Lens, S. M., K. Tesselaar, M. H. van Oers, and R. A. van Lier.** 1998. Control of lymphocyte function through CD27-CD70 interactions. Semin.Immunol. **10**:491-499.

65. **Lindberg, A. A., J. E. Schultz, M. Westling, J. E. Brown, S. W. Rothman, K. A. Karlsson, and N. Stromberg.** 1986. Identification of the receptor glycolipid for Shiga toxin produced by *Shigella dysenteriae* type 1. 439-446.

66. **Ling, H., A. Boodhoo, B. Hazes, M. D. Cummings, G. D. Armstrong, J. L. Brunton, and R. J. Read.** 1998. Structure of the shiga-like toxin I B-pentamer complexed with an analogue of its receptor Gb3. Biochemistry **37**:1777-1788.

67. **Lingwood, C. A., A. A. Khine, and S. Arab.** 1998. Globotriaosyl ceramide (Gb3) expression in human tumour cells: intracellular trafficking defines a new retrograde transport pathway from the cell surface to the nucleus, which correlates with sensitivity to verotoxin. Acta Biochim.Pol. **45**:351-359.

68. **Lingwood, C. A., H. Law, S. Richardson, M. Petric, J. L. Brunton, S. De Grandis, and M. Karmali.** 1987. Glycolipid binding of purified and recombinant *Escherichia coli* produced verotoxin *in vitro*. J.Biol.Chem. **262**:8834-8839.

69. **Liu, H., Y. Ma, L. J. Pagliari, H. Perlman, C. Yu, A. Lin, and R. M. Pope.** 2004. TNF-alpha-induced apoptosis of macrophages following inhibition of NF-kappa B: a central role for disruption of mitochondria. J.Immunol. **172**:1907-1915.

70. **Liu, J., T. Akahoshi, T. Sasahana, H. Kitasato, R. Namai, T. Sasaki, M. Inoue, and H. Kondo.** 1999. Inhibition of neutrophil apoptosis by verotoxin 2 derived from *Escherichia coli* O157:H7. Infect.Immun. **67**:6203-6205.

71. **Louise, C. B. and T. G. Obrig.** 1991. Shiga toxin-associated hemolytic-uremic syndrome: combined cytotoxic effects of Shiga toxin, interleukin-1 beta, and tumor necrosis factor alpha on human vascular endothelial cells *in vitro*. Infect.Immun. **59**:4173-4179.

72. **Louise, C. B., M. C. Tran, and T. G. Obrig.** 1997. Sensitization of human umbilical vein endothelial cells to Shiga toxin: involvement of protein kinase C and NF-kappaB. Infect.Immun. **65**:3337-3344.

73. **Lukacs, N. W., R. M. Strieter, V. M. Elner, H. L. Evanoff, M. Burdick, and S. L. Kunkel.** 1994. Intercellular adhesion molecule-1 mediates the

expression of monocyte-derived MIP-1 alpha during monocyte-endothelial cell interactions. Blood **83**:1174-1178.

74. **Mangan, D. F., G. R. Welch, and S. M. Wahl.** 1991. Lipopolysaccharide, tumor necrosis factor-alpha, and IL-1 beta prevent programmed cell death (apoptosis) in human peripheral blood monocytes. J.Immunol. **146**:1541-1546.

75. **Mangeney, M., C. A. Lingwood, S. Taga, B. Caillou, T. Tursz, and J. Wiels.** 1993. Apoptosis induced in Burkitt's lymphoma cells via Gb3/CD77, a glycolipid antigen. Cancer Res. **53**:5314-5319.

76. **Martinon, F., K. Burns, and J. Tschopp.** 2002. The inflammasome: a molecular platform triggering activation of inflammatory caspases and processing of proIL-beta. Mol.Cell **10**:417-426.

77. **McClure, P. J. and S. Hall.** 2000. Survival of *Escherichia coli* in foods. Symp.Ser.Soc.Appl.Microbiol. 61S-70S.

78. **Melton-Celsa, A. R., S. C. Darnell, and A. D. O'Brien.** 1996. Activation of Shiga-like toxins by mouse and human intestinal mucus correlates with virulence of enterohemorrhagic *Escherichia coli* O91:H21 isolates in orally infected, streptomycin-treated mice. Infect.Immun. **64**:1569-1576.

79. **Melton-Celsa, A. R. and A. D. O'Brien.** 1998. Structure, biology and relative toxicity of Shiga toxin family members for cells and animals. 121-128.

80. **Menten, P., A. Wuyts, and J. Van Damme.** 2002. Macrophage inflammatory protein-1. Cytokine Growth Factor Rev. **13**:455-481.

81. **Miyamoto, Y. and S. U. Kim.** 1999. Cytokine-induced production of macrophage inflammatory protein-1alpha (MIP-1alpha) in cultured human astrocytes. J.Neurosci.Res. **55**:245-251.

82. **Moake, J. L.** 2002. Thrombotic microangiopathies. N.Engl.J.Med. **347**:589-600.

83. **Moss, M. L., S. L. Jin, M. E. Milla, D. M. Bickett, W. Burkhart, H. L. Carter, W. J. Chen, W. C. Clay, J. R. Didsbury, D. Hassler, C. R. Hoffman, T. A. Kost, M. H. Lambert, M. A. Leesnitzer, P. McCauley, G. McGeehan, J. Mitchell, M. Moyer, G. Pahel, W. Rocque, L. K. Overton, F. Schoenen, T. Seaton, J. L. Su, J. D. Becherer, and .** 1997. Cloning of a

disintegrin metalloproteinase that processes precursor tumour-necrosis factor-alpha. Nature **385**:733-736.

84. **Moxley, R. A. and D. H. Francis.** 1998. Overview of animal models. 249-260.

85. **Nagata, S.** 2000. Apoptotic DNA fragmentation. Exp.Cell Res. **256**:12-18.

86. **Nau, G. J., J. F. Richmond, A. Schlesinger, E. G. Jennings, E. S. Lander, and R. A. Young.** 2002. Human macrophage activation programs induced by bacterial pathogens. Proc.Natl.Acad.Sci.U.S.A **99**:1503-1508.

87. **O'Brien, A. D., V. L. Tesh, A. Donohue-Rolfe, M. P. Jackson, S. Olsnes, K. Sandvig, A. A. Lindberg, and G. T. Keusch.** 1992. Shiga toxin: biochemistry, genetics, mode of action, and role in pathogenesis. Curr.Top.Microbiol.Immunol. **180**:65-94.

88. **Obrig, T. G., P. J. Del Vecchio, J. E. Brown, T. P. Moran, B. M. Rowland, T. K. Judge, and S. W. Rothman.** 1988. Direct cytotoxic action of Shiga toxin on human vascular endothelial cells. Infect.Immun. **56**:2373-2378.

89. **Obrig, T. G., T. P. Moran, and J. E. Brown.** 1987. The mode of action of Shiga toxin on peptide elongation of eukaryotic protein synthesis. Biochem.J. **244**:287-294.

90. **Ochoa, T. J. and T. G. Cleary.** 2003. Epidemiology and spectrum of disease of *Escherichia coli* O157. Curr.Opin.Infect.Dis. **16**:259-263.

91. **Parkos, C. A., C. Delp, M. A. Arnaout, and J. L. Madara.** 1991. Neutrophil migration across a cultured intestinal epithelium. Dependence on a CD11b/CD18-mediated event and enhanced efficiency in physiological direction. J.Clin.Invest **88**:1605-1612.

92. **Paton, J. C. and A. W. Paton.** 1998. Pathogenesis and diagnosis of Shiga toxin-producing *Escherichia coli* infections. Clin.Microbiol.Rev. **11**:450-479.

93. **Pellizzari, A., H. Pang, and C. A. Lingwood.** 1992. Binding of verocytotoxin 1 to its receptor is influenced by differences in receptor fatty acid content. Biochemistry **31**:1363-1370.

94. **Philpott, D. J., C. A. Ackerley, A. J. Kiliaan, M. A. Karmali, M. H. Perdue, and P. M. Sherman.** 1997. Translocation of verotoxin-1 across

T84 monolayers: mechanism of bacterial toxin penetration of epithelium. Am.J.Physiol **273**:G1349-G1358.

95. **Piecyk, M., S. Wax, A. R. Beck, N. Kedersha, M. Gupta, B. Maritim, S. Chen, C. Gueydan, V. Kruys, M. Streuli, and P. Anderson.** 2000. TIA-1 is a translational silencer that selectively regulates the expression of TNF-alpha. EMBO J. **19**:4154-4163.

96. **Prasad, K. V., Z. Ao, Y. Yoon, M. X. Wu, M. Rizk, S. Jacquot, and S. F. Schlossman.** 1997. CD27, a member of the tumor necrosis factor receptor family, induces apoptosis and binds to Siva, a proapoptotic protein. Proc.Natl.Acad.Sci.U.S.A **94**:6346-6351.

97. **Proulx, F., E. G. Seidman, and D. Karpman.** 2001. Pathogenesis of Shiga toxin-associated hemolytic uremic syndrome. Pediatr.Res. **50**:163-171.

98. **Ramegowda, B., J. E. Samuel, and V. L. Tesh.** 1999. Interaction of Shiga toxins with human brain microvascular endothelial cells: cytokines as sensitizing agents. J.Infect.Dis. **180**:1205-1213.

99. **Ramegowda, B. and V. L. Tesh.** 1996. Differentiation-associated toxin receptor modulation, cytokine production, and sensitivity to Shiga-like toxins in human monocytes and monocytic cell lines. Infect.Immun. **64**:1173-1180.

100. **Rhoades, K. L., S. H. Golub, and J. S. Economou.** 1992. The regulation of the human tumor necrosis factor alpha promoter region in macrophage, T cell, and B cell lines. J.Biol.Chem. **267**:22102-22107.

101. **Richardson, S. E., T. A. Rotman, V. Jay, C. R. Smith, L. E. Becker, M. Petric, N. F. Olivieri, and M. A. Karmali.** 1992. Experimental verocytotoxemia in rabbits. Infect.Immun. **60**:4154-4167.

102. **Rosenberger, C. M., M. G. Scott, M. R. Gold, R. E. Hancock, and B. B. Finlay.** 2000. *Salmonella typhimurium* infection and lipopolysaccharide stimulation induce similar changes in macrophage gene expression. J.Immunol. **164**:5894-5904.

103. **Ross, J.** 1995. mRNA stability in mammalian cells. Microbiol.Rev. **59**:423-450.

104. **Ruggenenti, P., M. Noris, and G. Remuzzi.** 2001. Thrombotic microangiopathy, hemolytic uremic syndrome, and thrombotic thrombocytopenic purpura. Kidney Int. **60**:831-846.

105. **Sakiri, R., B. Ramegowda, and V. L. Tesh.** 1998. Shiga toxin type 1 activates tumor necrosis factor-alpha gene transcription and nuclear translocation of the transcriptional activators nuclear factor-kappaB and activator protein-1. Blood **92**:558-566.

106. **Samuel, J. E., L. P. Perera, S. Ward, A. D. O'Brien, V. Ginsburg, and H. C. Krivan.** 1990. Comparison of the glycolipid receptor specificities of Shiga-like toxin type II and Shiga-like toxin type II variants. Infect.Immun. **58**:611-618.

107. **Sandvig, K., O. Garred, K. Prydz, J. V. Kozlov, S. H. Hansen, and B. van Deurs.** 1992. Retrograde transport of endocytosed Shiga toxin to the endoplasmic reticulum. Nature **358**:510-512.

108. **Sandvig, K., S. Grimmer, S. U. Lauvrak, M. L. Torgersen, G. Skretting, B. van Deurs, and T. G. Iversen.** 2002. Pathways followed by ricin and Shiga toxin into cells. Histochem.Cell Biol. **117**:131-141.

109. **Sandvig, K. and B. van Deurs.** 1996. Endocytosis, intracellular transport, and cytotoxic action of Shiga toxin and ricin. Physiol Rev. **76**:949-966.

110. **Sansonetti, P. J., C. Egile, and C. Wenneras.** 2001. Shigellosis: from disease symptoms to molecular and cellular pathogenesis. 335-385.

111. **Saxena, S. K., A. D. O'Brien, and E. J. Ackerman.** 1989. Shiga toxin, Shiga-like toxin II variant, and ricin are all single-site RNA N-glycosidases of 28 S RNA when microinjected into *Xenopus* oocytes. J.Biol.Chem. **264**:596-601.

112. **Schindler, R., B. D. Clark, and C. A. Dinarello.** 1990. Dissociation between interleukin-1 beta mRNA and protein synthesis in human peripheral blood mononuclear cells. J.Biol.Chem. **265**:10232-10237.

113. **Schuller, S., G. Frankel, and A. D. Phillips.** 2004. Interaction of Shiga toxin from *Escherichia coli* with human intestinal epithelial cell lines and explants: Stx2 induces epithelial damage in organ culture. Cell Microbiol. **6**:289-301.

114. **Shakhov, A. N., M. A. Collart, P. Vassalli, S. A. Nedospasov, and C. V. Jongeneel.** 1990. Kappa B-type enhancers are involved in lipopolysaccharide-mediated transcriptional activation of the tumor necrosis factor alpha gene in primary macrophages. J.Exp.Med. **171**:35-47.

115. **Shukaliak, J. A. and K. Dorovini-Zis.** 2000. Expression of the beta-chemokines RANTES and MIP-1 beta by human brain microvessel endothelial cells in primary culture. J.Neuropathol.Exp.Neurol. **59**:339-352.

116. **Siegler, R. L.** 1994. Spectrum of extrarenal involvement in postdiarrheal hemolytic-uremic syndrome. J.Pediatr. **125**:511-518.

117. **Siegler, R. L.** 1995. The hemolytic uremic syndrome. Pediatr.Clin.North Am. **42**:1505-1529.

118. **Siegler, R. L., T. J. Pysher, R. Lou, V. L. Tesh, and F. B. Taylor, Jr.** 2001. Response to Shiga toxin-1, with and without lipopolysaccharide, in a primate model of hemolytic uremic syndrome. Am.J.Nephrol. **21**:420-425.

119. **Slutsker, L., A. A. Ries, K. D. Greene, J. G. Wells, L. Hutwagner, and P. M. Griffin.** 1997. *Escherichia coli* O157:H7 diarrhea in the United States: clinical and epidemiologic features. Ann.Intern.Med. **126**:505-513.

120. **Smith, W. E., A. V. Kane, S. T. Campbell, D. W. Acheson, B. H. Cochran, and C. M. Thorpe.** 2003. Shiga toxin 1 triggers a ribotoxic stress response leading to p38 and JNK activation and induction of apoptosis in intestinal epithelial cells. Infect.Immun. **71**:1497-1504.

121. **Soldani, C., M. C. Lazze, M. G. Bottone, G. Tognon, M. Biggiogera, C. E. Pellicciari, and A. I. Scovassi.** 2001. Poly(ADP-ribose) polymerase cleavage during apoptosis: when and where? Exp.Cell Res. **269**:193-201.

122. **Stennicke, H. R. and G. S. Salvesen.** 2000. Caspases - controlling intracellular signals by protease zymogen activation. Biochim.Biophys.Acta **1477**:299-306.

123. **Stoecklin, G., M. Colombi, I. Raineri, S. Leuenberger, M. Mallaun, M. Schmidlin, B. Gross, M. Lu, T. Kitamura, and C. Moroni.** 2002. Functional cloning of BRF1, a regulator of ARE-dependent mRNA turnover. EMBO J. **21**:4709-4718.

124. **Strockbine, N. A., M. P. Jackson, L. M. Sung, R. K. Holmes, and A. D. O'Brien.** 1988. Cloning and sequencing of the genes for Shiga toxin from *Shigella dysenteriae* type 1. J.Bacteriol. **170**:1116-1122.

125. **Suzuki, T., M. Kobayashi, K. Isatsu, T. Nishihara, T. Aiuchi, K. Nakaya, and K. Hasegawa.** 2004. Mechanisms involved in apoptosis of human macrophages induced by lipopolysaccharide from *Actinobacillus actinomycetemcomitans* in the presence of cycloheximide. Infect.Immun. **72**:1856-1865.

126. **Taga, S., K. Carlier, Z. Mishal, C. Capoulade, M. Mangeney, Y. Lecluse, D. Coulaud, C. Tetaud, L. L. Pritchard, T. Tursz, and J. Wiels.** 1997. Intracellular signaling events in CD77-mediated apoptosis of Burkitt's lymphoma cells. Blood **90**:2757-2767.

127. **Taguchi, T., H. Uchida, N. Kiyokawa, T. Mori, N. Sato, H. Horie, T. Takeda, and J. Fujimoto.** 1998. Verotoxins induce apoptosis in human renal tubular epithelium derived cells. Kidney Int. **53**:1681-1688.

128. **Taylor, F. B., Jr., V. L. Tesh, L. DeBault, A. Li, A. C. Chang, S. D. Kosanke, T. J. Pysher, and R. L. Siegler.** 1999. Characterization of the baboon responses to Shiga-like toxin: descriptive study of a new primate model of toxic responses to Stx-1. Am.J.Pathol. **154**:1285-1299.

129. **te Loo, D. M., L. A. Monnens, T. J. Der Velden, M. A. Vermeer, F. Preyers, P. N. Demacker, L. P. van Den Heuvel, and V. W. van Hinsbergh.** 2000. Binding and transfer of verocytotoxin by polymorphonuclear leukocytes in hemolytic uremic syndrome. Blood **95**:3396-3402.

130. **Tesh, V. L.** 1998. Cytokine response to Shiga toxins. 226-235.

131. **Tesh, V. L., J. A. Burris, J. W. Owens, V. M. Gordon, E. A. Wadolkowski, A. D. O'Brien, and J. E. Samuel.** 1993. Comparison of the relative toxicities of Shiga-like toxins type I and type II for mice. Infect.Immun. **61**:3392-3402.

132. **Tesh, V. L. and A. D. O'Brien.** 1991. The pathogenic mechanisms of Shiga toxin and the Shiga-like toxins. Mol.Microbiol. **5**:1817-1822.

133. **Tesh, V. L., B. Ramegowda, and J. E. Samuel.** 1994. Purified Shiga-like toxins induce expression of proinflammatory cytokines from murine peritoneal macrophages. Infect.Immun. **62**:5085-5094.

134. **Tesh, V. L., J. E. Samuel, L. P. Perera, J. B. Sharefkin, and A. D. O'Brien.** 1991. Evaluation of the role of Shiga and Shiga-like toxins in mediating direct damage to human vascular endothelial cells. J.Infect.Dis. **164**:344-352.

135. **Tetaud, C., T. Falguieres, K. Carlier, Y. Lecluse, J. Garibal, D. Coulaud, P. Busson, R. Steffensen, H. Clausen, L. Johannes, and J. Wiels.** 2003. Two distinct Gb3/CD77 signaling pathways leading to apoptosis are triggered by anti-Gb3/CD77 mAb and verotoxin-1. J.Biol.Chem. **278**:45200-45208.

136. **Thorpe, C. M., B. P. Hurley, L. L. Lincicome, M. S. Jacewicz, G. T. Keusch, and D. W. Acheson.** 1999. Shiga toxins stimulate secretion of interleukin-8 from intestinal epithelial cells. Infect.Immun. **67**:5985-5993.

137. **Thorpe, C. M., W. E. Smith, B. P. Hurley, and D. W. Acheson.** 2001. Shiga toxins induce, superinduce, and stabilize a variety of C-X-C chemokine mRNAs in intestinal epithelial cells, resulting in increased chemokine expression. Infect.Immun. **69**:6140-6147.

138. **Tsuchiya, S., M. Yamabe, Y. Yamaguchi, Y. Kobayashi, T. Konno, and K. Tada.** 1980. Establishment and characterization of a human acute monocytic leukemia cell line (THP-1). Int.J.Cancer **26**:171-176.

139. **van de Kar, N. C., L. A. Monnens, M. A. Karmali, and V. W. van Hinsbergh.** 1992. Tumor necrosis factor and interleukin-1 induce expression of the verocytotoxin receptor globotriaosylceramide on human endothelial cells: implications for the pathogenesis of the hemolytic uremic syndrome. Blood **80**:2755-2764.

140. **Van Setten, P. A., L. A. Monnens, R. G. Verstraten, L. P. van Den Heuvel, and V. W. van Hinsbergh.** 1996. Effects of verocytotoxin-1 on nonadherent human monocytes: binding characteristics, protein synthesis, and induction of cytokine release. Blood **88**:174-183.

141. **Van Setten, P. A., V. W. van Hinsbergh, L. P. van Den Heuvel, F. Preyers, H. B. Dijkman, K. J. Assmann, T. J. van der Velden, and L. A. Monnens.** 1998. Monocyte chemoattractant protein-1 and interleukin-8

levels in urine and serum of patents with hemolytic uremic syndrome. Pediatr.Res. **43**:759-767.

142. **Van Setten, P. A., V. W. van Hinsbergh, T. J. van der Velden, N. C. van de Kar, M. Vermeer, J. D. Mahan, K. J. Assmann, L. P. van Den Heuvel, and L. A. Monnens.** 1997. Effects of TNF alpha on verocytotoxin cytotoxicity in purified human glomerular microvascular endothelial cells. Kidney Int. **51**:1245-1256.

143. **Wajant, H., K. Pfizenmaier, and P. Scheurich.** 2003. Tumor necrosis factor signaling. Cell Death.Differ. **10**:45-65.

144. **Wallace, J. L., A. Higa, G. W. McKnight, and D. E. MacIntyre.** 1992. Prevention and reversal of experimental colitis by a monoclonal antibody which inhibits leukocyte adherence. Inflammation **16**:343-354.

145. **Wang, Z. M., C. Liu, and R. Dziarski.** 2000. Chemokines are the main proinflammatory mediators in human monocytes activated by *Staphylococcus aureus*, peptidoglycan, and endotoxin. J.Biol.Chem. **275**:20260-20267.

146. **Wozniak, A., W. H. Betts, G. A. Murphy, and M. Rokicinski.** 1993. Interleukin-8 primes human neutrophils for enhanced superoxide anion production. Immunology **79**:608-615.

147. **Yamasaki, C., Y. Natori, X. T. Zeng, M. Ohmura, S. Yamasaki, Y. Takeda, and Y. Natori.** 1999. Induction of cytokines in a human colon epithelial cell line by Shiga toxin 1 (Stx1) and Stx2 but not by non-toxic mutant Stx1 which lacks N-glycosidase activity. FEBS Lett. **442**:231-234.

148. **Yamasaki, C., K. Nishikawa, X. T. Zeng, Y. Katayama, Y. Natori, N. Komatsu, T. Oda, and Y. Natori.** 2004. Induction of cytokines by toxins that have an identical RNA N-glycosidase activity: Shiga toxin, ricin, and modeccin. Biochim.Biophys.Acta **1671**:44-50.

149. **Zimmermann, K. C., C. Bonzon, and D. R. Green.** 2001. The machinery of programmed cell death. Pharmacol.Ther. **92**:57-70.

VITA

LISA MARGARET HARRISON

ADDRESS

Department of Medical Microbiology and Immunology
Texas A&M University Health Science Center
Rm. 407 Reynolds Medical Building
College Station, TX 77843-1114

EDUCATION

Ph.D. Medical Sciences
Texas A&M University
August 2004

B.S. Microbiology
University of California Davis
June 1997

PUBLICATIONS

Han, M., **L. Harrison**, P. Kehn, K. Stevenson, J. Currier, M.A. Robinson. 1999. Invariant or highly conserved TCR α are expressed on double-negative ($CD3^+CD4^-CD8^-$) and $CD8^+$ T cells. J. Immunol. 163: 301-311.

Harrison, L.M., W.C.E. van Haaften, and V.L. Tesh. 2004. Regulation of pro-inflammatory cytokine expression by Shiga toxin 1 and/or lipopolysaccharides in the human monocytic cell line THP-1. Infect. Immun.72: 2618-262.

Harrison, L.M., R.P. Cherla, C. van den Hoogen, W.C.E. van Haaften, and V.L. Tesh. 2004. Comparative evaluation of apoptosis induced by Shiga toxin 1 and/or lipopolysaccharides in human monocytic and macrophage-like cells. (Submitted for publication)

Harrison, L.M., C. van den Hoogen, W.C.E. van Haaften, and V.L. Tesh. 2004. Chemokine expression in the monocytic cell line THP-1 in reponse to purified Shiga toxin 1 and/or lipopolysaccharides. (Submitted for publication).